



Review

A Review of the Recent Development in the Synthesis and Biological Evaluations of Pyrazole Derivatives

Oluwakemi Ebenezer ^{1,2} , Michael Shapi ¹ and Jack A. Tuszynski ^{2,3,4,*} 

¹ Department of Chemistry, Faculty of Natural Science, Mangosuthu University of Technology, Durban 4026, South Africa; ebenezer.oluwakemi@mut.ac.za (O.E.); mshapi@mut.ac.za (M.S.)

² Department of Physics, University of Alberta, Edmonton, AB T6G 2E1, Canada

³ Department of Oncology, Cross Cancer Institute, University of Alberta, Edmonton, AB T6G 1Z2, Canada

⁴ Department of Mechanical and Aerospace Engineering, (DIMEAS), Politecnico di Torino, 10129 Turin, Italy

* Correspondence: jact@ualberta.ca

Abstract: Pyrazoles are five-membered heterocyclic compounds that contain nitrogen. They are an important class of compounds for drug development; thus, they have attracted much attention. In the meantime, pyrazole derivatives have been synthesized as target structures and have demonstrated numerous biological activities such as antituberculosis, antimicrobial, antifungal, and anti-inflammatory. This review summarizes the results of published research on pyrazole derivatives synthesis and biological activities. The published research works on pyrazole derivatives synthesis and biological activities between January 2018 and December 2021 were retrieved from the Scopus database and reviewed accordingly.

Keywords: heterocycle; pyrazole; derivatives; synthesis; biological activities; recent development



Citation: Ebenezer, O.; Shapi, M.; Tuszynski, J.A. A Review of the Recent Development in the Synthesis and Biological Evaluations of Pyrazole Derivatives. *Biomedicines* **2022**, *10*, 1124. <https://doi.org/10.3390/biomedicines10051124>

Academic Editor: Ken-Ichi Sano

Received: 5 April 2022

Accepted: 6 May 2022

Published: 12 May 2022

Publisher's Note: MDPI stays neutral with regard to jurisdictional claims in published maps and institutional affiliations.



Copyright: © 2022 by the authors. Licensee MDPI, Basel, Switzerland. This article is an open access article distributed under the terms and conditions of the Creative Commons Attribution (CC BY) license (<https://creativecommons.org/licenses/by/4.0/>).

1. Introduction

Heterocycles are a fundamental and unique class of compounds; they account for over half of all known organic compounds and have a broad range of physical, chemical, and biological properties, covering a broad spectrum of reactivity and stability [1]. Furthermore, their synthetic usefulness as synthetic intermediates, the protective groups, the chiral auxiliaries, the organocatalysts, and the metallic ligands in the asymmetric catalysts in pharmaceutical agents have rendered them multiple units of interest. Among heterocyclic compounds, five-membered rings containing nitrogen atoms constitute a vast and differentiated group with a broad spectrum of biological activity [2–4]. The members of this group, such as pyrazole, imidazole, oxazole, triazole, tetrazole, oxadiazole, thiazole, and isoxazole, are particularly important antibacterial and antifungal agents [3–5]. The pyrazole ring is a five-membered heterocycle containing two adjacent nitrogen atoms. It is a moiety found in many molecules that possess many applications. Additionally, naturally occurring pyrazoles and their synthetic derivatives are well-known to have a broad spectrum of biological properties (Figure 1). In recent years, some of the FDA-approved and commercialized drugs, including patented ones, have been developed from pyrazole derivatives (Figure 2), which implies ample usage of these groups in new-fangled bioactive molecules. This review focuses on a concise overview of the pyrazole pharmacophore synthesis and biological activities reported between 2018 and 2021. Thus, it will serve as a helpful reference guide for researchers interested in the field. This review is loosely categorized into chemical synthesis and biological applications. The first section includes the synthesis of pyrazole derivatives, and the second section describes the biological applications.

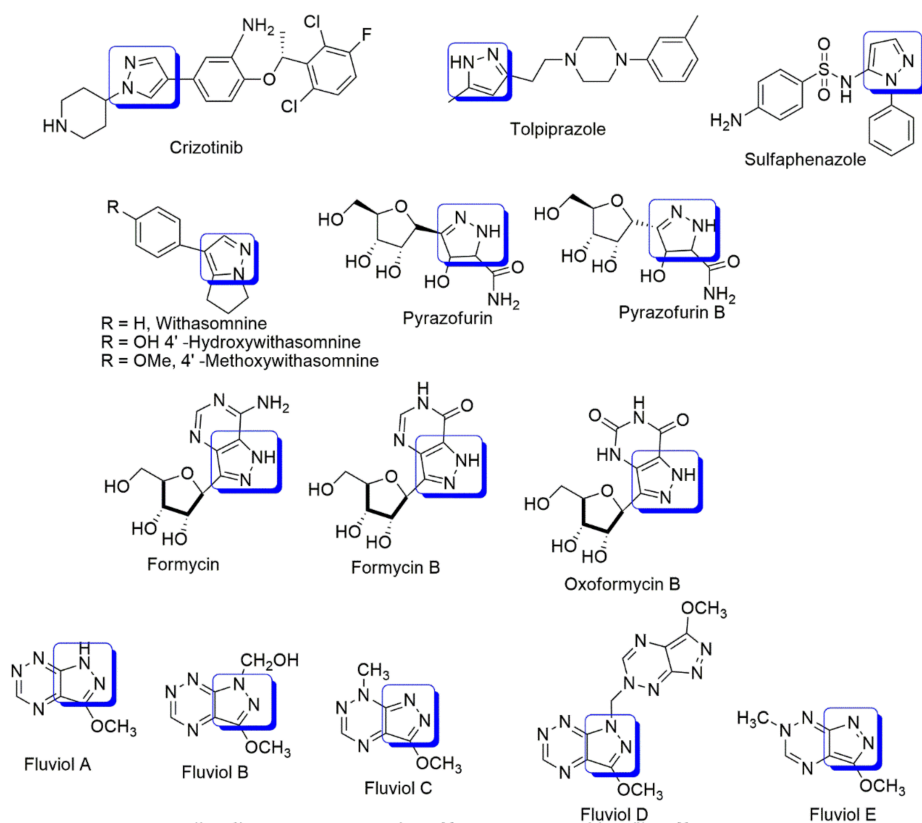


Figure 1. Naturally occurring bioactive compounds containing the pyrazole scaffold.

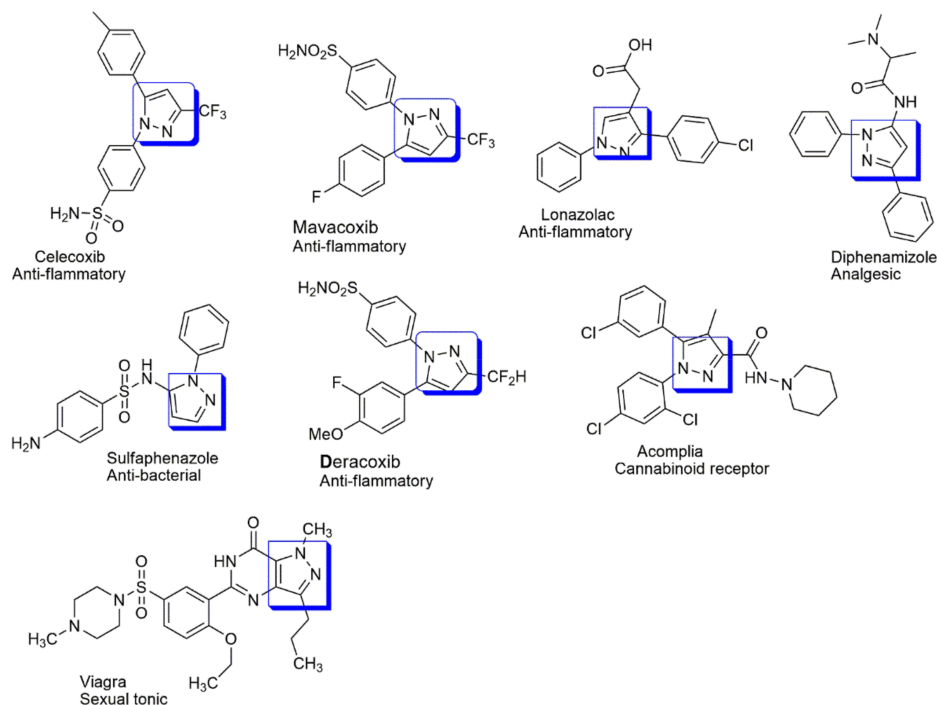


Figure 2. Some biologically active molecules containing pyrazole conjugates.

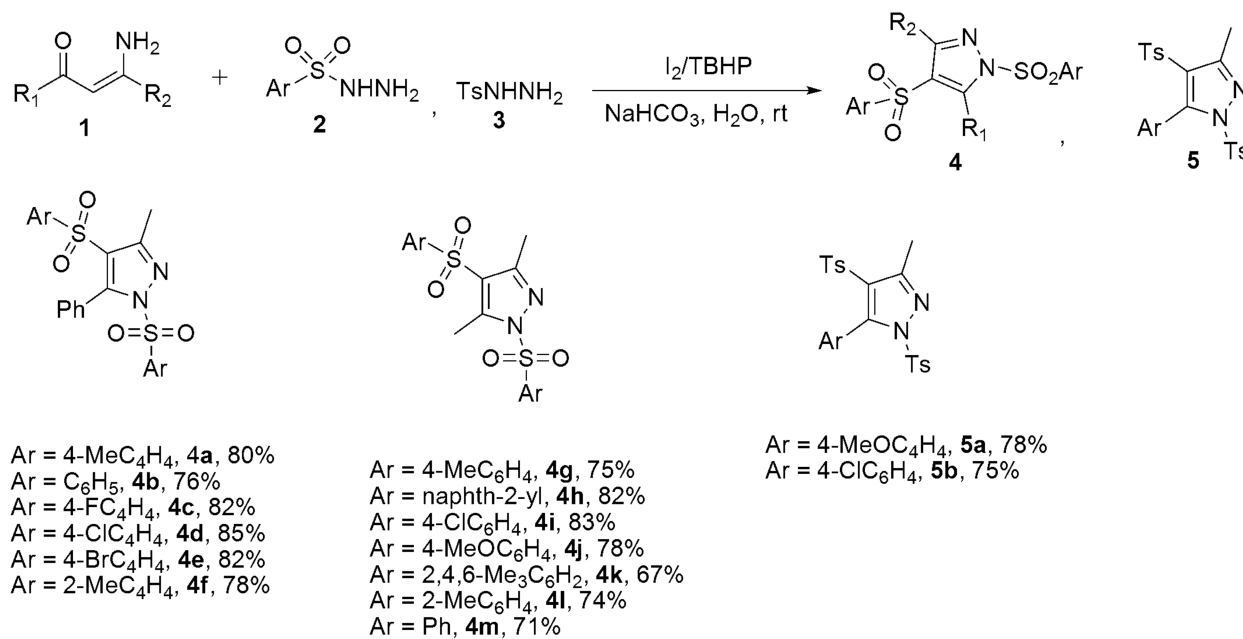
2. Synthesis of Pyrazole Derivatives

2.1. Condensation of Hydrazine's or Similar Nuclei with Carbonyl Functional Group Compounds

2.1.1. Pyrazoles from Vinyl Ketones

The tandem reactions between amine-functionalized enaminones **1** and aryl sulfonyl hydrazine or tosylhydrazone derivatives **2** and **3** in the absence of a metal catalyst have

been reported [6]. The synthesis of the substituted pyrazoles **4** and **5** occurred in water, TBHP, and NaHCO₃, respectively. In addition, when alkyl-based sulfonyl hydrazine such as methyl sulfonyl hydrazine was incorporated, the reaction was not successful. Additionally, when the reaction was carried out in EtOH and DMF, all the analogs were obtained with a good yield. The expected products with a lower yield were formed by introducing double-ethyl functionalized enaminone (R₁ = R₂ = ethyl). (see Scheme 1).

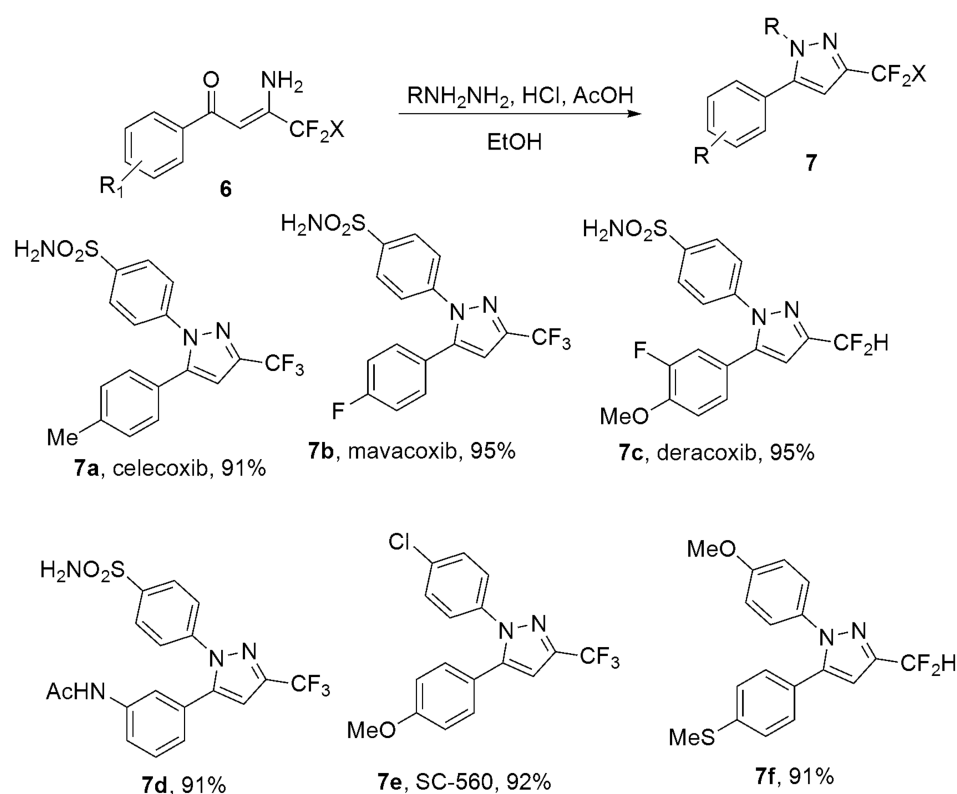


Scheme 1. Synthesis of the substituted pyrazoles using hydrazine [6].

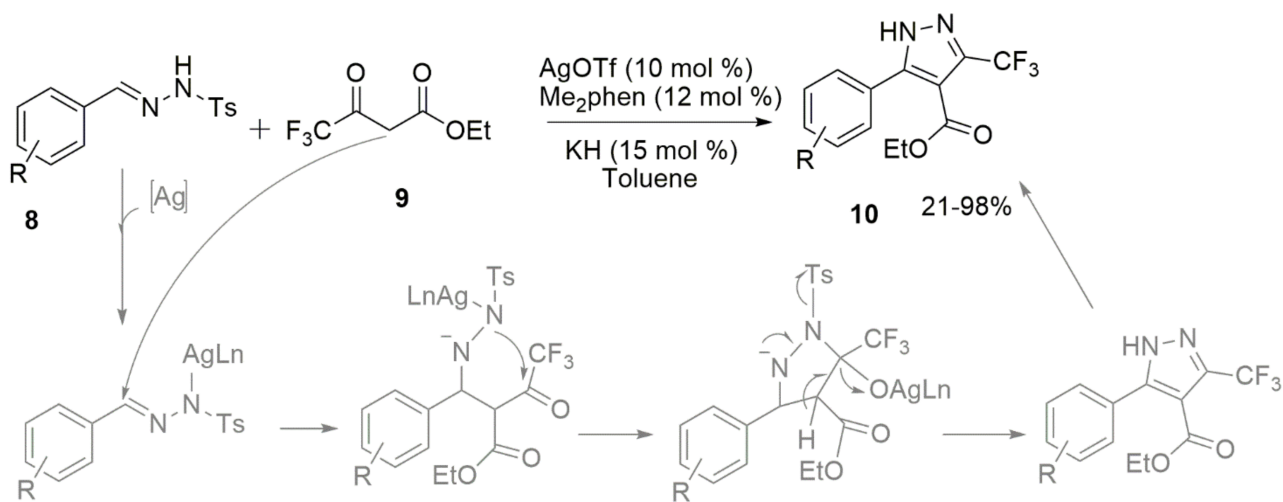
Wan et al. [7] reported a different synthetic route to forming-substituted pyrazole derivatives, including celecoxib (**7a**), mavacoxib (**7b**), and deracoxib (**7c**), respectively. The compounds were synthesized using enaminones and aryl hydrazines in ethanol with acetic acid. The reaction produced regioselective compounds with a high yield. Notably, compared to the other synthetic methods, using fluoroalkylated pyrazoles [8], β -diketones [9], and ynones [10], this method gives an excellent yield, a regioselective product. The synthetic route can be explored to synthesize pyrazole derivatives that are not easy to get from fluoroalkyl β -diketones. (see Scheme 2).

2.1.2. Pyrazoles from 1,3-Diketones

A silver-catalyzed synthesis of 5-aryl-3-trifluoromethyl pyrazoles using *N'*-benzylidene tolylsulfonylhydrazides **8** with ethyl 4,4,4-trifluoro-3-oxobutanoate **9** as precursors has been reported [11]. The reaction involved consecutive nucleophilic addition, intramolecular cyclization, elimination, and finally, [1,5]-*H* shift. This led to trifluoromethylated pyrazole derivatives **10** with moderate to excellent yields (see Scheme 3). In optimizing the product, the yield improved by increasing the reaction temperature to 60 °C, but increasing the reaction temperature above 60 °C resulted in a lower yield. The Cu(OTf)₂ transition catalyst afforded 60% yield, while Fe(OTf)₃ was unproductive. THF or dioxane gave a poor yield of the product compared to toluene. Meanwhile, K₂CO₃ was more effective than NaH, KO*t*-Bu, and NaO*t*-Bu. Additionally, the use of Me₂phen as a ligand yielded the best performance (>99%), compared to using bpy or phen as a ligand (57% or 92%).

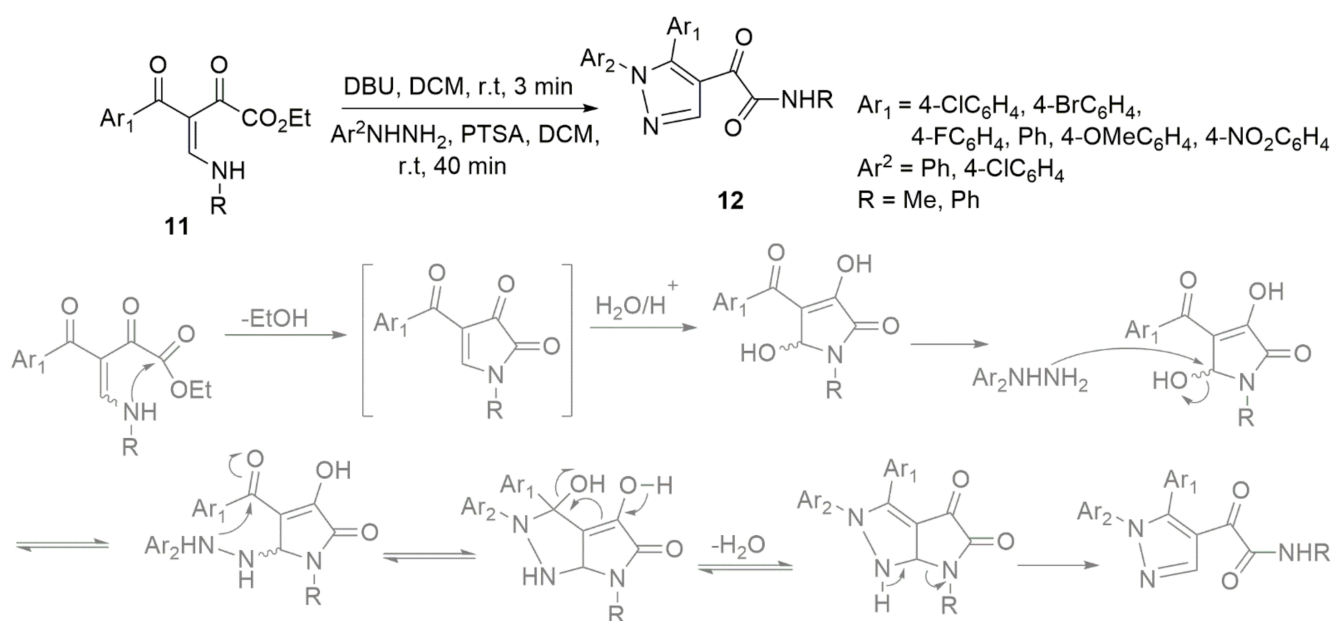


Scheme 2. Synthetic route to the formation of celecoxib, deracoxib, and mavacoxib using hydrazine [7].



Scheme 3. Synthesis of 5-aryl-3-trifluoromethyl pyrazole derivatives in the presence of a silver catalyst [11].

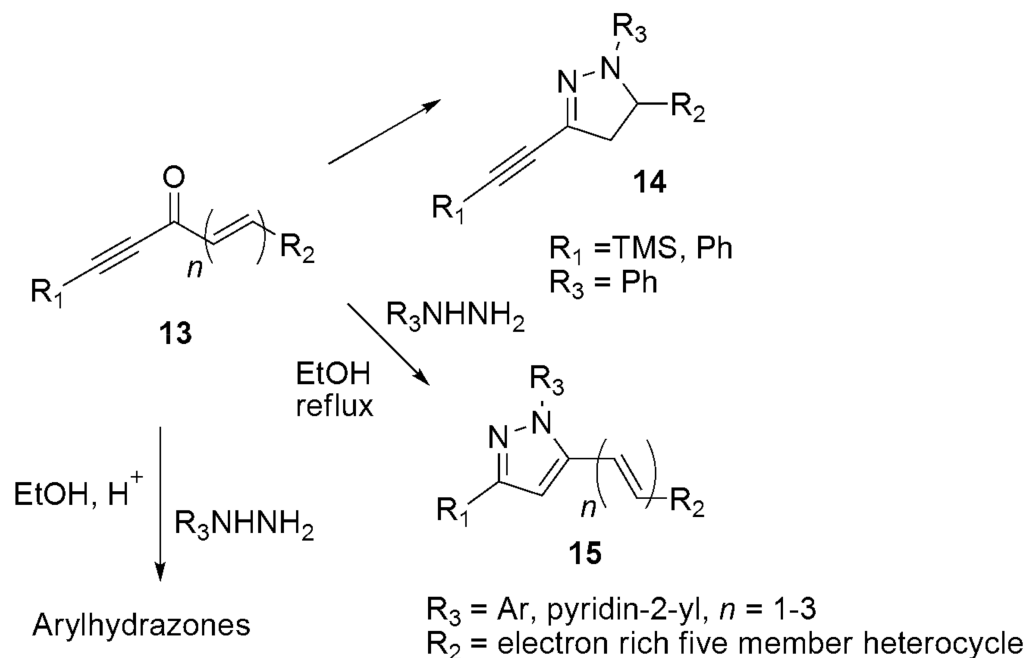
Poletto et al. [12] reported the one-pot synthetic strategy for synthesizing highly regioselective α -ketoamide *N*-arylpyrazoles **28**, the secondary β -enamine diketone, and arylhydrazines as precursors. Notably, the intermediate 4-acyl 3,5-dihydroxypyrralone, produced in situ, went through nucleophilic substitution at C-5 by arylhydrazine. Afterward, heterocyclization occurred at the carbonyl carbon of the acyl group (see Scheme 4).



Scheme 4. Synthesis of the arylpyrazoles from secondary β -enamino diketone and arylhydrazine [12].

2.1.3. Pyrazoles from Acetylenic Ketones

The merging of substrates with five electron-rich heteroaromatic nuclei interacts with arylhydrazines with the carbonyl group and triple carbon bond. The cyclo-condensation of cross-conjugated enynones **13** with hydrazines has produced pyrazole derivatives **14** and **15** in good yield [13] (see Scheme 5).



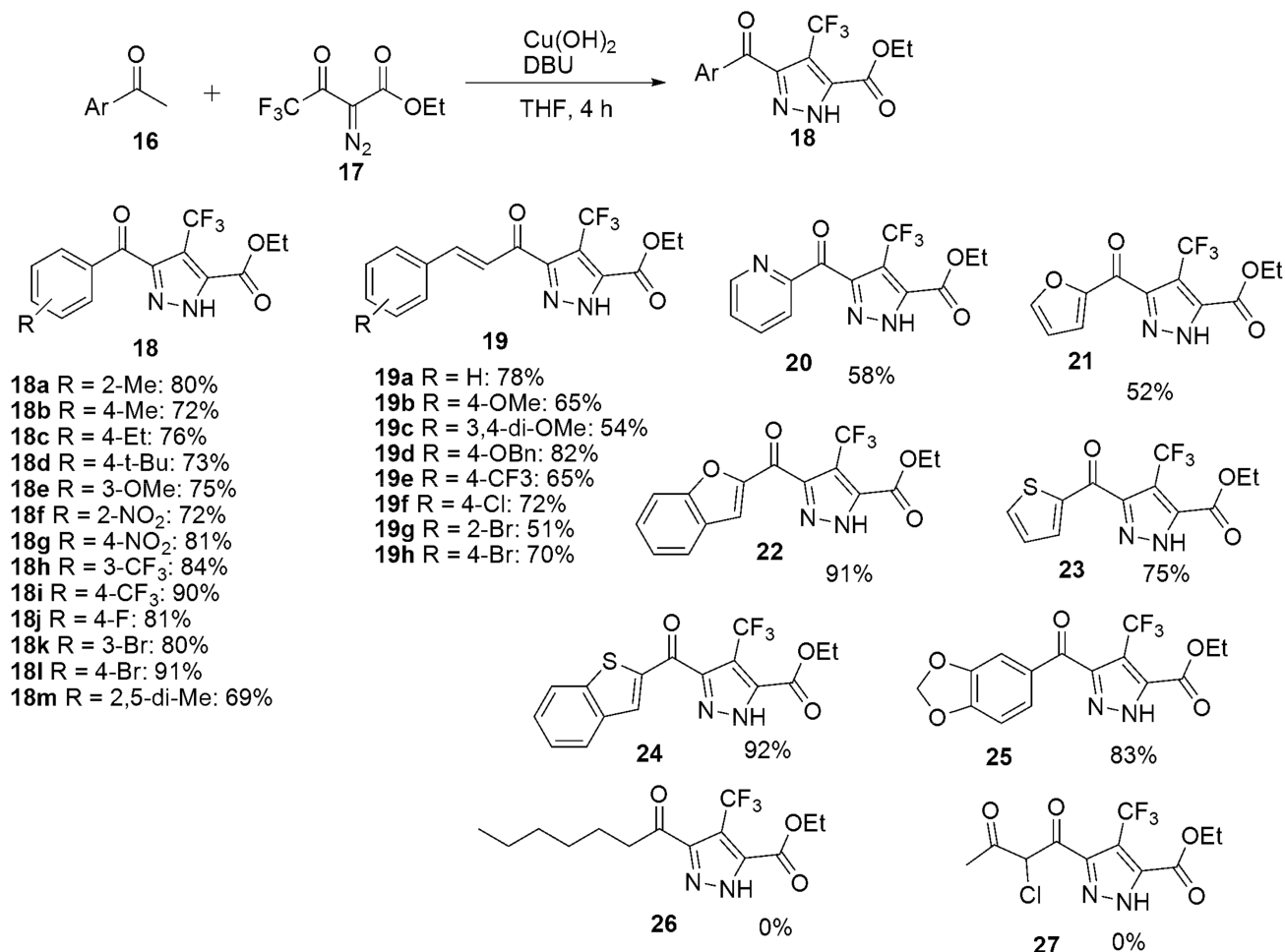
Scheme 5. Synthesis of pyrazole derivatives via the cyclo-condensation of cross-conjugated enynones with hydrazines [13].

2.2. Dipolar Cycloadditions

2.2.1. Pyrazoles from Diazoester

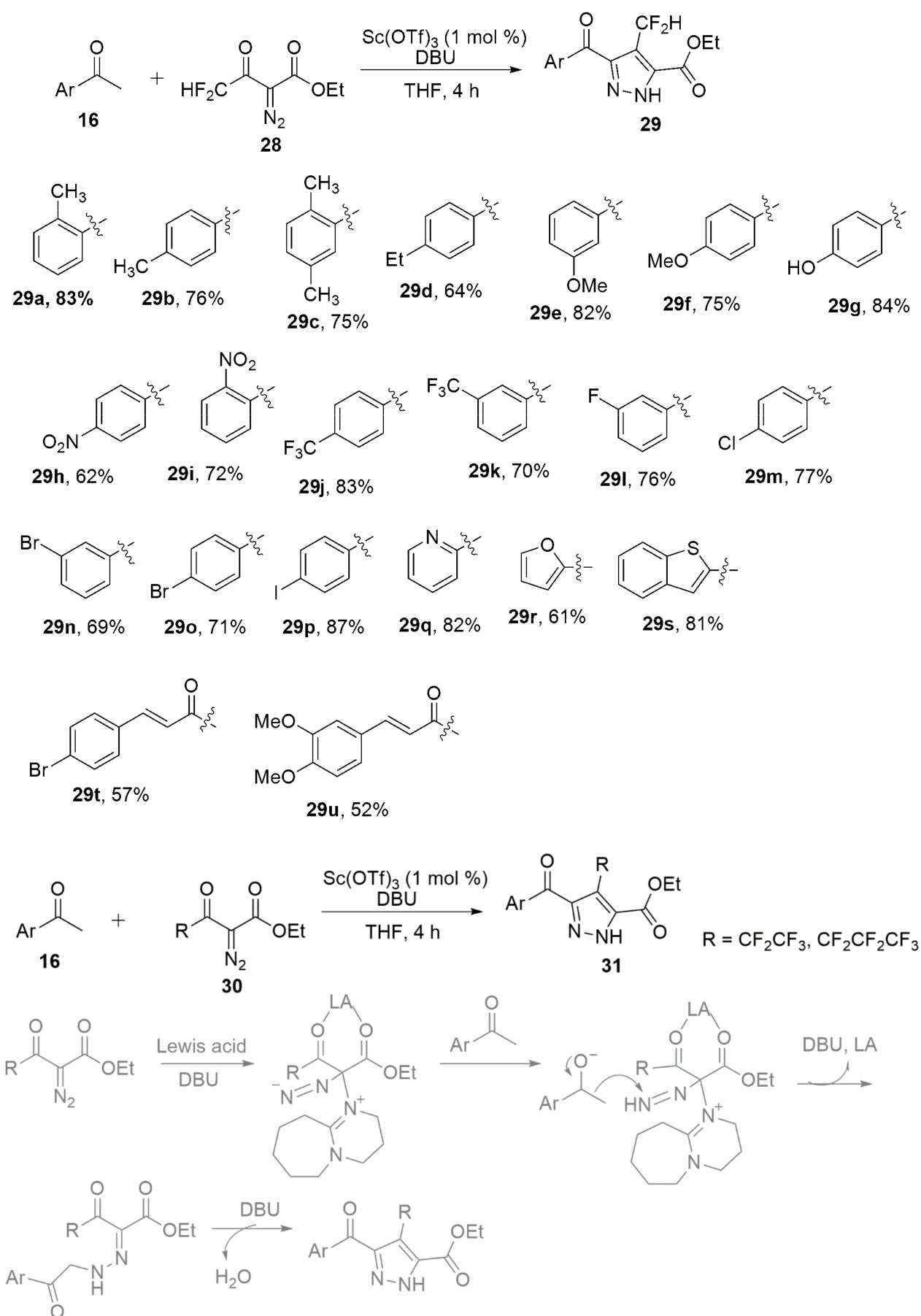
Fang et al. [14] reported the designed and synthesized polysubstituted 4-trifluoromethylpyrazoles using ketones **16** and trifluoroacetyl diazoester **17**. The ketones reacted with the terminal nitrogen atom of the trifluoroacetyl diazoester, followed by cycliza-

tion, forming 4-trifluoromethylpyrazole derivatives **18–27**. Meanwhile, the replacement of DBU with NEt_3 , NaOt-Bu , CsF , Cs_2CO_3 , and Na_2CO_3 resulted in a poor yield (see Scheme 6). Notably, dialkyl ketones did not afford the corresponding 4-(trifluoromethyl)pyrazoles **26** and **27**, using DBU and NEt_3 , which could be due to the relative lower reactivity of the α -hydrogen of dialkyl ketones.



Scheme 6. Synthesis of polysubstituted-4-trifluoromethylpyrazoles using ketones and trifluoroacetyl diazoester [14].

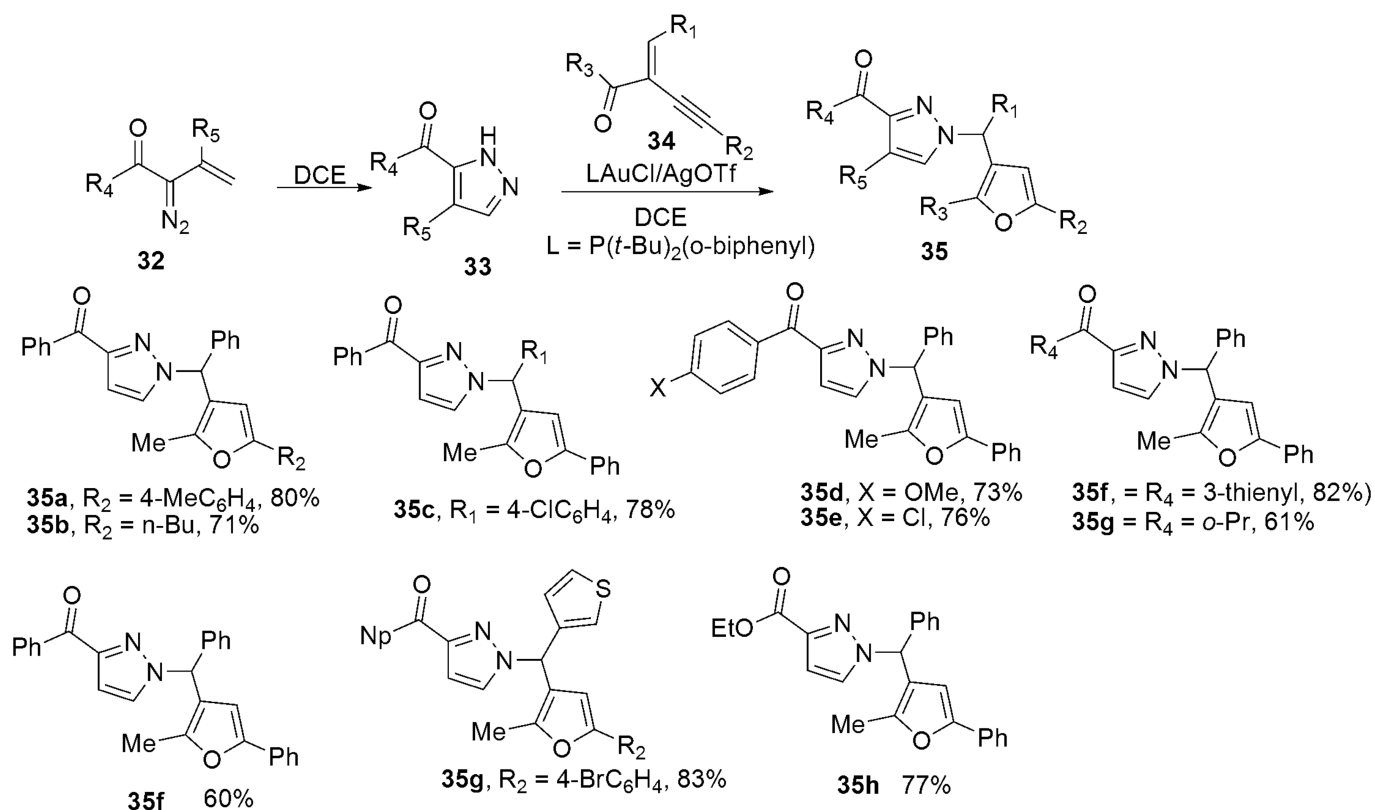
Chen et al. [15] reported a synthetic approach for synthesizing polysubstituted 4-difluoromethyl **28** and perfluoroalkyl **31** pyrazole derivatives. The authors utilized a Lewis acid and base co-mediated reaction of perfluoroacetyl diazoester with ketones (see Scheme 7). Catalysts such as $\text{Cu}(\text{OTf})_2$, CuCN , $\text{Sc}(\text{OTf})_3$, NiCl_2 , FeCl_3 , $\text{Fe}(\text{OTf})_3$, CoCl_2 , and ZnI_2 were explored for the optimization of the reaction. Particularly, the $\text{Sc}(\text{OTf})_3$ catalyst displayed the best performance with 97% yield in the presence of DBU as the base. Meanwhile, the base, such as Et_3N , $t\text{-BuOK}$, K_2CO_3 , and K_3PO_4 , did not give the expected product.



Scheme 7. Synthetic route to 4-difluoromethyl pyrazole derivatives using Sc(OTf)₃ as the catalyst [15].

2.2.2. Pyrazoles from Vinyldiazo Ketones

The synthesis of pyrazole-based triarylmethanes using 2-(1-alkynyl)-2-alken-1-ones and vinyldiazo ketones has been reported [16], as shown in Scheme 8. The first stage of the reaction involved heating vinyldiazo ketones **32** in dichloroethane, which produced 1*H*-pyrazoles **33**, followed by a reaction with enynones **34** to produce pyrazole-based triarylmethanes **35**.

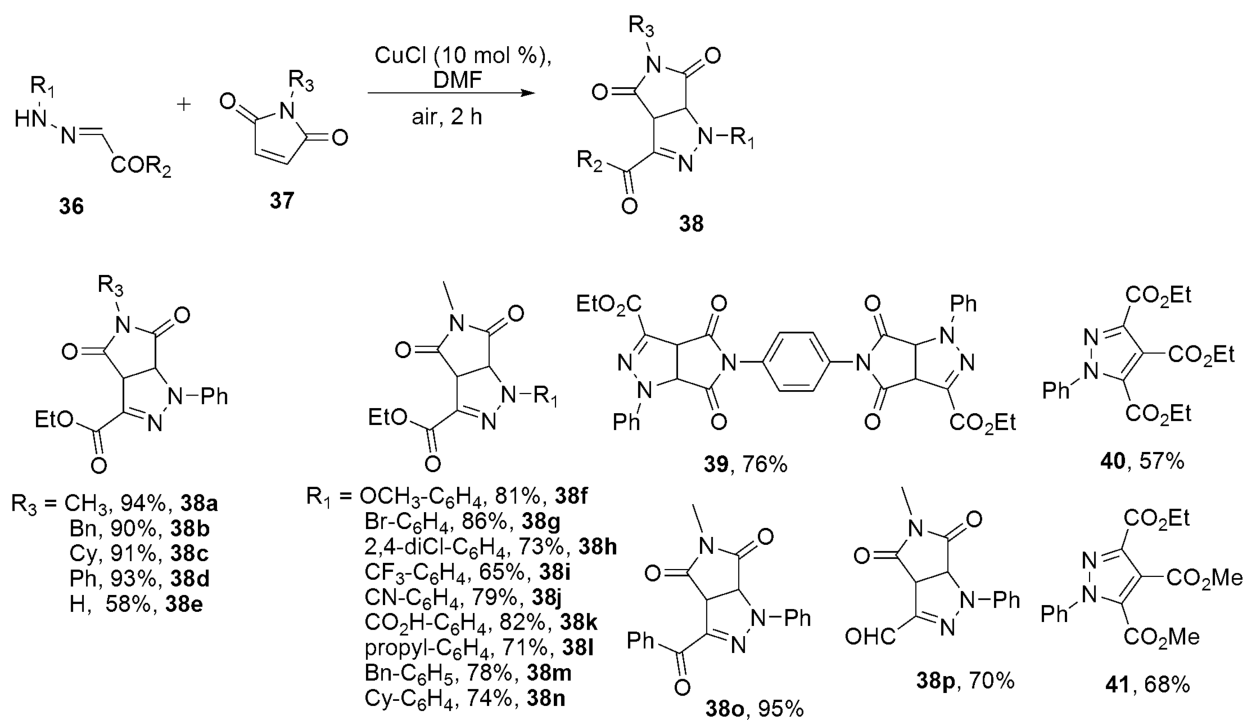


Scheme 8. Synthesis of pyrazole-based triarylmethanes using a gold catalyst [16].

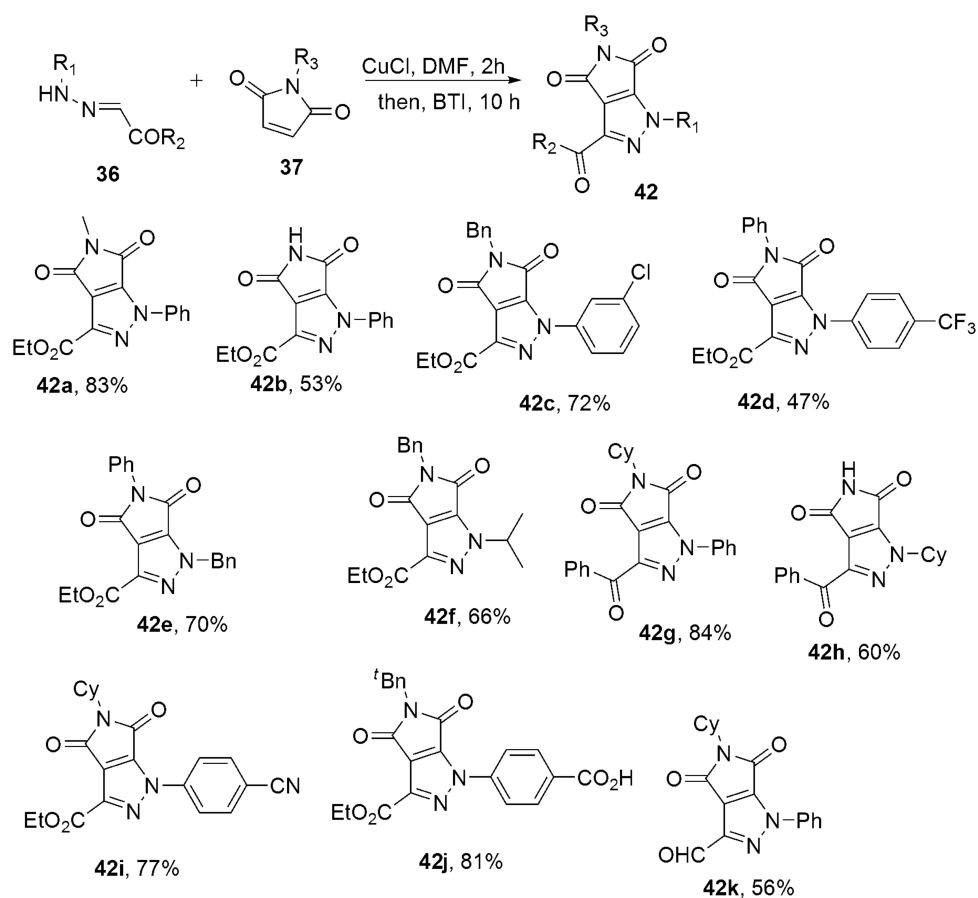
2.2.3. Pyrazoles from Hydrazones

Zhu and colleagues [17] investigated the oxidative coupling reaction of phenylhydrazone **36** and maleimide **37** to synthesize pyrazoles derivatives. The reaction was carried out with CuCl as the catalyst, and dimethylformamide (DMF) was used as a solvent (see Schemes 9 and 10). In the reaction, it produced 12% yield in the presence of 20 mol% Cu(OAc)₂ in dimethylsulfoxide (DMSO) at 80 °C for 2 h. Additionally, other Cu(II) salts did not enhance the reaction. The reaction yielded 86% when CuCl as the catalyst in DMSO was utilized, while Cu(I) salts, mainly CuOAc, CuBr, CuI, and CuSCN, led to product reduction. Moreover, catalysts such as Mn(OAc)₃, Ag₂CO₃, FeCl₃, and Pd(OAc)₂ were inefficient.

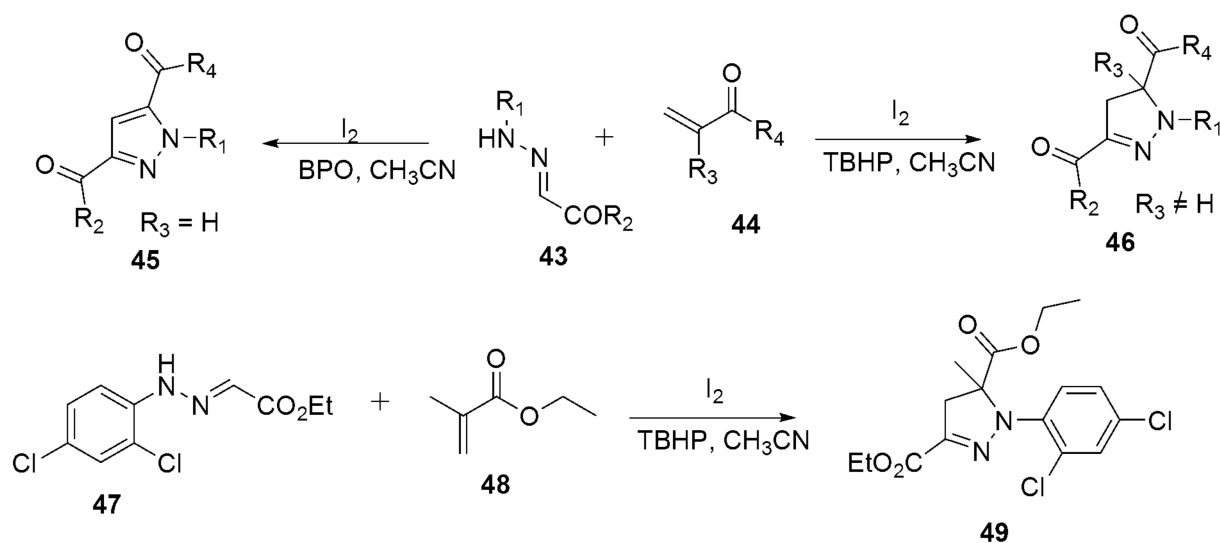
An effective protocol for synthesizing pyrazoles derivatives **46** and **49** via an iodine-catalyzed reaction of aldehyde hydrazones with electron-deficient olefins has been reported [18] (see Scheme 11). The transformation of the reaction produced a 35% yield in the presence of 20 mol% I₂ and 3.0 equiv of TBHP in DMF at 80 °C. The solvents, such as CH₃CN, displayed a moderate yield. When different oxidants were utilized, BPO displayed a superior performance up to an 81% yield compared to TBHP, K₂S₂SO₈, DTBP, BTL, H₂O₂, and *m*-CPBA. The product was reduced by replacing molecular iodine with other iodides, such as NaI, NIS, or TBAI.



Scheme 9. Synthesis of pyrazole derivatives via copper-catalyzed oxidative coupling reaction [17].

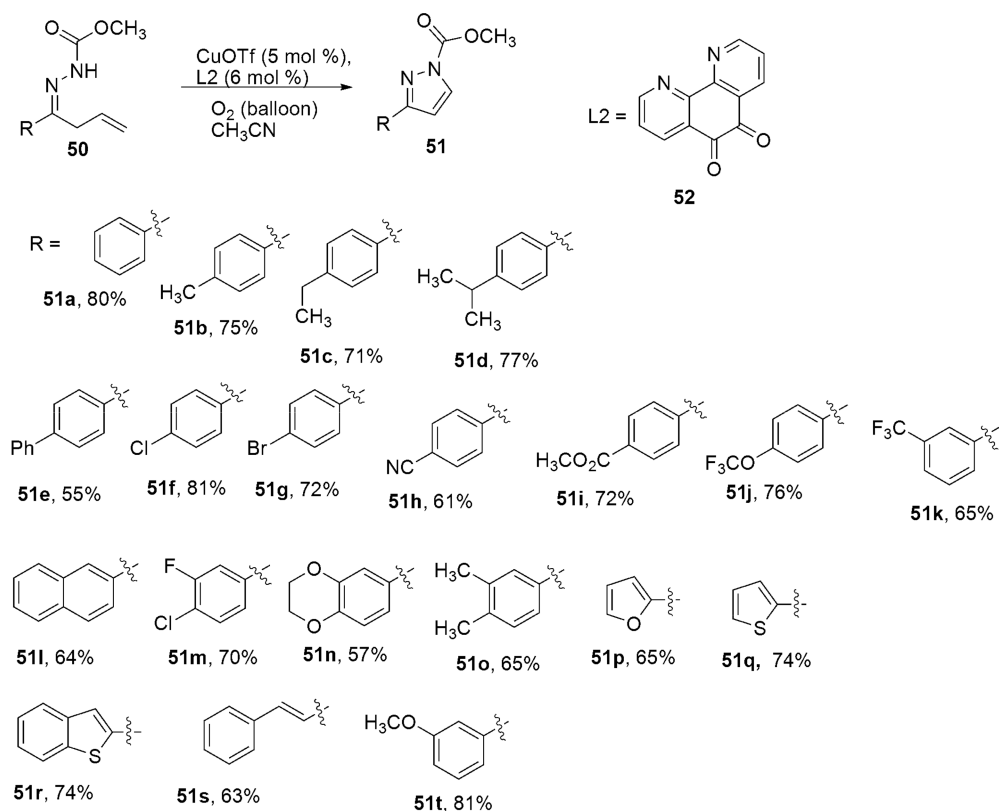


Scheme 10. Synthesis of the pyrazole derivatives from aldehyde hydrazones via a copper-catalyzed oxidative coupling reaction [17].

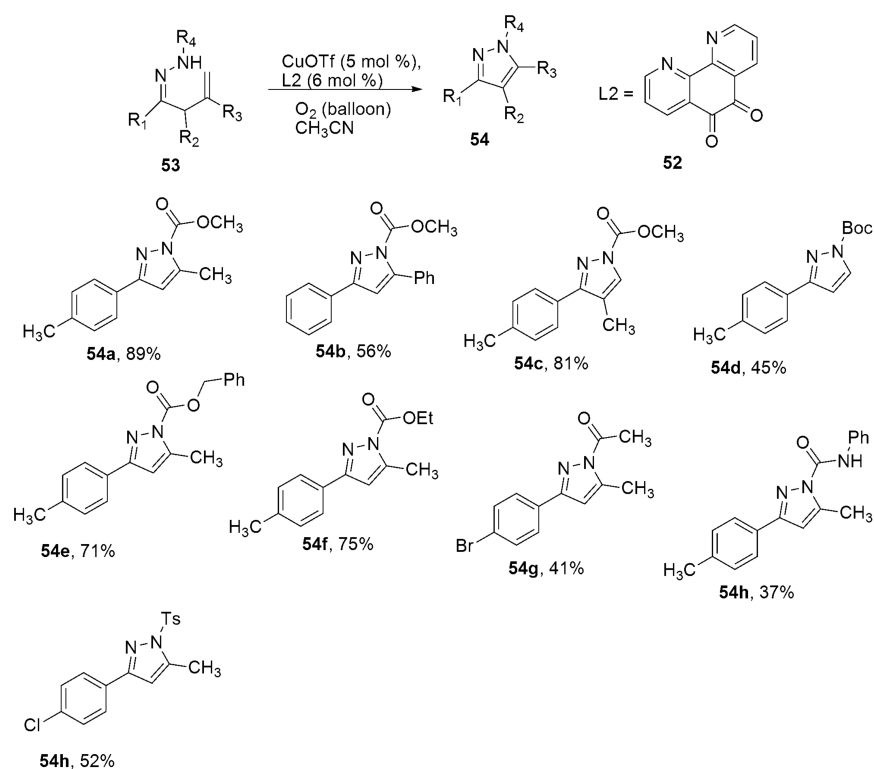


Scheme 11. Synthesizing of pyrazoles derivatives via an iodine-catalyzed reaction [18].

A facile one-pot, copper-catalyzed aerobic cyclization has been consecutively used to synthesize the pyrazole derivatives (**51** and **54**) by Fan and coworkers [19]. In this reaction, β and γ -unsaturated hydrazones were readily available substrates. While O_2 acted as the terminal oxidant and economic Cu(I) salt was used as the catalytic agent, CuOTf showed the best performance compared to other employed catalysts such as CuOAc, CuBr, Cu(acac)₂, CuOTf, and Cu(OTf)₂ (see Schemes 12 and 13).

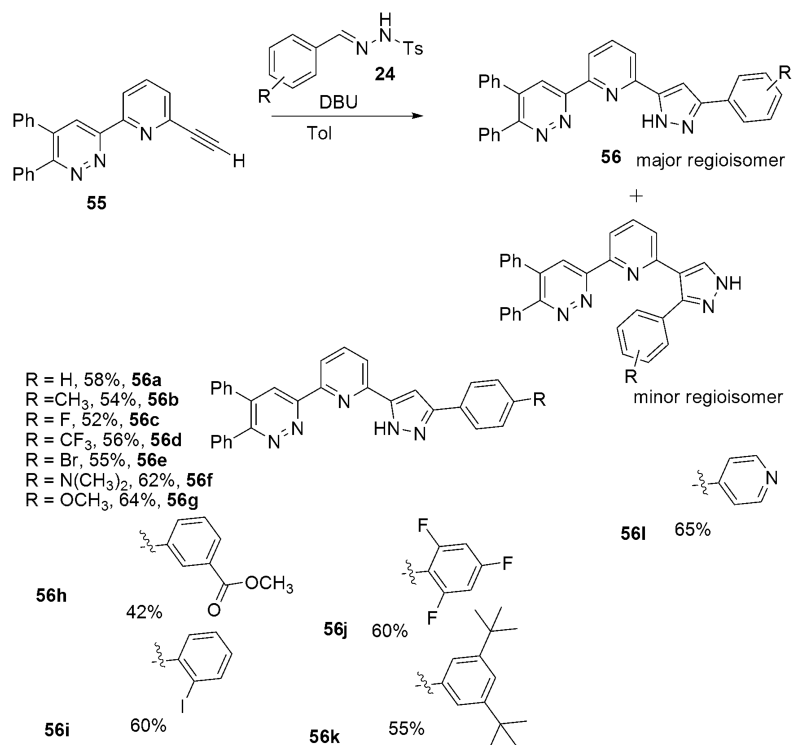


Scheme 12. Synthesis of the pyrazole derivatives in the presence of terminal oxidant and copper salt [19].



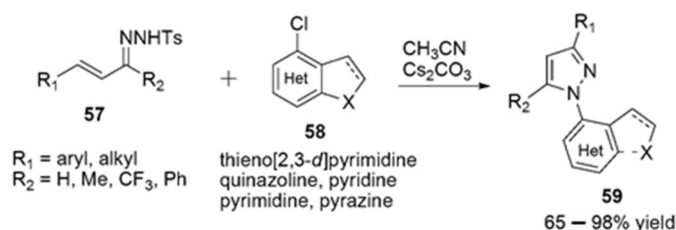
Scheme 13. Synthesis of the pyrazole derivatives from β,γ -unsaturated hydrazones [19].

The intermolecular, thermally activated, and DBU-aided [3 + 2] cycloaddition of pyridin-2-yl-[1,2,4]-triazine dipolarophiles **55** with structurally varied 4-methylbenzenesulfonylhydrazides **24** produced **57** as the major isomer with an excellent yield [20] (see Scheme 14).



Scheme 14. Synthesis of pyrazole derivatives via the dipolar cycloaddition of terminal ethynyl pyridines with tosylhydrazides [20].

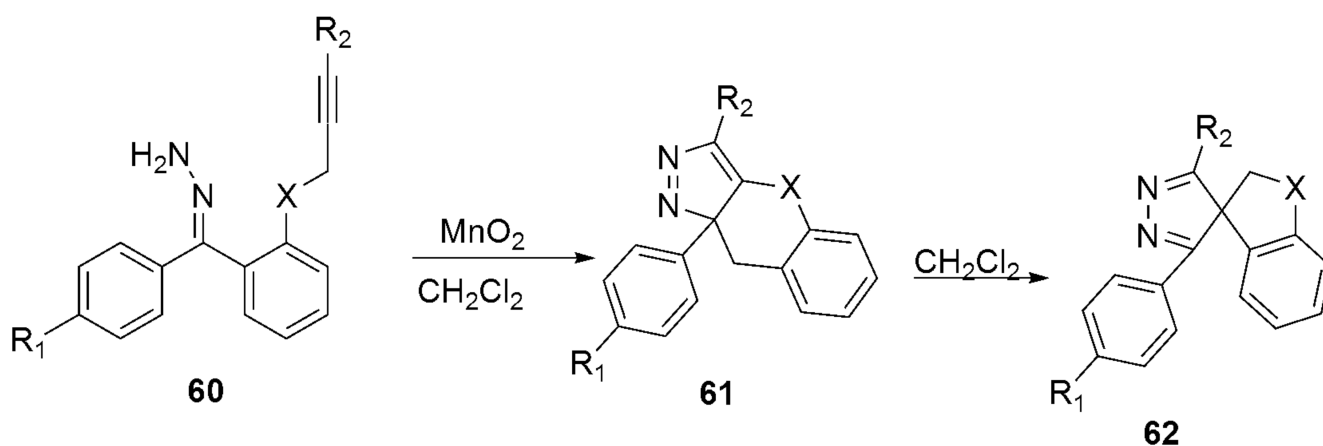
Zheng et al. [21] used a metal-free protocol to synthesize pyrazolylthienopyrimidines and other *N*-heteroaryl pyrazole derivatives **57** from α,β -unsaturated *N*-tosylhydrazones **103** and *N*-heteroaryl chlorides **58** under mild reaction conditions. The bi(heteroaryl) pyrazole derivatives were obtained in good to excellent yields (see Scheme 15).



Scheme 15. Synthesis of pyrazole derivatives from α,β -unsaturated *N*-tosylhydrazones and *N*-heteroaryl chlorides [21].

2.2.4. Pyrazoles from Diazo Intermediates and Alkynes

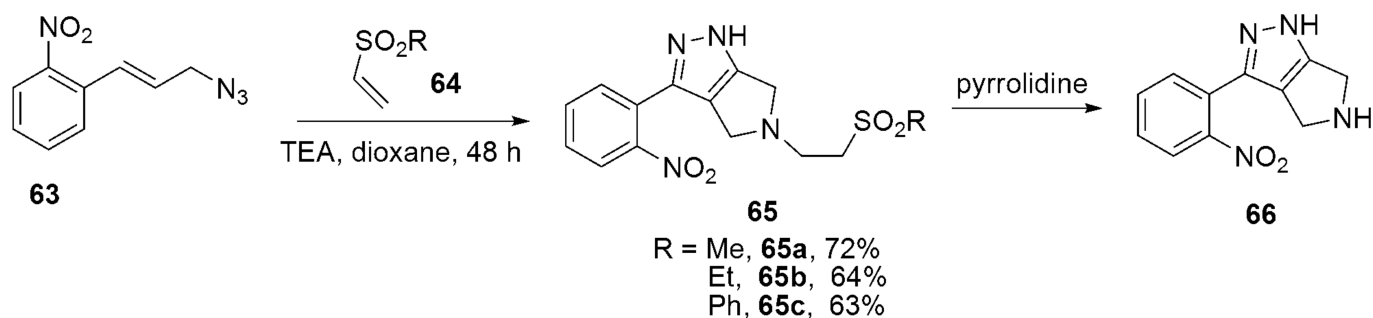
Dimirjian and colleagues [22] developed a synthetic approach for synthesizing fused pyrazoles via an intramolecular reaction. Notably, 1,3-dipolar cycloadditions of diazo intermediates with alkynes **60** produced the spirocyclic product of pyrazole derivatives **62** (see Scheme 16).



Scheme 16. Synthetic route to the formation of spirocyclic pyrazole via 1,3-dipolar cycloadditions of diazo intermediates with alkynes [22].

2.2.5. Pyrazoles from Vinyl Sulfone

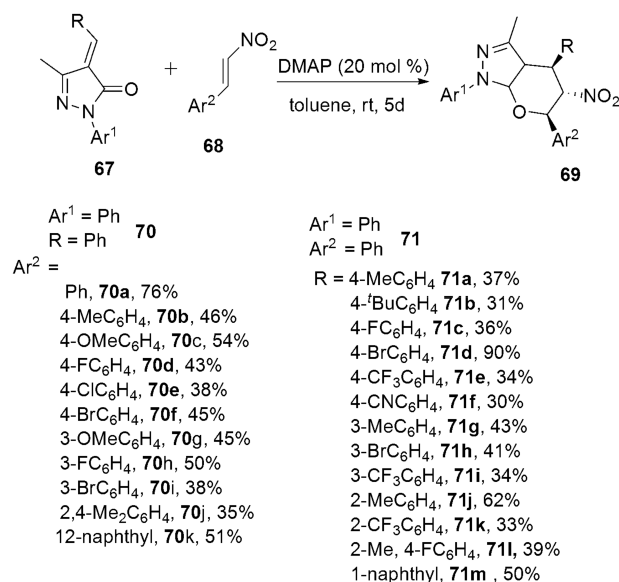
Dihydro-pyrrolo-pyrazoles have been synthesized through a cascade reaction involving cinnamyl azides and vinyl sulfones with moderate to good yields [23]. The protecting group, ethylene sulfone, can be removed by heating the product in pyrrolidine (see Scheme 17). The reaction tolerated a range of solvents such as benzene, acetonitrile, methanol, 1,3-dichloroethene, isopropanol, and dioxane. However, dioxane with triethylamine as a base produced dihydro-pyrrolo-pyrazole excellently compared to dioxane and diisopropylethylamine (DIPEA) or diisopropanolamine (DIPA).



Scheme 17. Synthesis of dihydro-pyrrolo-pyrazoles from vinyl sulfones [23].

2.2.6. Pyrazoles from Nitro-Olefins

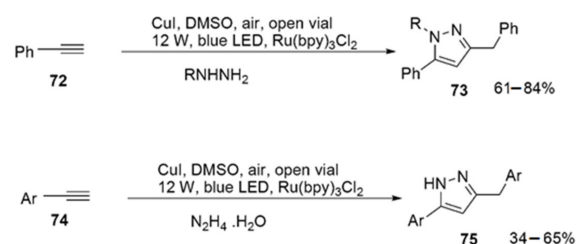
The Rauhut–Currier cyclization reaction was reported for the synthesized trisubstituted pyrazole derivatives [24]. The trisubstituted tetrahydropyrano [2,3-c]pyrazoles were obtained from the domino Rauhut–Currier cyclization reaction. The reaction occurred between alkylidene pyrazolones and nitro-olefins (see Scheme 18).



Scheme 18. Synthesis of the trisubstituted tetrahydropyrano [2,3-c]pyrazoles domino Rauhut–Currier cyclization reaction [24].

2.2.7. Pyrazoles from Alkynes

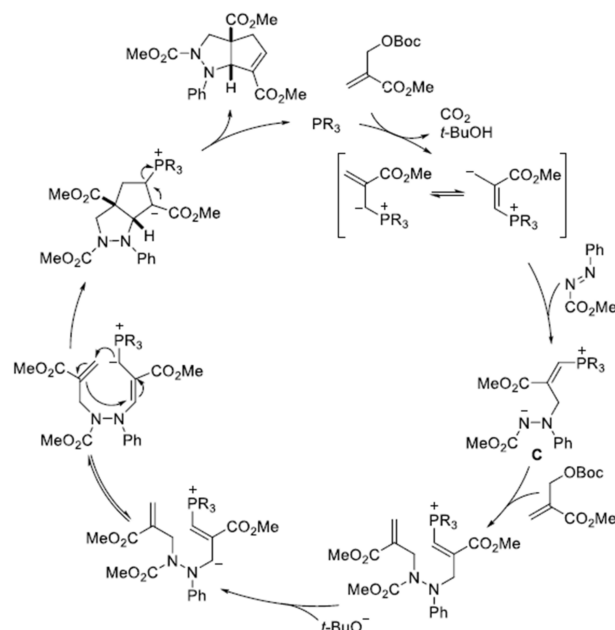
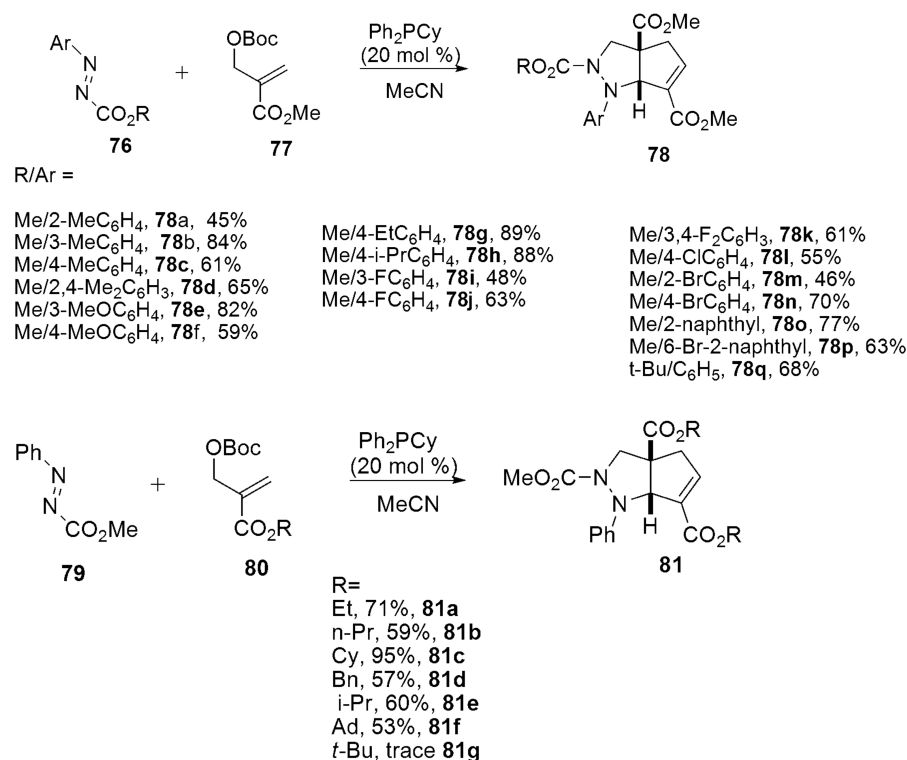
A visible light-promoted cascade of Glaser coupling/annulation alkynes and hydrazines has been utilized to synthesize polysubstituted pyrazoles **73** and **75** [25] (see Scheme 19). The replacement of CuI with CuCl, CuCl₂, Cu(OTf)₂, and Cu(OAc)₂ in the reaction using maintaining Ru(bpy)₃Cl₂ as the photocatalyst did not improve the reaction product.



Scheme 19. Synthetic route to forming polysubstituted pyrazoles from Glaser coupling/annulation of alkynes with hydrazines [25].

2.2.8. Pyrazoles from Morita–Baylis–Hillman (MBH) Carbonates

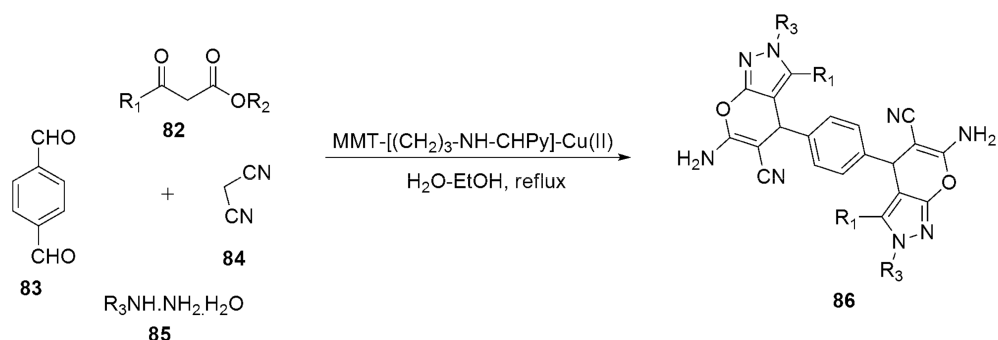
Under mild reaction conditions, phosphine-catalyzed domino Morita–Baylis–Hillman (MBH) carbonates with diazenes yielded tetrahydropyrazole-fused heterocycles **78** and **81** with moderate to excellent yields [26] (see Scheme 20). The substitution of *tert*-butyl (**81g**) with MBH carbonate was not reactive, probably due to its steric barrier. It is noteworthy that MBH carbonates derived from other aldehydes, namely benzaldehyde, did not function in this reaction.



Scheme 20. Synthesis of tetrahydropyrazole-fused heterocycles from Morita–Baylis–Hillman (MBH) carbonates [26].

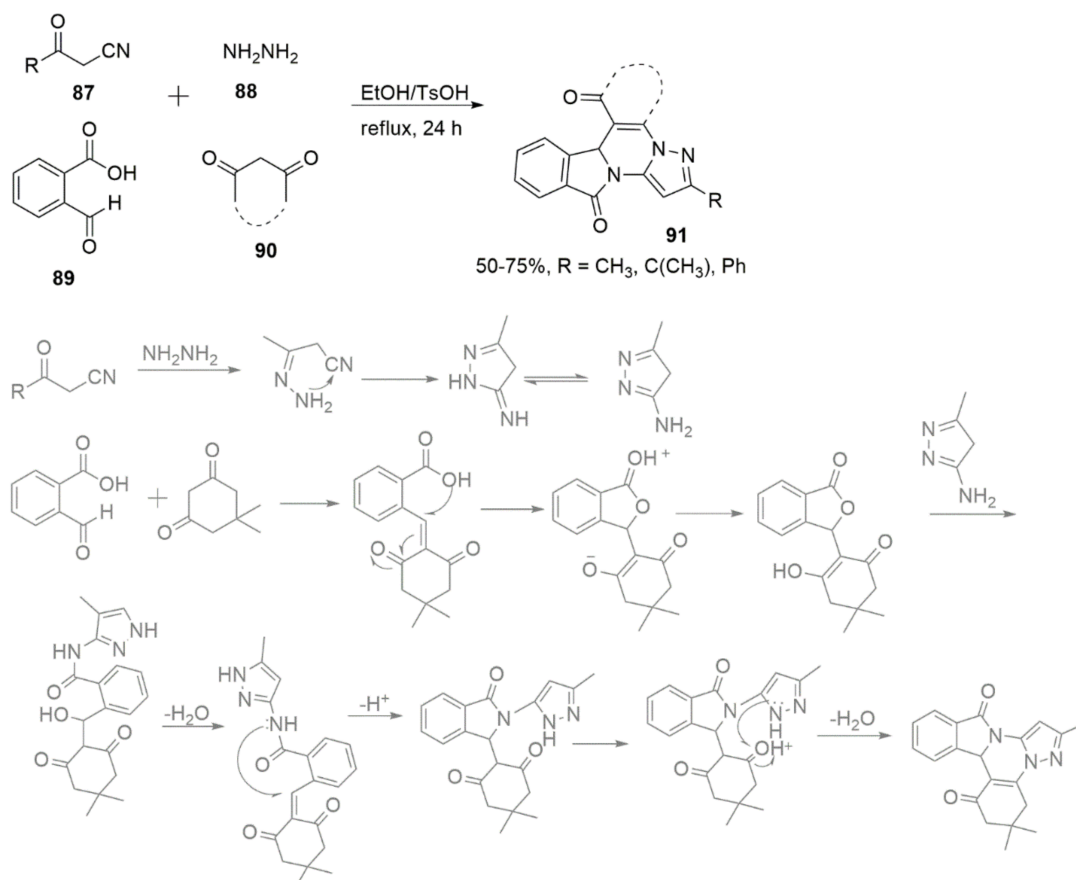
Multicomponent Strategies

A one-pot multicomponent reaction for synthesizing bispyranopyrazole **86** derivatives using MMT K10 as a support heterogeneous catalytic system has been reported [27] (see Scheme 21). Notably, the economic and environmentally friendly catalyst was recycled and reused five times in the reaction, and no lack of activity was observed.



Scheme 21. Synthesis of bispyranopyrazole under a support heterogeneous catalytic system [27].

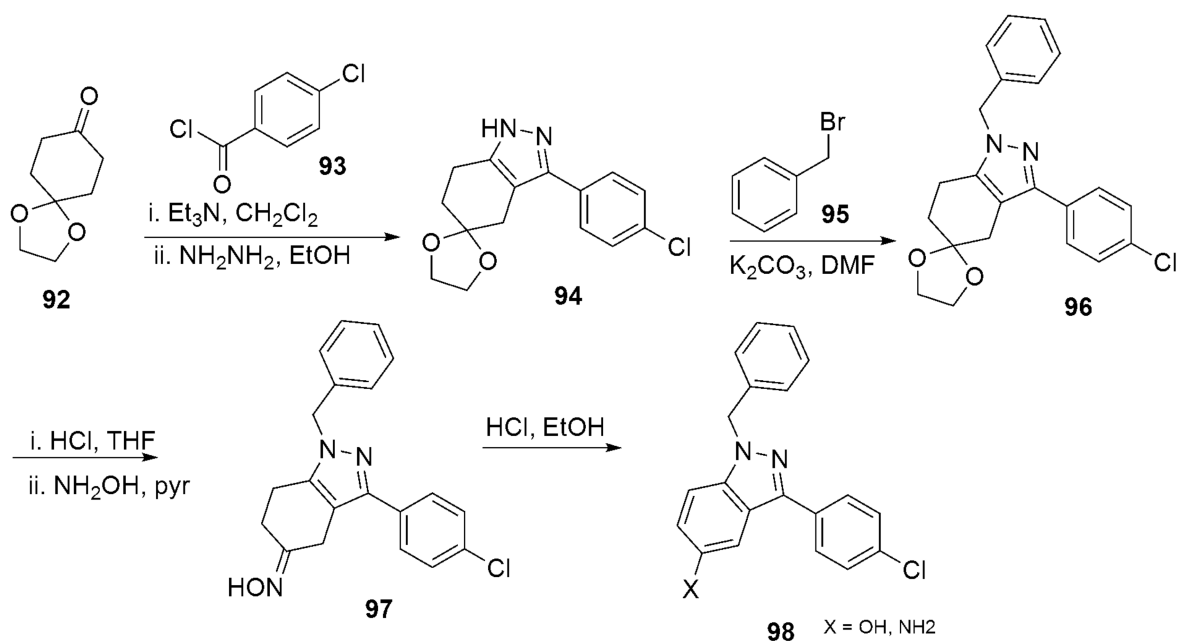
Alizadeh-Kouzehrash et al. [28] reported new *N*-fused pyrazole derivatives **91** via an efficient one-pot multicomponent reaction. Using a cheap catalyst, namely 4-toluenesulfonic and ethanol, as a green organic solvent (see Scheme 22), the best yields were reached in ethanol as a solvent under the reflux temperature, and in the absence of a catalyst, the yields percentage of reactions were reduced.



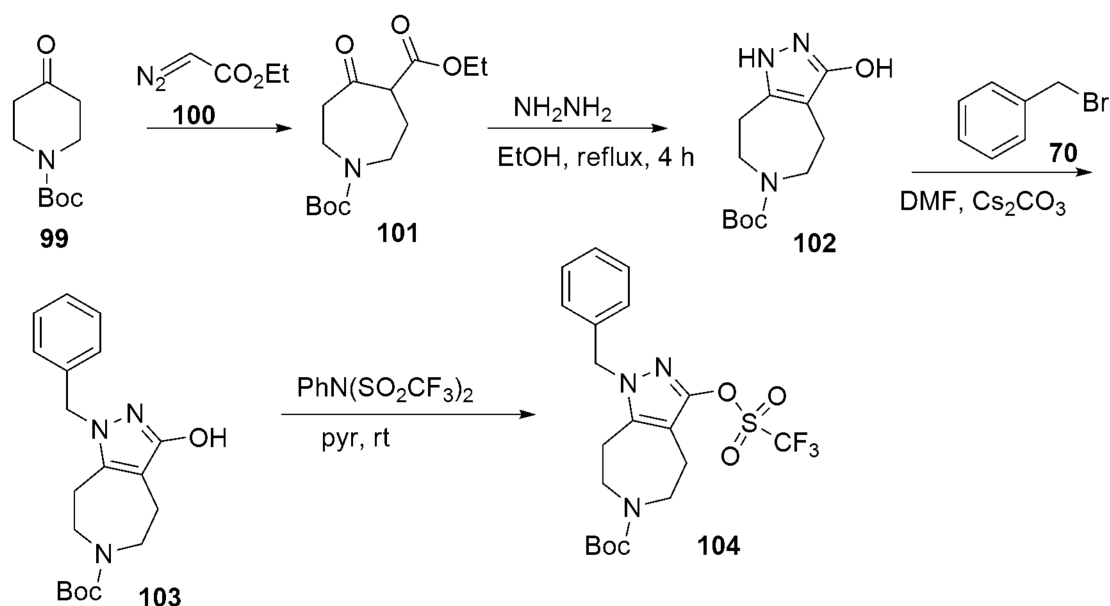
Scheme 22. Synthesis of fused pyrazole derivatives using 4-toluenesulfonic as the catalyst [28].

3. Miscellaneous

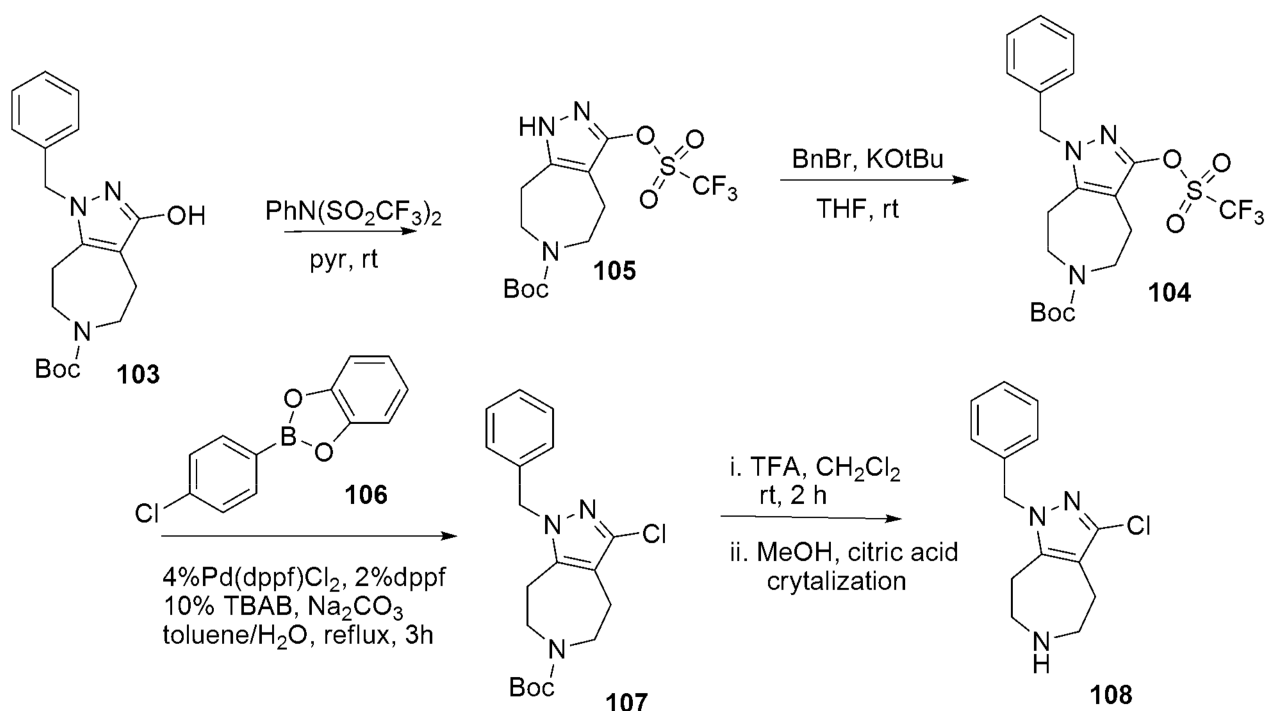
The synthetic route to JNJ-18038683 **83** and other fused pyrazole derivatives were reported by Dvorak et al. [29]. Two synthetic routes were employed to construct the fused pyrazole-azepine heterocyclic core (see Schemes 23–25). In the reaction path to pyrazole triflate **107**, a bi-phasic solvent system of toluene/water was optimal, and no triflate hydrolysis was identified. Meanwhile, the displacement of the BOC-protecting group was achieved by treating **107** with trifluoroacetic acid to give the free base of the amine. Subsequently, the free base was converted into citrate salt, and the salt formation was then performed with a free base and citric acid in methanol. The final recrystallization yielded clinical candidate **108** as a nonhygroscopic free-flow powder.



Scheme 23. Synthetic route to the formation of fused pyrazole [29].

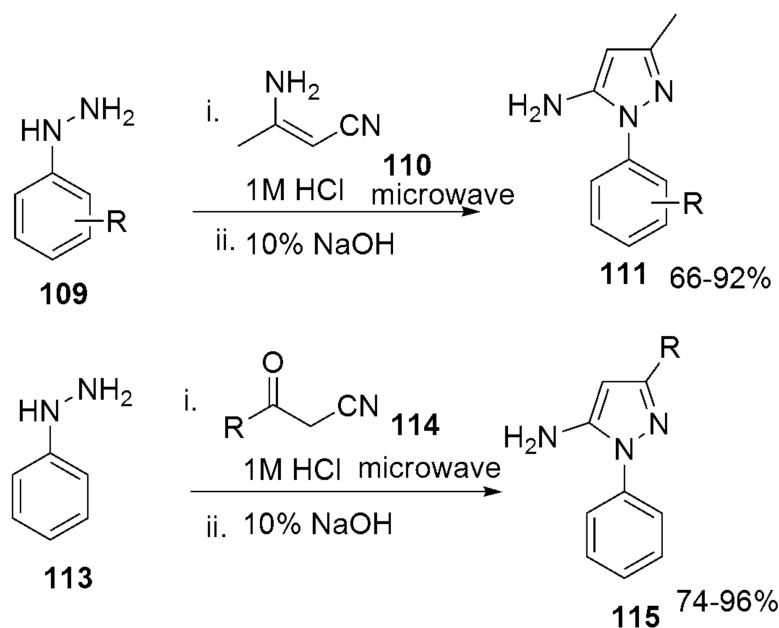


Scheme 24. Synthetic route to the formation of pyrazole triflate using *N*-phenyltriflamide in pyridine [29].



Scheme 25. Synthetic route to the formation of the JNJ-18038683 heterocyclic compound [29].

1*H*-pyrazole-5-amines were obtained from the microwave reaction of arylhydrazines **108** with 3-aminocrotonitrile **109** in moderate to excellent yields after 10 min of irradiation [30]. In addition, the reaction of phenylhydrazine **110** with α -cyanoketones **110** under similar conditions produced many functionalized 1*H*-pyrazole-5-amines. Meanwhile, the *m*-nitrophenyl and *p*-nitrophenyl-3-oxopropanenitrile substituents did not react with phenylhydrazine, even at a longer heating time. However, the reaction conditions tolerated other functionalized aromatic groups such as trifluoromethyl and methyl sulfone (see Scheme 26).



Scheme 26. Synthesis of pyrazole derivatives via the microwave reaction of arylhydrazines with 3-aminocrotonitrile [30].

4. Biological Activity of Pyrazole Derivatives

4.1. Anti-Inflammatory

Bhale et al. [31] reported synthesizing 1,3,4,5-tetrasubstituted pyrazole derivatives and their in vitro anti-inflammatory effect (see Figure 3). Compound **117a** showed excellent inhibition (93.80%) compared to the standard diclofenac sodium (90.21%) at a 1 mM concentration. El-Karim et al. [32] reported compounds **118a–118f** (edema inhibition% = 98.16%, 96.73%, 88.81%, 81.5%, 76.17%, and 76.68%, respectively) as potent candidates producing rapid onset and a long duration of anti-inflammatory activity, as well as a good safety GIT profile. Meanwhile, the analgesic evaluation revealed that **118b–118e** produced potent and long-acting analgesia accompanied by a significant inhibition of the inflammatory cytokine TNF- α level compared to the standard drugs. The inhibition in the protein denaturation of bovine albumin with IC₅₀ of 34.1 μ g/mL using diclofenac sodium as the standard drug (IC₅₀ = 31.4 μ g/mL). Out of the 15 novel compounds synthesized by Akhtar et al. [33], **123a–123d** demonstrated a significant in vitro anti-inflammatory activity, with IC₅₀ values of 71.11, 81.77, 76.58, and 73.35 μ g/mL, respectively, compared with the standard diclofenac. The benzylidene substituent attached remarkably influenced the anti-inflammatory potency. Abdellatif et al. [34] synthesized a new series of pyrazole derivatives. The inhibition efficacy of the target compounds to ovine COX-1 and human recombinant COX-2 was analyzed using an immune enzyme assay (EIA) kit. Most of the tested compounds showed high COX-2 inhibitory activity with IC₅₀ values ranging from 0.02–0.04 μ M. Meanwhile, **119a** and **119b** had the most suitable COX-2 selectivity index (SI = 462.91 and 334.25, respectively), superior to celecoxib (SI = 313.12) and indomethacin (SI = 1.37). Compounds **119a** and **119b** (SO₂NH₂ as the selective COX-2 pharmacophore) also showed the highest anti-inflammatory activity (ED₅₀ = 136 and 126 μ mol/kg, sequentially). In addition, they have the lowest ulcerogenic liability (Ulcer Index = 1.25 and 1.00, respectively), reflecting their expected safe GI profiles. Shi and coworkers [35] discovered **120** as the most potent anti-inflammatory agent (IC₅₀ = 3.17 μ M), with low toxicity and strong inhibitory NO release (inhibitory rates (IR) = 90.4% at 10 μ M). This compound also showed potent inhibition of iNOS with an IC₅₀ value of 1.12 μ M. The treatment of compound **120** on acute inflammatory models in AA rats displayed a remarkable inhibitory effect on hind paw swelling and body weight loss, comparable to the effect identified in the aspirin-treated group. Of all the compounds investigated by Sivaramakarthykeyan et al. [36], the *para*-nitrophenyl moiety linked to a pyrazole conjugate **121** (93.53 \pm 1.37%) displayed the highest anti-inflammatory activity in the anti-inflammatory assay using the protein denaturation method. This is superior to the standard, diclofenac sodium (90.13 \pm 1.45%). Nayak et al. [37] revealed that compound **122a** showed remarkable sodium and celecoxib, which showed IC₅₀ values of 55.65 and 44.81 μ g/mL, respectively. The potent compounds were further evaluated for their in vitro COX-2 inhibitory activities using an enzyme immunoassay. Compound **123d** demonstrated able selectivity toward COX-2 with a selectivity index (SI) of 80.03 compared with the standard celecoxib, with an SI of 95.84. Dimmito et al. [38] reported that compound **124a** displayed a good analgesic effect after subcutaneous and intracerebroventricular management in vivo. Additionally, **124a** showed an excellent anti-inflammatory effect after subcutaneous administration, indicating prospective activity at the periphery. Harras and colleagues [39] synthesized a series of pyrazole derivatives and evaluated their in vitro COX-1/COX-2 inhibition and in vivo anti-inflammatory activity using the carrageenan rat paw edema model. It was noted that the targeted compounds exhibited more potent inhibitory activity against COX-2 than COX-1. Meanwhile, all compounds' selectivity indexes (SI) were analyzed and compared to celecoxib (SI = 8.17). Compounds **125a** and **125b** displayed an outstanding COX-2 selectivity index of 8.22 and 9.31, respectively. Meanwhile, the histopathological investigation of the rats' stomach, liver, and kidneys revealed that **125a** and **125b** triggered minimal degenerative changes, suggesting these derivatives' safety. Sivaramakarthykeyan et al. [40] reported the anti-inflammatory activity of the pyrazole derivatives. The derivative, lacking substitution on the aryl entity **126**, exhibited the highest anti-inflammatory profile. Ab-

dellatif et al. [41] synthesized a series of substituted pyrazole derivatives. The targeted compounds were screened for their COX-1/COX-2 inhibitory activity. Additionally, the carrageenan-induced rat paw edema model and histopathological study were demonstrated to examine their anti-inflammatory effectiveness and gastric safety. Compound **127** was the most potent anti-inflammatory agent ($ED_{50} = 65.6 \mu\text{mol/kg}$) compared to the reference drug, celecoxib ($ED_{50} = 78.8 \mu\text{mol/kg}$). In addition, the potent compound possessed minimum ulcerogenic (Ulcer Index = 7.25) Figure 3.

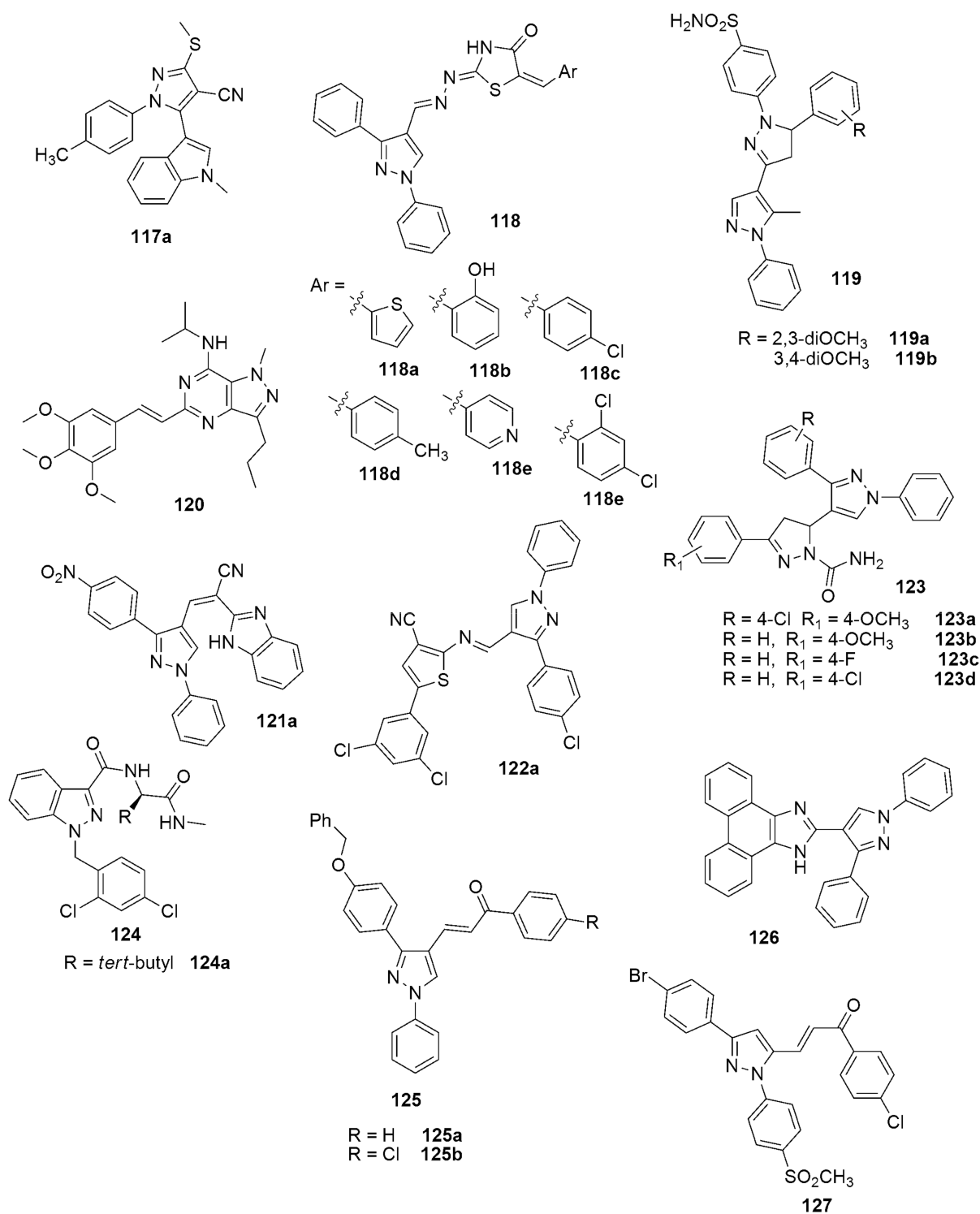


Figure 3. Structures of pyrazole derivatives with anti-inflammatory activity.

A new series of thiazolidindione **128** and thiazolidinone **129** containing a pyrazole core has been synthesized as hybrid structures [42]. The synthesized compounds were further evaluated for COX-1/COX-2 in vitro anti-inflammatory activity and ulcerogenic liability (Figure 3). The most COX-2-selective derivatives **128a** and **128b** and **129a** and **129b** showed the highest anti-inflammatory activities and the lowest ulcerogenic. Among the potent compounds, the thiazolidindione with a methoxy substituent **129b** displayed excellent activity against COX-2 ($IC_{50} = 0.88 \mu\text{M}$) with the highest COX-2 selectivity index ($SI = 9.26$). While compound **128c** with a methoxy substituent displayed the highest potent inhibitory against COX-2 ($IC_{50} = 0.62 \mu\text{M}$) with the highest COX-2 selectivity index ($SI = 8.85$). The highest anti-inflammatory (AI) activities were observed in **129a** and **128b** (after 1 h, AI = 82.34 and 81.15%; after 3 h, AI = 79.00 and 97.68%; and after 5 h, AI = 80.15 and 97.68%, respectively). Additionally, **128a** was slightly more potent ($ED_{50} = 79.12 \mu\text{mol/kg}$) than celecoxib ($ED_{50} = 82.2 \mu\text{mol/kg}$), while **128b** showed a superior ED_{50} value of $5.63 \mu\text{mol/kg}$ with a more than 14-fold effectiveness of celecoxib. Some pyrazolopyrimidine hybrids were prepared using Schiff base by Abdelall and coworkers [43]. All the synthesized compounds were evaluated in vivo against carrageenan-induced rat paw edema as anti-inflammatory agents. Regarding the anti-inflammatory activity compounds, **130** and **131** showed excellent activity compared to celecoxib. Thangarasu et al. [44] reported the anti-inflammatory effect of pyrazole moieties, and compound **132b** was found to have dominated activity potentials with an IC_{50} value of 3.5 nM in the COX-2 inhibition studies.

Murahari et al. [45] designed and synthesized novel pyrazole-based derivatives using the ligand-based approach. Among the synthesized compounds, **133** showed excellent in vivo anti-inflammatory activity with 0.8575 mmol/kg as ED_{50} . The design and synthesis of novel thiophene–pyrazole hybrids have been investigated [46]. The thienopyrimidine analogs **134a–134b** and the thiophene derivative **135** are promising non-toxic, gastrointestinal-safe anti-inflammatory candidates with good oral bioavailability and physicochemical properties. A series of 1,2,3-triazole-linked 3-(1,3-diphenyl-1*H*-pyrazol-4-yl)acrylates was synthesized following a multi-step reaction [47] (Figure 4). Three of the evaluated compounds demonstrated significant anti-inflammatory activity, with IC_{50} values of 60.56, 57.24, and 69.15 $\mu\text{g/mL}$ for compounds **136a–13c**, respectively, comparable to the standard diclofenac sodium with an IC_{50} value of $54.65 \mu\text{g/mL}$.

Taher and colleagues [48] reported the synthesis and pharmacologic evaluation of novel pyrazole and pyrazoline derivatives. The study presents the effect of lengthening the carbon chain in different pyrazole derivatives bearing various amine moieties. Their results showed that lengthening of the aliphatic chain in **137a–137c** (26.19%, 30.95%, and 28.57%, respectively) led to higher activity. Meanwhile, the cyclization of chalcones into pyrazolines were more potently anti-inflammatory in compounds **138**, **139a** and **139b** (21.43%, 26.19%, and 28.57%). Compounds **138** and **140** exhibited the highest analgesic activity among all the examined compounds (75.9% and 84.5%, respectively). Mustafa et al. [49] presented a novel series of celecoxib derivatives. The in vivo anti-inflammatory activity of the synthesized compounds was evaluated using celecoxib as a reference standard by the paw oedema model on albino Wistars. Most of the compounds showed higher in vivo anti-inflammatory activity compared to celecoxib. Different substituents on the triazole moiety played a crucial role in the percentage inhibition of anti-inflammatory effects at 1h. Derivatives with chlorine atoms **141a–141d** and the nitro derivative **141e** showed good anti-inflammatory potency (Figure 4). A series of novel benzophenones conjugated with an oxadiazole sulfur bridge pyrazole has been designed, synthesized, and characterized [50]. It was afterward evaluated for anti-inflammatory and analgesic effects. Among the series, compound **142** (65.38% edema inhibition) with an electron-withdrawing group (fluoro) at the *para* position of the benzoyl ring of benzophenone was characterized by great activity compared to the standard drug. The analgesics activity data also revealed that compound **142** was the highest potent compound among the compounds evaluated for an analgesic effect on the acetic acid-induced writhing response and thermal pain (see Figure 4).

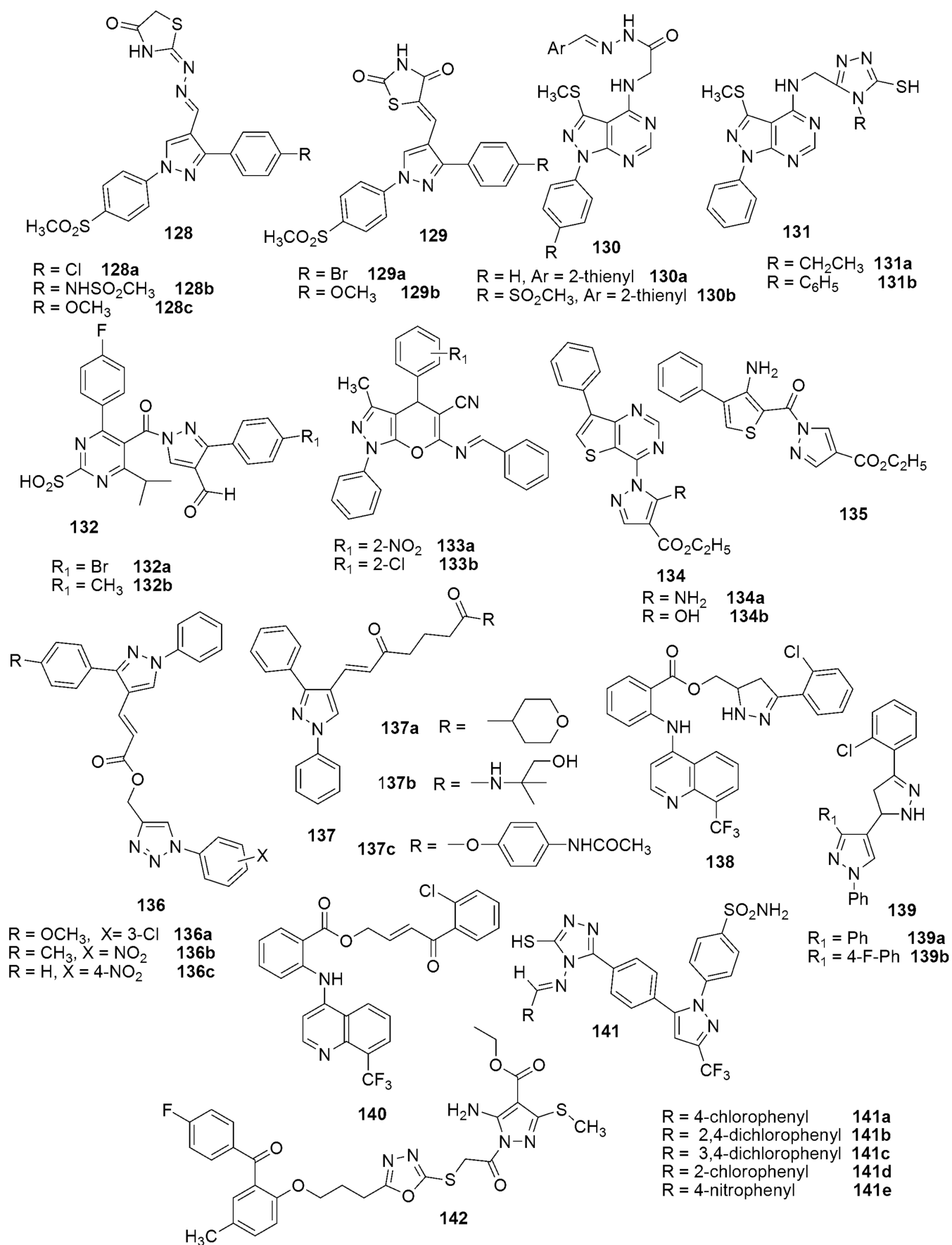


Figure 4. Structures of the pyrazole derivative with anti-inflammatory activity.

A novel series of pyrazole hybrids, such as pyrazole-thiohydantoin and pyrazole-methylsulfonyl, was synthesized by Abdellatif et al. [51]. The hybrids were evaluated *in vivo* for their anti-inflammatory activity (Figure 5). Compounds **143a–143d** were found to have the most active anti-inflammation. The unsubstituted **143b** and **143d** showed comparable ED₅₀ (78.90 and 88.28 µmol/kg) with celecoxib (ED₅₀ = 78.53 µmol/kg), while the methoxy-substituted compounds **143a**, **143c**, and **143e** (ED₅₀ = 62.61, 55.83, and 58.49 µmol/kg, respectively) showed superior activity to celecoxib. Thirteen pyrazole derivatives were synthesized and evaluated for their anti-inflammatory activity (*in vitro* and *in vivo*) and ulcerogenic liability [52]. Nine compounds **144–146** exhibited a moderate to high edema inhibition percentage (78.9–96%) than celecoxib (82.8%). Additionally, they were found to have potent COX-2 inhibitory activity, with the IC₅₀ values ranging from 0.034 to 0.052 µM. Compound **145a** was the benign pyrazole with respect to the ulcerogenic effect (UI = 0.7) on the stomach, which may be ascribed to its high COX-2 enzyme selectivity (SI = 353.8), while compounds **144a**, **145b**, and **146a–c** exhibited ulcer index values (UI = 0.8–2) comparable to celecoxib. Sulphonyl derivatives **147** and **148** have been reported to be selective for the COX-2 isozyme with COX-2 selectivity indexes of 9.78, 8.57, 10.78, and 10.47, respectively, compared to celecoxib (S.I. = 8.68) [53]. Meanwhile **147** and **148** were observed as excellent anti-inflammatory derivatives with ED₅₀ = 51.51, 46.98, 53.65, and 54.45 µmol/kg better than celecoxib (ED₅₀ = 76.09 µmol/kg). Gedawy et al. [54] reported novel pyrazole sulfonamide derivatives as dual COX-2/5-LOX inhibitors. The benzothiophen-2-yl pyrazole carboxylic acid derivative **149** showed the most potent analgesic and anti-inflammatory activity superior to celecoxib and indomethacin. It showed potent COX-1, COX-2, and 5-LOX inhibitory activities, with IC₅₀ of 5.40, 0.01, and 1.78 µM, respectively, showing a selectivity index of 344.56 superior to the reference standards (see Figure 5).

A new pyrazole sulfonate series has been reported [55]. Among the series, 4-iodophenyl 5-methyl-3-(*p*-tolyl)-1H-pyrazole-1-sulfonate **150a** and phenyl 5-methyl-3-(4-(trifluoromethyl)phenyl)-1H-pyrazole-1-sulfonate **150b** displayed superior anti-inflammatory activity (% inhibition of auricular edemas = 27.0 and 35.9, respectively); while the *in vivo* analgesic activity of **150c** and **150d** was more effective with an inhibition of 50.7% and 48.5% separately, and compounds **150a**, **150c**, and **150d** were identified as selective COX-2 inhibitors (SI = 455, 10,497, and >189, respectively). In addition, the acute oral toxicity *in vivo* analysis showed lethal doses of 50 (LD₅₀) of **150a** and **150d** to mice to be more than 2000 mg/kg. A novel series of 1,5-diaryl pyrazole-3-carboxamides was synthesized and evaluated against COX-1, COX-2, and sEH enzymes as dual COX-2/sEH inhibitors [56]. The anti-inflammatory activities of compounds **151a–c** were superior (edema inhibition percentages of 62%, 71%, and 65%) to the reference drug celecoxib (22%). Compounds **151a–c**, the most potent dual COX-2/sEH inhibitors *in vitro*, displayed the highest analgesic activity, with a % inhibition of 62.68, 71.64, and 67.16, respectively, and potencies 4.66, 5.33, and 5, respectively. Furthermore, compounds **151b** and **151c** substantially decreased the serum concentration of TNF-α with a % inhibition of 77% and 75%, respectively, when compared to celecoxib (64%). Compounds **152** and **153** have been reported as promising anti-inflammatory agents [57]. The compounds inhibited the lipoxygenase enzyme with IC₅₀ values of 2.17 ± 0.12 and 2.53 ± 0.06 µM, respectively, compared to the standard quercetin (IC₅₀ value = 3.35 ± 0.01 µM) (see Figure 5).

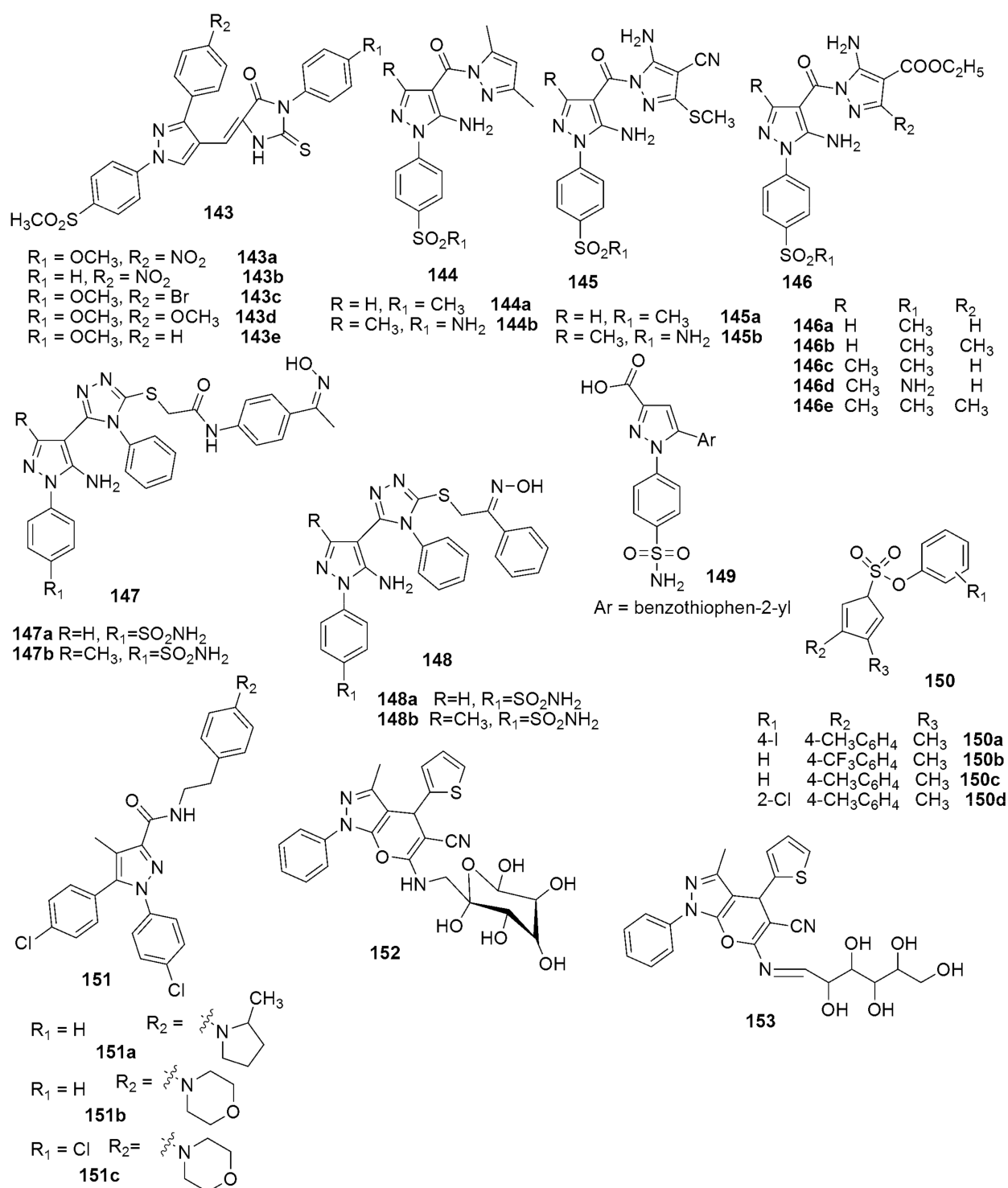


Figure 5. Structures of promising pyrazole derivatives with anti-inflammatory and analgesic activity.

4.2. Anticancer

Compound 5-(5-Bromo-1-methyl-1H-indol-3-yl)-1-(4-cyano-phenyl)-3-methylsulfanyl-1H-pyrazole-4-carbonitrile **117b** showed significant cytotoxicity against MCF 7 ($\text{GI}_{50} = 15.6 \mu\text{M}$) with low cytotoxicity against a normal Vero cell line [31] (see Figure 4). Sivaramakarthikeyan et al. [36] reported that the evaluation of the anticancer potency of the synthesized pyrazole-benzimidazole hybrids revealed that the hybrids bearing a *para*-fluorophenyl unit tethered at the pyrazole nucleus (**121b**) showed the highest activity against both the pancreatic cancer cells (SW1990 and AsPC1) with IC_{50} of 30.9 ± 0.77

and $32.8 \pm 3.44 \mu\text{M}$ compared to the reference compound, gemcitabine 35.09 ± 1.78 and $39.27 \pm 4.44 \mu\text{M}$. Akhtar et al. [33] revealed that **123b** was active against A549, SiHa, COLO205, and HepG2 cancer cell lines, with IC_{50} values of 4.94, 4.54, 4.86, and $2.09 \mu\text{M}$. The potent compound **123b** was also nontoxic against normal cells (cell line HaCaT), with an IC_{50} value greater than $50 \mu\text{M}$ (see Figure 6).

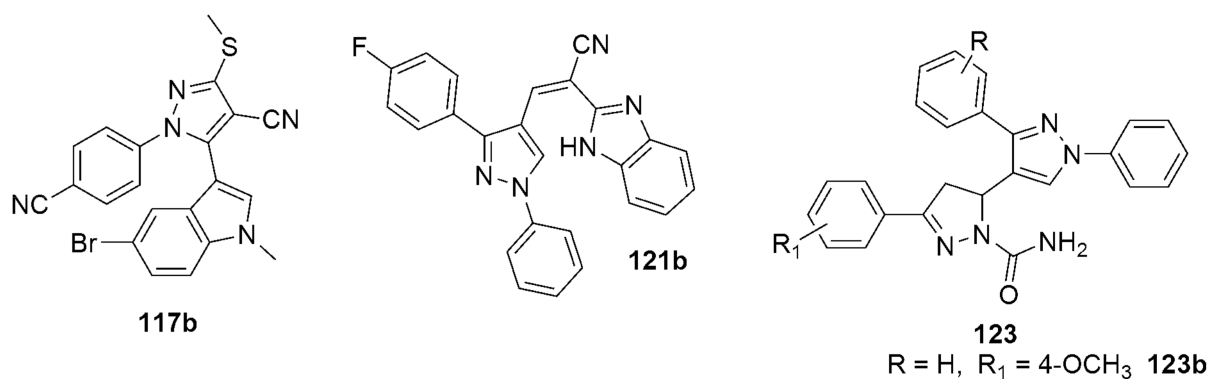


Figure 6. Pyrazole hybrids with anticancer activity.

Sivaramakarthykeyan et al. [40] showed that **126** exhibited significant activity against both the pancreatic cell lines—namely, AsPC1 and SW1990—with IC_{50} values of 30.3 ± 0.45 , $32.4 \pm 0.65 \mu\text{M}$ and noncancerous cell—namely, MRC5 with an IC_{50} value of $55.5 \pm 3.50 \mu\text{M}$ (Figure 3). The synthesis and anticancer evaluation of a series of 1,2,3-triazole linked 3-(1,3-diphenyl-1*H*-pyrazol-4-yl)acrylates have been carried out [47]. Compound **136b** showed the most promising anticancer effects among the synthesized compounds, with IC_{50} values of 1.962, 3.597, 1.764, and $4.496 \mu\text{M}$ against the A549, HCT-116, MCF-7, and HT-29 cell lines, respectively. The sulphamoyl derivatives **148a** and **148b** exhibited the most potent activity, with IC_{50} of 5.34 and $6.48 \mu\text{M}$ against A549 and IC_{50} of 4.71 and $5.33 \mu\text{M}$ against MCF-7. Additionally, the compounds showed potent activity, with IC_{50} values of 4.39 and $5.12 \mu\text{M}$ against HCT-116 and IC_{50} of 3.66 and $4.37 \mu\text{M}$ against PC-3 [53]. A further analysis disclosed that compounds **148a** and **148b** arrested the cell cycle activity on the PC-3 cell line with greater selectivity. Meanwhile, the antiproliferation potency of compounds **148a** and **148b** on PC-3 cells is due to cell cycle arrest and apoptosis-inducing activity categorized by the Bax/Bcl-2 ratio increase (see Figure 7).

Compounds **154–156** were effective VEGFR-2 kinase inhibitors with IC_{50} of 913.51, 225.17, and 828.23 nM , respectively, compared to sorafenib ($\text{IC}_{50} = 186.54 \text{ nM}$) [58]. Further, the cellular mechanistic studies of **156** revealed its promptness towards pre-G1 apoptosis and cell growth termination at the G2/M phase.

A new series of pyrazolo [1,5-*a*]pyrimidine derivatives has been designed and evaluated for their cytotoxic activities on a human breast adenocarcinoma cell line (MCF-7) and colon cancer cell line (HTC-116) [59]. The results revealed that **157** was the most potent among the tested compounds against HTC-116, with an IC_{50} value of $1.51 \mu\text{M}$, while **158** ($\text{IC}_{50} = 7.68 \mu\text{M}$) displayed an excellent cytotoxic effect superior to reference doxorubicin against MCF-7. The tetrahydrothiochromeno [4,3-*c*]pyrazole derivatives were synthesized and evaluated for anticancer activity using MTT [60]. Most of these compounds showed potential anticancer activity and low cytotoxicity on the normal cells in vitro. Compounds **159a** and **159b** displayed excellent anticancer activity, with IC_{50} values of $15.43 \mu\text{M}$ and $20.54 \mu\text{M}$ towards MGC-803, respectively. Additionally, the potent compounds **159a** and **159b** induced G2/M cell cycle arrest and apoptosis in MGC-803 cells. New pyrazole Schiff bases containing azo groups **160** have been reported as promising anticancer agents [61]. A new series of novel pyrazole-containing imide derivatives were synthesized and evaluated for their anticancer activities against the A-549, Bel7402, and HCT-8 cell lines [62]. Among the evaluated compounds, **161a–161d** exhibited potent inhibitory activity against the A-549 cell line, with IC_{50} values at 4.91, 3.22, 27.43, and $18.14 \mu\text{M}$, respectively, superior to

5-fluorouracil ($IC_{50} = 59.27 \mu M$). Additionally, **161a–161c** exhibited substantial inhibitory activity towards the HCT-8 and Bel7402 cell lines (see Figure 7).

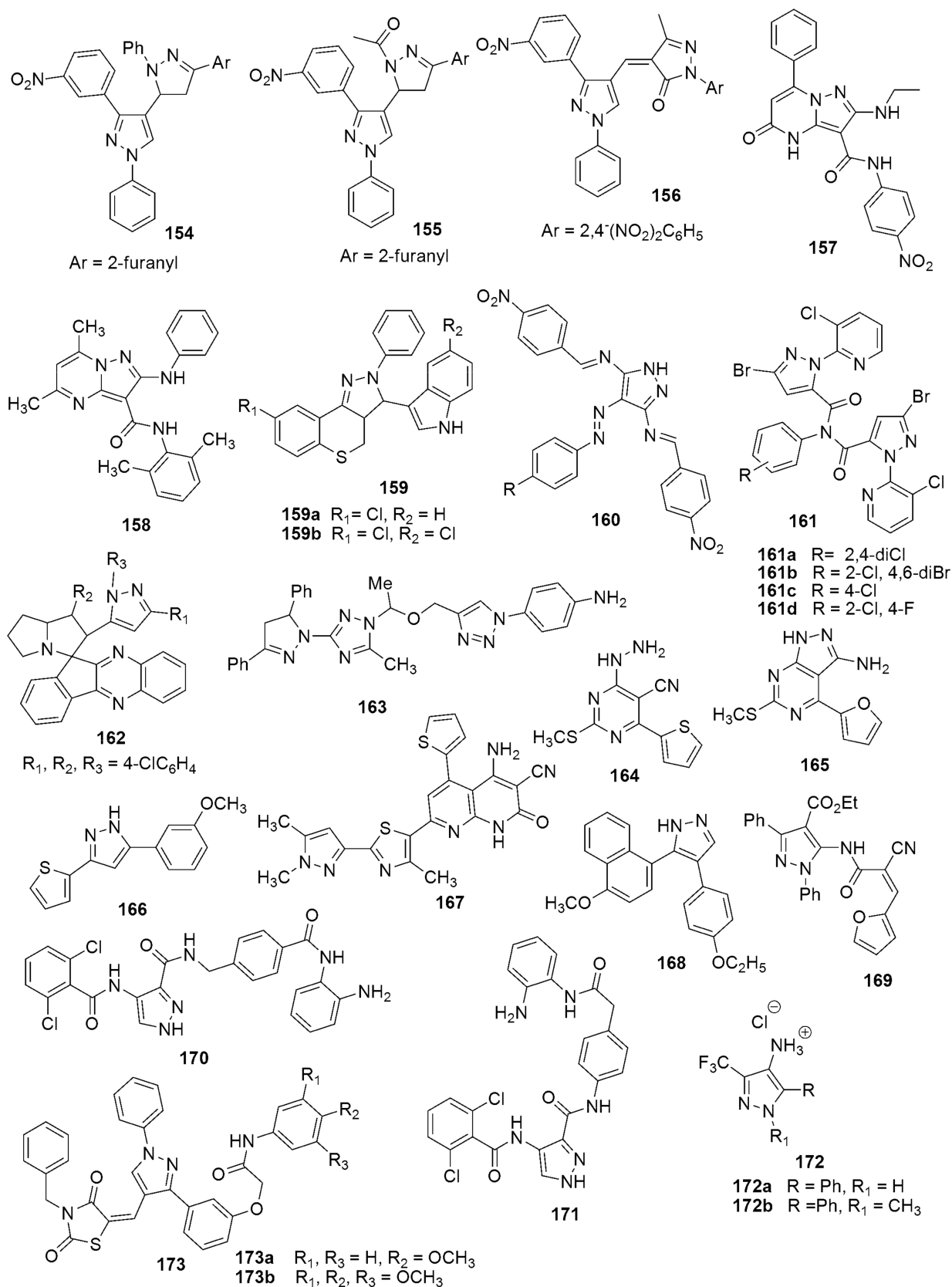


Figure 7. Structures of pyrazole derivatives with anticancer activity.

The cytotoxic activity of spirocycloadducts and *N*-arylpyrazole hybrids against the HeLa cancer cell line was evaluated using an MTT assay [63]. Spiro[indenoquinoline-pyrrolizidine]-*N*-arylpyrazole conjugate **162** bearing a *p*-chlorophenyl substituent exhibited the highest antiproliferative activity against cancer cell line HeLa ($IC_{50} = 1.93 \mu M$). The IC_{50} is comparable to camptothecin's standard drug ($IC_{50} = 1.66 \mu M$) (see Figure 7). A novel series of 1,2,3-triazole-pyrazole hybrids were designed and synthesized using the Cu-catalyst [64]. The synthesized compounds were evaluated for anticancer activity using three cancer cell line panels. Compound **163** was the most potent cytotoxic candidate for HepG-2, HCT-116, and MCF-7, with $IC_{50} = 12.22, 14.16,$ and $14.64 \mu M$, respectively, comparable to the standard drug doxorubicin ($IC_{50} = 11.21, 12.46,$ and $13.45 \mu M$). Ragab et al. [65] revealed compounds **164** and **165** as promising leads for colon cancer treatment. Compounds **164** and **165** were active against the KM12 cell line, with an IC_{50} value of 1.73 and 1.21 μM and high selectivity index (SI) (18.82 and 35.49, respectively). Compared to the standard drug 5-FU with an IC_{50} value of 12.26 μM and SI value of 1.93. The potent compound displayed selective cytotoxic activity against KM12 cells in the annexin V-FITC staining assay.

Mohamady et al. [66] designed and synthesized diarylpyrazole derivatives. The compounds were screened against the MCF7 and HepG2 cell lines. Among the evaluated compounds, **166**, which contained a thiophene ring, was observed to have the highest antiproliferative activity against HepG2 cells, with an IC_{50} of 0.083 μM . The compound caused cell cycle arrest at the G2, and the 7.7-fold increase in caspase-3 confirmed its apoptotic effect on HepG2 cells. Additionally, **166** caused a noticeable decrease in Hsp90 proteins (Akt, c-Met, c-Raf, and EGFR) and a 1.57-fold upsurge in Hsp70.

Pyrazolothiazole-substituted pyridine conjugates were synthesized and evaluated for cytotoxicity activity [67]. Compound **167**—namely, 4-amino-7-(2-(1,5-dimethyl-1*H*pyrazol-3-yl)-4-methylthiazol-5-yl)-2-oxo-5-(thiophen-2-yl)-1,2-dihydro-1,8-naphthyridine-3-carbonitrile—has the highest cytotoxicity activity towards PC-3 ($IC_{50} = 17.50 \mu M$), NCI-H460 ($IC_{50} = 15.42 \mu M$) and Hela ($IC_{50} = 14.62 \mu M$), comparable to the anticancer potential of standard drug etoposide ($IC_{50} = 17.15, 14.28,$ and $13.34 \mu M$, respectively).

Wang et al. [68] investigated a new series of pyrazole-naphthalene derivatives. The synthesized compounds were evaluated for their anticancer activity against breast cancer cell lines (MCF-7). Compound **168** ($IC_{50} = 2.78 \pm 0.24 \mu M$), with substituted ethoxy at position 4 of the phenyl ring, exhibited the highest activity, and the activity was 5-fold more active than the reference drug cisplatin ($IC_{50} = 15.24 \pm 1.27 \mu M$). Additionally, **168** showed inhibited tubulin polymerization with an IC_{50} value of 4.6 μM . Mohamed and coworkers [69] recommended cyanoacrylamide compound **169** as a new promising chemotherapeutic agent. The compound exhibited high cytotoxic activity toward colorectal carcinoma. Compounds **170** and **171** displayed excellent antiproliferative activities towards HDAC2, with IC_{50} values of 0.25 and 0.24 nM, respectively, and CDK2 with IC_{50} values of 0.30 and 0.56 nM, respectively. The potent compounds **170** and **171** pointedly inhibited the movement of the A375 and H460 cells, arrested the cell cycle in the G2/M phase, and promoted apoptosis in A375, HCT116, H460, and Hela cells, related to proliferating the intracellular reactive oxygen species (ROS) levels. Notably, **170** has good pharmacokinetic properties, with an intraperitoneal bioavailability of 63.6% in ICR mice. Additionally, the compound was effective in vivo for antitumor activity in the HCT116 xenograft model. Thus, the authors proposed compound **171** as a favorable agent for treating malignant tumors. Burgart and colleagues [70] found 4-aminopyrazole derivatives **172a** and **172b** to be cytotoxic against HeLa cells and human dermal fibroblasts cancer cells. A novel series of pyrazole-arylacetamide hybrids has been synthesized and evaluated for cytotoxicity activity. Compounds **173a** and **173b** exhibited a potent cytotoxic effect on the MCF-7 cancer cell line, with IC_{50} values of 0.604 μM and 0.665 μM compared to the standard drug cisplatin ($0.636 \pm 0.458 \mu M$) (see Figure 7).

Answer et al. [71] synthesized some novel pyrazole hybrids using 5-amino-3-(4-(dimethylamino) phenyl)-1-phenyl-1*H*-pyrazole-4-carbonitrile as a precursor. Including

different nucleophilic and electrophilic compounds, among the synthesized compounds, the anticancer activities of the synthesized compounds **174**, **175**, **176**, and **177** (6.50 ± 0.5 , 3.74 ± 0.3 , 3.18 ± 0.2 , and 8.67 ± 0.9 μM , respectively) exhibited strong cytotoxic activity against MCF-7 and HCT-116 (7.80 ± 0.6 , 4.93 ± 0.3 , 4.63 ± 0.4 , and 10.02 ± 1.0 μM , respectively) (see Figure 7). Hassan et al. [72] synthesized a novel series of pyrazolopyrimidines and screened the compounds against a panel of 60 human cancer cell lines. Compounds, 5-amino-1H-pyrazole-4-carbonitrile derivative **177**, pyrazolo [5,1-b]quinazoline-11-carbonitrile derivative **178**, and 1-amino-2,4-dihydro-5H-benzo [4,5]imidazo [1,2 c]pyrazolo [4,3-e]pyrimidin-5-one **179** exhibited anticancer activity against some cancer cell lines (Figure 7). Compounds **180a–180c** have been reported to displayed anticancer [73] compounds **180a–180c** bearing an electron-donating group, such as methoxy substituent at the *para* position; the 3,4 dimethoxy and 3,4,5 trimethoxy derivatives demonstrated noticeable cytotoxic activity with IC_{50} values of 0.604 μM , 1.057 μM , and 0.665 μM respectively, against the MCF-7 cancer cell lines.

Thiazolyl pyrazole carbaldehyde hybrids have been synthesized and screened for their in vitro anticancer activity by Mamidala and colleagues [74]. Compound **181** exhibited the highest antiproliferative activity against the HeLa, MCF-7, and A549 cancer cell lines, with IC_{50} values of 9.05 ± 0.04 , 7.12 ± 0.04 , and 6.34 ± 0.06 μM , respectively. Raghu et al. [75] designed and synthesized a new series of 1,3,5-triazine-based pyrazole hybrids with anticancer activity targeting the epidermal growth factor (EGFR) tyrosine kinase. Compounds **182a–182c** exhibited potent anticancer activity against the MCF-7 (human breast), HepG2 (human liver), HCT116 (human colorectal), PC-3 (human prostate), LoVo (human colon), and LoVo/DX (doxorubicin-resistant) cancer cell lines. According to the EGFR tyrosine kinase test, **182a–182c** demonstrated excellent activity, with an IC_{50} value of 395.1, 286.9, and 229.4 nM. Compared to the reference doxorubicin (63.8 nM) and erlotinib (103.8 nM), compound **182c**, with a trifluoromethyl group at the *para* position on the phenyl rings, exhibited the most potent anticancer activity. Thus, the anticancer activity of the tested compounds was affected by the physicochemical properties of the substituent on the pyrazole-bound phenyl nucleus. Compounds **183a–183c** have been reported as promising antiproliferative agents [76]. Suryanarayana et al. [77] synthesized a novel series of dinitrophenylpyrazole-bearing triazole and further investigated their anticancer activity using three tumor cell lines—namely, MCF-7, HeLa, and HeLa Caco-2. Among the synthesized compounds **184a–184c** with the methoxy group on the phenyl ring at the *ortho*, *meta*, or *para* position exhibited excellent inhibitory activity against the HeLa ($\text{IC}_{50} = 4.0$ μM , 5.0 μM , and 6.0 μM) compared to the standard drug combretastatin-A4 ($\text{IC}_{50} = 9.0$ μM). Compound **185c** exhibited excellent inhibitory activity against the MCF-7 cell line, with an IC_{50} value of 8.0 μM . Compound **185** has been reported as a promising anticancer agent that reduced the level of CDK2, stopped MCF-7 cells in the G0/G1 phase, caused ROS growth, damaged the MMP, and accelerated the apoptosis of MCF-7 cells [78] (see Figure 8). Among the new library of pyrazole derivatives investigated for antiproliferative activity by Signorello and coworkers, compounds **186a** and **186b** exhibited antiproliferative effectiveness [79]. Compound **186a** displayed moderate inhibition (25–30% at 10 μM) toward melanoma (SK-MEL-5, UACC-62) and renal cancer cell lines (UO-31 cancer cell lines). Compound **186b** displayed a broad spectrum of action (25–30%) towards leukemia (CCFR-CEM and RPMI-8226), non-small cell lung (NCI-H522), CNS (SF-295 and SNB-75), ovarian (OVCAR-4) and the breast (BT-549 and MDA-MB-468) cancer cell line. Additionally, compound **186b** demonstrated 50–60% inhibition towards melanoma (SK-MEL-5 and UACC-62), renal (CAK-1 and UO-31), and prostate (PC-3) cancer cell lines. The water-soluble, BBB4-loaded NPs (BBB4-G4K NPs, **187**), achieved from BBB4 in a non-bioactive, polyester-based, lysine-containing fourth-generation cationic dendrimer (G4K) has been reported to have an excellent antibacterial profile and highly selective toward the *Staphylococcus* genus [80]. The synthesis and biological screening of 5- pyrazolyl urea as potential antiangiogenic compounds were investigated by Morretta et al. [81]. Among the targeted compounds, compound **188a** displayed 100% inhibition on leukemia cancer cell

lines, while **188b** and **188c** impeded non-small cell lung cancer cell lines. Compound **188d**, similar to the STIRUR-41 pharmacophore, exhibited 40% inhibition in the non-small cell lung cancer cell lines. Additionally, compounds **188e** and **188f**, containing a trifluoromethyl substituent on the urea moiety, displayed excellent inhibitory activity. Meanwhile, the mechanism of action detailed that **188e** may likely exert its antiproliferative activity by targeting different signaling pathways, including ERK/MAPK and phosphatases, or the crosstalk between these two associated intracellular mechanisms. Compound **188e** can regulate ERK1/2 phosphorylation and PP1g action.

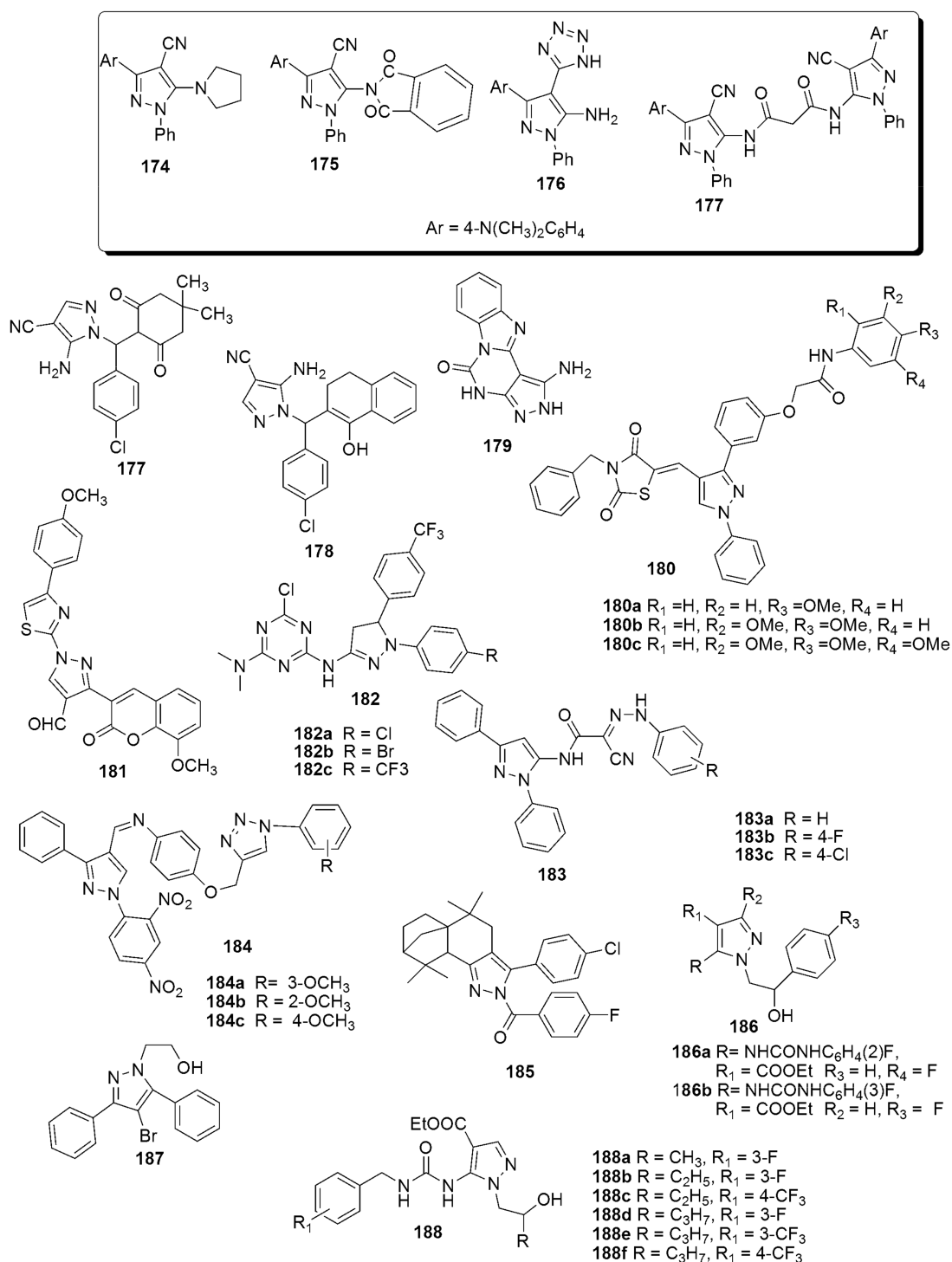


Figure 8. Structures of pyrazole derivatives acting as anticancer agents.

4.3. Antibacterial

Nayak et al. [37] reported **122a–122g** as promising antibacterial agents (Figure 3). Ebenezer et al. [82] reported a designed and synthesized library of novel pyrazole–imidazo [1,2- α]pyridine scaffolds through a one-pot three-component tandem reaction. All selected compounds (zone of inhibition 9 mm) showed excellent bactericidal activity. In most cases, except for MRSA, the activity of the compounds was better than that of the standard ciprofloxacin. Compounds **189a–189e** had excellent activity against *S. aureus*, *E. coli*, *S. typhimurium*, *K. pneumoniae*, and *P. aeruginosa*, with minimum bactericidal concentrations (MBC) <0.1 $\mu\text{g}/\text{mL}$. Pyrazoloquinoline derivatives have been synthesized and their antibacterial activity evaluated using the Agar diffusion method [83]. The ketonic compounds **190a** and **190b** showed activity percentages of 112% and 95% (*Streptococcus pneumoniae*) and 86% and 83%, respectively (*Bacillus subtilis*), compared to the standard control. The halogenated ketonic derivative **190b** showed improved activity compared to gentamicin (109%), and no activity was observed in *Pseudomonas aeruginosa*. Hansa and coworkers [84] reported 4-(4-(anilinomethyl)-3-[4-(trifluoromethyl)phenyl]-1H-pyrazol-1-yl)benzoic acid derivatives as potent anti-Gram-positive bacterial agents. Many of the evaluated compounds are potent growth inhibitors of Gram-positive bacteria and showed low toxicity of human cultured cells. Among the compounds, **191a** and **191b** exhibited excellent inhibition against *Staphylococcus aureus*. A novel series of multi-substituted benzo-indole pyrazole derivatives with antibacterial activity targeting DNA gyrase has been investigated [85]. Compound **192** exhibited excellent antibacterial activity against four drug-resistant *E. coli* bacteria strains (*E564c*, *E68d*, *E48e*, and *E109*, respectively) with IC_{50} values of 7.0 and 17.0, 13.5, and 1.0 μM , respectively. The substitution of fluorine or chlorine at R_2 enhanced the bacteriostatic effect. The derivative bearing a Cl atom at R_1 and R_2 exhibited a superior antibacterial effect. Additionally, compound **192** displayed potent inhibition against DNA gyrase, with IC_{50} values of 0.10 μM in the in vitro enzyme inhibitory assay. A library of twenty-three novel pyrazole–phenylthiazole hybrids was synthesized and screened for antimicrobial activity against five bacterial species and two fungi [86]. Compound **193** displayed a promising antibacterial effect against the Gram-positive methicillin-resistant *Staphylococcus aureus* (MRSA) strain with a MIC value of 4 $\mu\text{g}/\text{mL}$. Compound **193** was nontoxic to mammalian cells—namely, human embryonic kidney cells and human red blood cells. All the synthesized compounds except **194** (moderate growth inhibition of 40.8%) showed poor antifungal activity. Analogs of pyrazole–thiazolidinone and pyrazole–thiosemicarbazone were designed using a molecular hybridization approach and further synthesized through a Vilsmeier–Haack approach [87]. The compounds were tested for antimicrobial activity against two Gram-positive bacteria, such as *Staphylococcus aureus* and methicillin-resistant *Staphylococcus aureus*. Additionally, four Gram-negative bacteria such as *Escherichia coli*, *Salmonella typhimurium*, *Klebsiella pneumoniae*, and *Pseudomonas aeruginosa* were used in the biological assay. Derivatives **195** and **196** appeared as the most active antimicrobial compounds, with an MBC value of <0.2 μM against MRSA and *S. aureus*. The presence of 2,4-dichloro group on **195** enhanced its antibacterial activity. A new pyrazole containing isonicotinoyl derivatives from substituted chalcones and isoniazid by using sulfamic acid and their pharmacological activity evaluation have been investigated [88]. All examined compounds showed inferior activity against *E. coli*. The MIC values divulged that compounds **197a**, **197c**, and **197d** (MIC values = 14, 17, and 14 μM) exhibited good antimicrobial activity against *Staphylococcus aureus*, while compounds **197a** and **197b** (MIC values = 14 and 29 μM) displayed superior antimicrobial activity against *Pseudomonas aeruginosa*. Compounds **197b** and **197d** (MIC values = 117 and 114 μM) exhibited noticeable activity against *Salmonella typhi*. Notably, the electro-donating group at the R position improved the antimicrobial activities more than the insertion of the electro-withdrawing group. Additionally, electron-donating substituents at position three enhanced the antimicrobial activity compared to position four. The one-pot reaction of bis-hydrazonoyl bromide with active methylene reagents furnished new bis-thiazolyl-pyrazole derivatives [89]. The insertion of acetyl (COCH_3) and methyl (CH_3) groups improved the

activity of compound **198** against Gram-positive strains with MIC values 2, 8, and 8 μM towards *S. aureus*, *B. subtilis*, and *E. faecalis*, respectively. In comparison, **198** showed moderate antifungal and no substantial activity against Gram-negative strains with MIC > 32 μM . The most potent compound against the Gram-positive bacterial strains was **200** with MIC values of 0.12, 1, and 0.5 μM for *S. aureus*, *B. subtilis*, and *E. faecalis*, respectively, compared to the standard drug vancomycin (1 to 2 μM). The lipophilic aryl substituent at position five and cyano at position four in the pyrazole ring improved the antibacterial activity of **200**. Compounds **198**, **199b**, and **200** exhibited more potent inhibitory activity of DHFR with IC₅₀ values (6.34 ± 0.26 , 7.49 ± 0.28 , and 3.81 ± 0.16 μM), respectively, compared with Trimethoprim (8.34 ± 0.11 μM). However, *bis*-1-(thiazol-2-yl)-5-(amino)-1*H*-pyrazole-4-carbonitrile derivative **199a** was revealed to be the least inhibited toward DHFR in comparison to Trimethoprim and other tested derivatives, with an IC₅₀ value 19.38 ± 0.68 μM , and that may be related to the presence of the carboxamide group in position four at the pyrazole ring rather than acetyl or carbonitrile as pyrazole derivatives **198**, **199b**, and **200**. Desai and colleagues [90] synthesized analogs of pyrazole, pyrazoline-clubbed pyridine compounds, and examined their antibacterial and antifungal activities. Among the test compounds, **201a** (3-OH) and **201b** (4-F) exhibited good activity (MIC = 50 $\mu\text{g}/\text{mL}$) against *S. aureus* and *E. coli*, respectively. Compound **201c** (2,4-dichloro) showed superior activity (MIC = 12.5 $\mu\text{g}/\text{mL}$) against *P. aeruginosa* and very good activity (MIC = 25 $\mu\text{g}/\text{mL}$) against *S. pyogenes* compared to the standard drug ampicillin (100 $\mu\text{g}/\text{mL}$) and chloramphenicol (50 $\mu\text{g}/\text{mL}$). The derivatives bearing electron-donating groups (2-OH, 3-OH, 4-CH₃, and 4-OH-3-OCH₃) showed significant antifungal and antibacterial activity, while the derivatives bearing electron-withdrawing groups (4-F and 2,4-dichloro) showed an augmentation in the antibacterial potency. Compound **202** has been reported as a promising antibacterial agent (*B. cereus*, *S. aureus*, *P. aeruginosa*, and *E. coli*) with the closest inhibition zones (17–20 mm) [91] (see Figure 9).

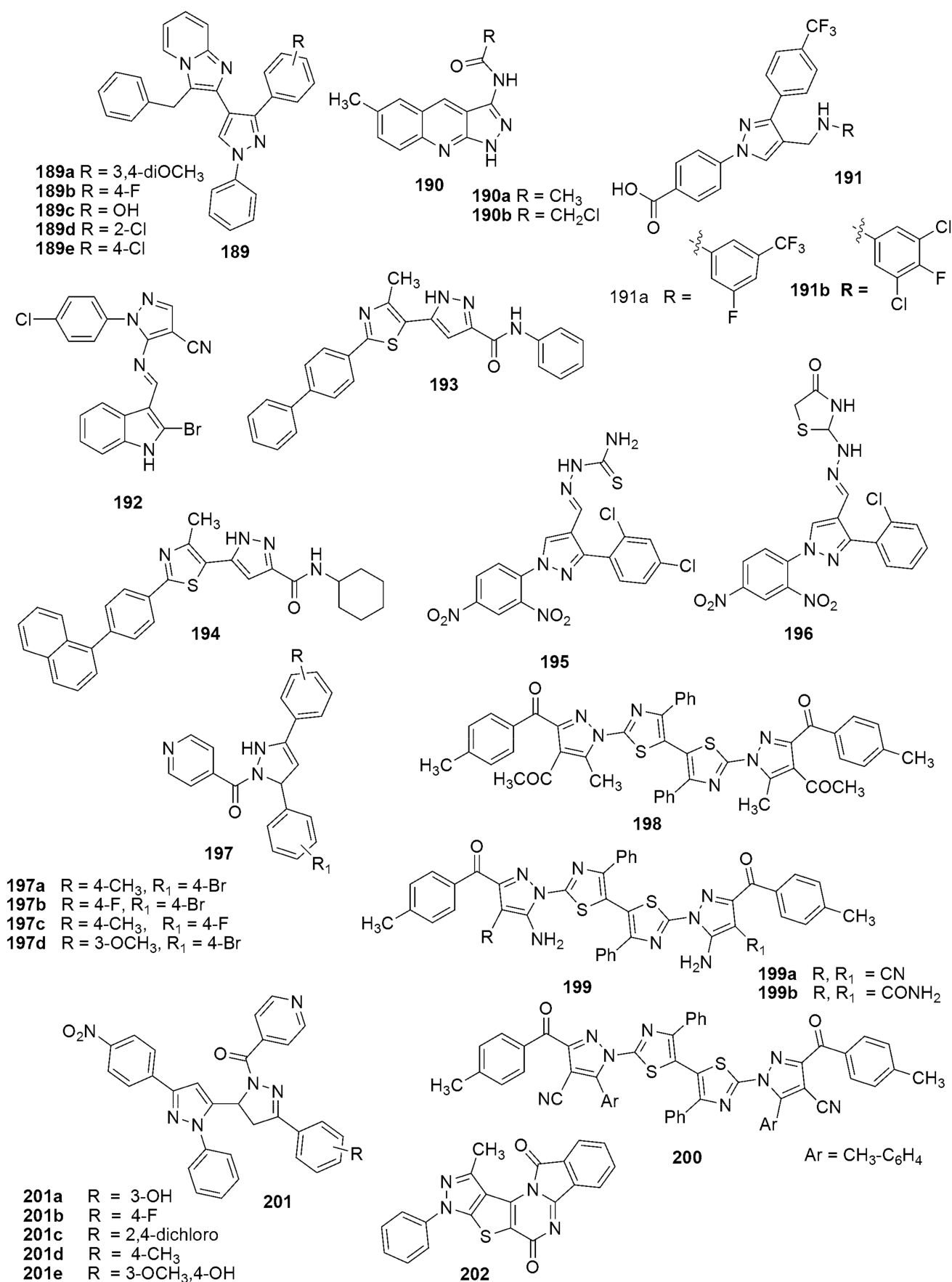


Figure 9. Structures of promising pyrazole derivatives with antibacterial activity.

4.4. Antifungal

Compounds **201d** (4-CH₃) and **201e** (4-OH-3-OCH₃) showed significant antifungal activity towards diverse fungal strains [90]. Compound **201d** (4-CH₃) displayed significant activity (MIC = 12.5 µg/mL) towards *A. niger*, and compound **201e** (4-OH-3-OCH₃) showed excellent activity (MIC = 12.5 µg/mL) against *C. albicans* and *A. clavatus* (Figure 9). Othman et al. [92] reported novel heterocyclic hybrids of pyrazole and their antimicrobial activity. Compounds bearing a benzenesulphonamide group fused with 3-methyl-5-oxo-1H-pyrazol-4-(5H)-ylidene) hydrazine **203** and 6-amino-7-cyano-3-methyl-5H-pyrazolo [4,3-c]pyridazine **204** showed significant and broad-spectrum antimicrobial activity. Compound **204** displayed excellent antifungal activity toward *A. fumigates* with a MIC value of 0.98 µg/mL. While **203** and **205** are equipotent with the reference, amphotericin B against *A. fumigates* with a MIC value of 1.95 µg/mL exhibited 2-fold decrease in the effectiveness compared to the standard, ciprofloxacin against *S. pneumonia* (MIC = 1.95 and 0.98 µg/mL, respectively). Compound **203** was equipotent in the antifungal activity with the reference (MIC = 3.9 µg/mL) against *C. albicans*.

A series of novel pyrazole-thiazole carboxamides were designed, synthesized, and investigated for their antifungal activity [93]. The outcomes showed that compounds **206**, **207**, and **208** have promising in vitro activities against *Rhizoctonia cerealis*, with EC₅₀ values from 1.1 to 4.9 mg/L, superior to thifluzamide (EC₅₀ = 23.1 mg/L). The antifungal activity of **207** (EC₅₀ value = 1.1 mg/L) was ~21-fold more active than thifluzamide and ~2-fold more active than compound **206** (EC₅₀ = 2.0 mg/L). Meanwhile, **208** exhibited excellent antifungal activity towards *S. sclerotiorum*, with an EC₅₀ value of 0.8 mg/L, which was ~6-fold higher than thifluzamide (EC₅₀ = 4.9 mg/L). The conjugates bearing an aniline moiety with a single substituent at the *ortho*- or *meta*-position exhibited promising antifungal activity. Additionally, the in vivo antifungal assay showed that **206** (90% at 10 mg/L) exhibited higher antifungal activity than thifluzamide against *R. solani* (90% at 10 mg/L). The synthetic route to pyrazole-4-formylhydrazine derivatives bearing a diphenyl ether fragment was reported by Wang et al. [94]. The synthesized compounds were evaluated for their antifungal activity by targeting a succinate dehydrogenase. Among the tested compounds, **209a** against *Rhizoctonia solani*, **209b** against *Fusarium graminearum*, and **209c** against *Botrytis cinerea*, exhibited superior antifungal activity. The compounds displayed EC₅₀ values of 0.14, 0.27, and 0.52 µg/mL higher than carbendazim against *R. solani* (0.34 µg/mL) and *F. graminearum* (0.57 µg/mL), along with penthiopyrad against *B. cinerea* (0.83 µg/mL). Compound **209a** was ~2- and 15-fold higher than the marketed fungicides carbendazim (0.34 µg/mL) and boscalid (2.21 µg/mL) towards *R. solani*. The results from the determination of the inhibitory effects of **209a** against the SDH collected from the mycelia of *R. solani* showed IC₅₀ values of 3.99 µM (1.58 µg/mL). The in vivo anti-*R. solani* control effectiveness of the most potent compound, **209a** (73.25% at 200 µg/mL), was significantly superior to carbendazim under the same conditions (59.81%). Compound **210** has been reported as an excellent antifungal agent with equivalent activity to the marketed fungicide drug thifluzamide, and its EC₅₀ value was 0.022 mg/L against *R. solani* [95] (see Figure 10).

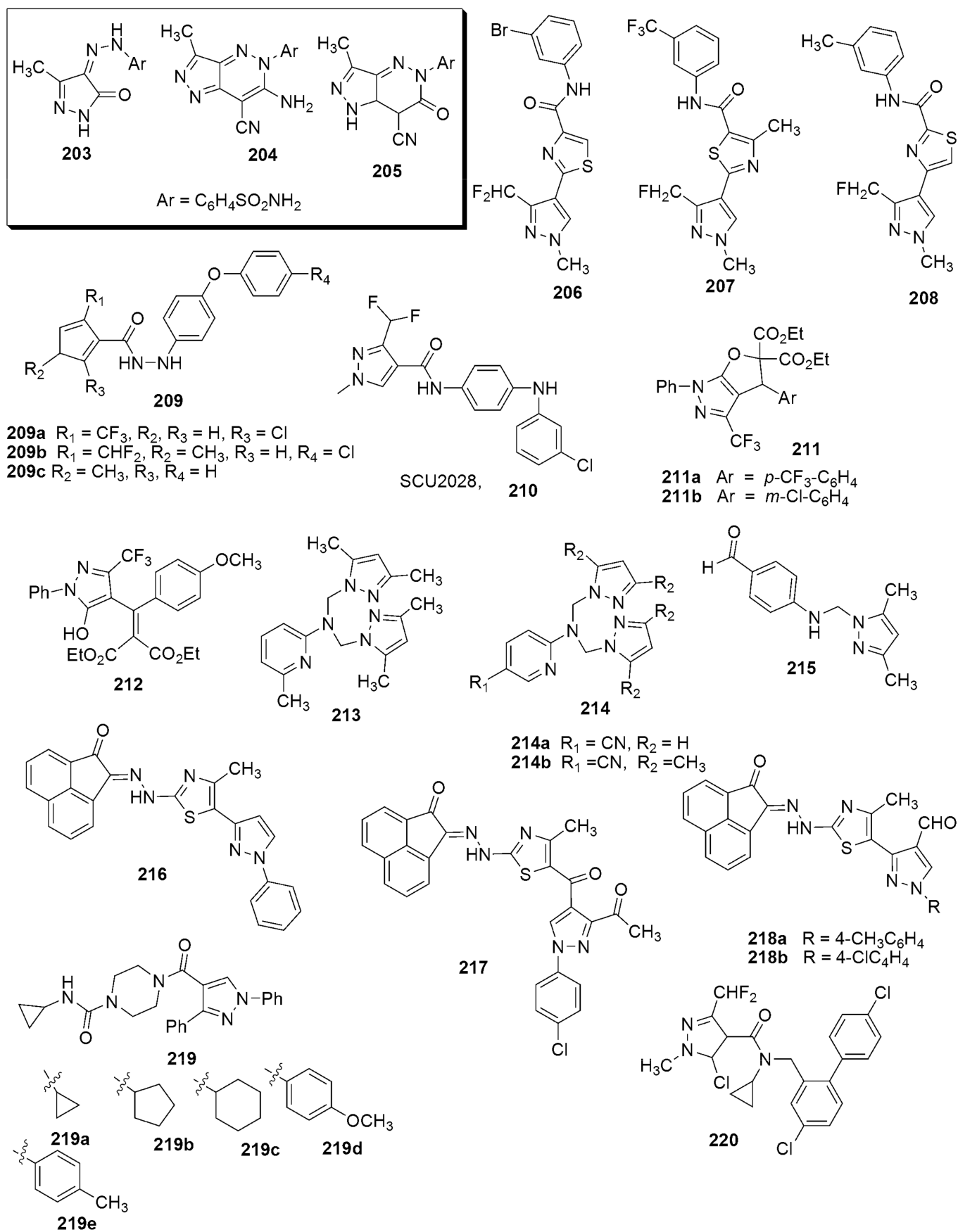


Figure 10. Pyrazole derivative with antifungal activity.

A synthetic route to substituted 3-(trifluoromethyl)-4,5-dihydro-1H-furo [2,3-c] pyrazole conjugates using the [3 + 2] Michael/Alkylation approach was developed by Tan et al. [96]. The antifungal activity of the synthesized compounds was further examined, and **211a** exhibited excellent antifungal activity against *A. solani* with IC₅₀ values of 5.44 µM. Compounds **211b** and **212** also displayed good antifungal effects, with corresponding IC₅₀ values of 9.00 and 31.45 µM, respectively. The antifungal effects of the most active compounds **211a** and **211b** and **212** were relatively superior to the standard compound cycloheximide (IC₅₀ = 71.00 µM). The conjugates bearing the electron-deficient group on the aromatic ring displayed higher inhibitory effects. At the same time, the compound bearing an electron-donating substituent on the aromatic ring showed reduced inhibitory effects. Compounds **213**, **214a** and **214b**, and **215** have been unveiled to exhibit good antifungal activity toward *Fusarium Oxysporum f. sp.* and *Albedinis (FOA) fungus* with IC₅₀ values ranging from 25.6 to 33.2 µg/mL [97]. Compound **216** has been reported to have superior antifungal inhibitory activity against *C. albicans* (MIC = ≤146 µg/mL) compared to **217**, which displayed a MIC = ≤183 µg/mL. Meanwhile, **218a** and **218b** exhibited significant antifungal effectiveness concentrations against *C. albicans* compared to the reference compound cycloheximide with the corresponding MIC values ≥ 168 µg/mL and ≥165 µg/mL, respectively [98]. Piperazine-pyrazole-4-carboxylic acids have shown good antifungal inhibitory effects. Compounds **219a–219e** showed equipotent antifungal activity with the reference miconazole against *C. albicans* (MIC value = 78.1 µg/mL) [99] (see Figure 10).

Dong and coworkers [100] synthesized a series of novel pyrazole-4-carboxamides hybrids and further evaluated their antifungal activity (see Figure 10). Compound **220** was the most potent compound against *A. solani* in vitro, with an EC₅₀ value of 3.06 µg/mL. It displayed 100% (10 µg/mL) inhibitory activity against *A. solani* in vivo compared to the standard drug boscalid. Makhanya et al. [101] revealed compounds **221a** and **221b** as promising antifungal agents. The antifungal assay showed that **221a** and **221b** exhibited significant inhibitory activity against *Saccharomyces cerevisiae* (zone inhibition (ZI) = 23 and 20 mm, respectively), with a MIC value of 0.18 µM. Comparable with the standard drug amphotericin, B. Bayazeed et al. [102] detected four chromen-3-yl-pyrazole derivatives: **222a**, **222b**, **223a**, and **223b** to have superior antifungal activity. Compared to the standard drug ketoconazole against *Aspergillus fumigatus* with the corresponding % ZI values of 164%, 147.1%, 158.8%, and 147.1%, respectively. In addition, compounds **222b** (% ZI value = 150%) and **223b** (% ZI value = 150%) have 1.5-fold superior activity against *C. albicans* compared to the reference ketoconazole (% ZI value = 150%). Notably, the insertion of two ester groups in compound **222a** improved its antifungal activity. Meanwhile, incorporating electron-donating groups (OCH₃ and CH₃) at the *para*-position of the aromatic ring in **222b**, **223a**, and **223b** enhanced their antifungal activity. Wang et al. [103] reported a novel series of pyrazole-4-acetohydrazide derivatives targeting fungal SDH, further evaluating their antifungal properties towards *R. solani*, *F. graminearum*, and *B. cinerea*. Among the evaluated compounds, the antifungal activity of **224a** against *R. solani*, **224b** against *F. graminearum*, and **224c** against *B. cinerea* had EC₅₀ values of 0.27, 1.94, and 1.93 µg/mL, respectively. These values were superior to the standard reference boscalid against *R. solani* (0.94 µg/mL) and fluopyram against *F. graminearum* (9.37 µg/mL) and *B. cinerea* (1.94 µg/mL). Additionally, the compounds with hydroxyl group substituents at the R₁ position displayed higher anti-*R. solani* activity than the corresponding conjugates bearing an ethoxy group substituent. The in vivo studies detailed that compound **224a** was effective toward *R. solani* (79.83% at 200 µg/mL), comparable to validamycin (86.56%) and thifluzamide (83.49%). Compound **224a** was predicted as an SDH inhibitor (see Figure 11).

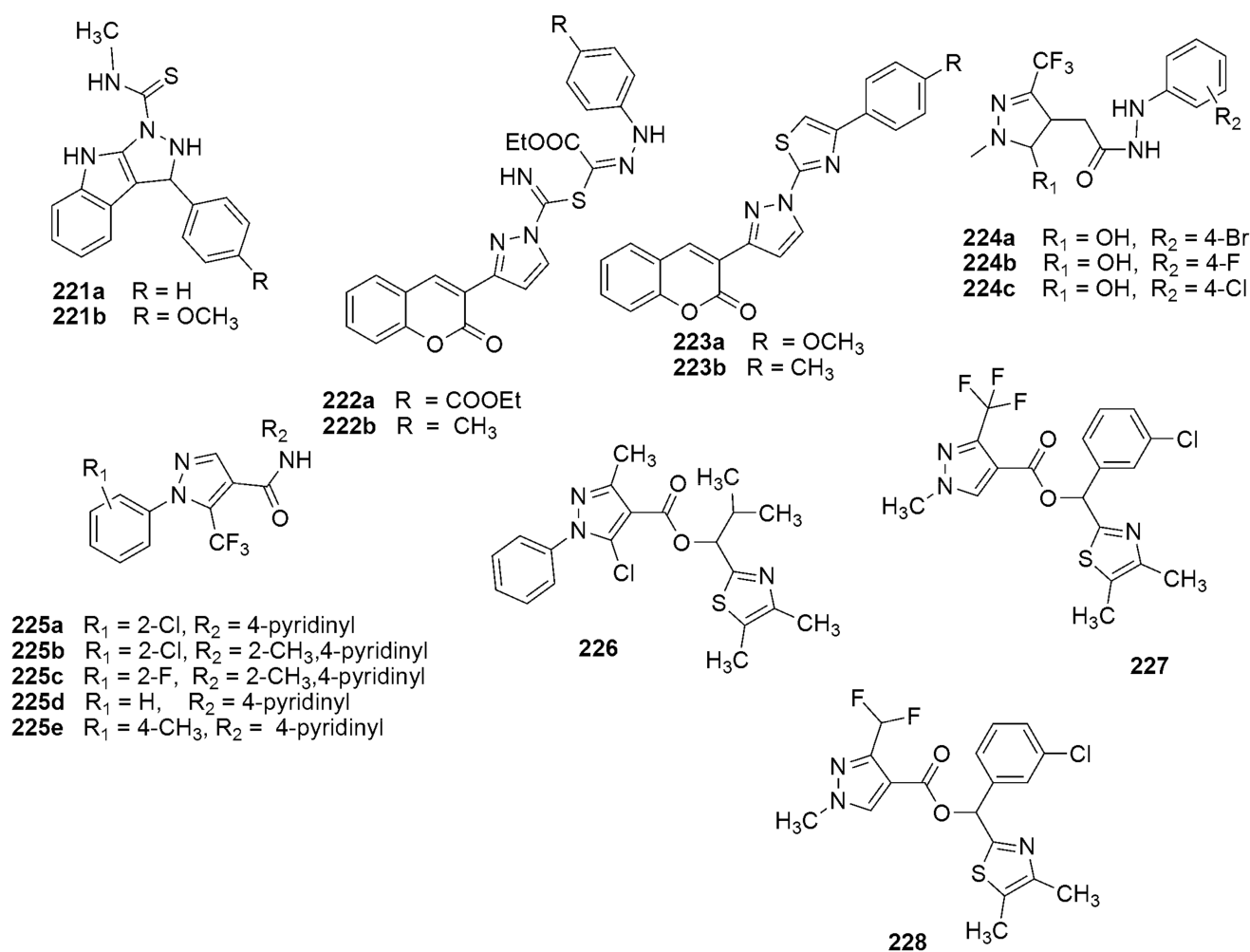


Figure 11. Structures of pyrazole derivatives as antifungal agents.

A series of new pyrazole-4-carboxamide conjugates were designed and synthesized by Wu et al. [104]. The synthesized compounds were evaluated for their antifungal activity using four phytopathogenic fungi (*G. zeae*, *F. oxysporum*, *C. mandshurica*, and *P. infestans*). The EC₅₀ values were 1.8 µg/mL for **225a** against *G. zeae*, 1.5 and 3.6 µg/mL for **225b** against *F. oxysporum* and *C. mandshurica*, respectively, and 6.8 µg/mL for **225c** against *P. infestans*. Meanwhile, the SDH enzymatic effectiveness unveiled corresponding IC₅₀ values of 6.9, 12.5, 135.3, and 223.9 µg/mL, for **225c**, **222d**, **225e**, and penthiopyrad, respectively. Incorporating substituents (CH₃, F, or Cl) into the 2-phenyl and methyl into 2-pyridinyl positions enhanced the antifungal activity. While the introduction substituent into the 3-phenyl and 3-pyridinyl positions decreased the antifungal properties. Xia et al. [105] reported novel pyrazole carboxylate derivatives bearing thiazole as potent fungicides. The antifungal studies revealed compound **226** displayed superior activities against *Botrytis cinerea* and *Sclerotinia sclerotiorum*, with EC₅₀ values of 0.40 and 3.54 mg/L, respectively. Compound **227** displayed superb antifungal activity against *Valsa mali*, with an EC₅₀ value of 0.32 mg/L. The in vivo fungicide control studies against *B. cinerea* and *V. mali* revealed that compounds **226** and **228** at 25 mg/L, respectively, were influential on cherry tomatoes and apple branches. Compound **227** displayed an inhibitory activity toward SDH, with an IC₅₀ value of 82.26 µM. Nevertheless, compounds **226** and **228** lack inhibitory activity toward SDH in the in vivo studies (see Figure 11).

4.5. Antidiabetics

Thiazolidindione **128a** and **128b** and thiazolidinone derivatives **129a** and **129b** displayed significant inhibitory activities against α - and β -glucosidase (% inhibitory activity = 62.15, 55.30, 65.37, and 59.08 for α -glucosidase and 57.42, 60.07, 58.19, and 66.90 for β -glucosidase, respectively) than the reference compounds: acarbose with % inhibitory activity = 49.50 for α -glucosidase and *D*-saccharic acid 1,4-lactone monohydrate with % inhibitory activity = 53.42 for β -glucosidase. Compared to pioglitazone and rosiglitazone, the potent compounds showed good PPAR- γ activation and hypoglycemic effectiveness [42]. Kattimani et al. [106] reported the ring alteration of 3-arylsydnone into 1-aryl-1*H*-pyrazole-3-carbonitriles via a [3 + 2] cycloaddition reaction and were subsequently converted into 5-(1-aryl-1*H*-pyrazol-3-yl)-1*H*-tetrazole. The synthesized compounds were screened for in vivo antihyperglycemic activity using albino Wistar rats. Compounds **229a** and **229b** and **230a–230d** pointedly reduced the blood glucose levels and prevented vascular difficulties in streptozotocin-induced diabetic rats (Figure 12). Compounds **231** and **232** were potent inhibitors of the α -amylase enzyme [107]. Compound **231** showed excellent activity against α -amylase, with an IC_{50} value of 4.08 μ g/mL, followed by **232** with an IC_{50} value of 7.59 μ g/mL. The potency of the compounds was superior to acarbose (IC_{50} value = 8.0 μ g/mL). Pogaku et al. [108] designed and synthesized new pyrazole–triazolopyrimidine hybrids as potent α -glucosidase inhibitors using a one-pot multicomponent approach. Among the evaluated compounds, **233a–c** bearing an electron-withdrawing group on the phenyl ring displayed significant inhibitory activity against the α -glucosidase enzyme. Compound **233a** with the 4-Cl group showed the highest inhibition, with an IC_{50} value of 12.45 μ M, equipotent to the standard drug acarbose (IC_{50} value = 12.68 μ M). In contrast, **233b** with a fluoro substitution at the *para* position displayed an IC_{50} value of 14.47 μ M, followed by **233c** bearing a 4-NO₂ group (IC_{50} value 17.27 μ M). Karrouchi et al. [109] designed and synthesized a pyrazole-3-carbohydrazide, **234**. The in vitro α -glucosidase inhibition study of **234** showed good activity for a concentration of 0.08 mM with a percent inhibition of 79.83%, superior to acarbose (29%). The β -galactosidase evaluation displayed a good inhibitory activity with a percentage of 64.6%, comparable to quercetin (68%) for a concentration of 3.30 mM, while the α -amylase inhibition results revealed an inhibitory activity of 20.51% comparative to the acarbose with a percentage of 36% for a concentration of 3.53 mM. The Rhodanine–pyrazole conjugates were designed and synthesized by Singh et al. [110]. The compounds were further tested for their antidiabetic activity. Among the evaluated compounds, **235a** ($IC_{50} = 2.259 \times 10^{-6}$ mol/L) was the most potent compound, 42-fold superior to acarbose. The unsubstituted hybrid **235b** ($IC_{50} = 2.854 \times 10^{-5}$ mol/L) was 3-fold superior to acarbose. Meanwhile, **235c** ($IC_{50} = 6.377 \times 10^{-5}$ mol/L) and **235d** ($IC_{50} = 1.325 \times 10^{-4}$ mol/L) exhibited strong inhibitory activity against α -amylase comparable to acarbose. Compound **236** has been reported to showed a promising bifunctional antidiabetic effect [111]. A series of new benzo[*d*][1,2,3]triazol-1-yl-pyrazole-bearing dihydro-[1,2,4] triazolo [4,3-*a*]pyrimidine groups have been designed and synthesized [112]. All synthesized compounds were screened in vitro for α -glucosidase inhibition, anticancer (A549 and MCF-7 cell lines), and antioxidant studies. Among all the compounds tested for antidiabetic potential, **237a**, **237b**, and **237c** exhibited substantial inhibition activity, with IC_{50} values of 20.12 ± 0.19 μ M, 21.55 ± 0.46 μ M, and 24.92 ± 0.98 μ M, respectively, compared to the reference compound acarbose ($IC_{50} = 12.68$ μ M) (see Figure 12).

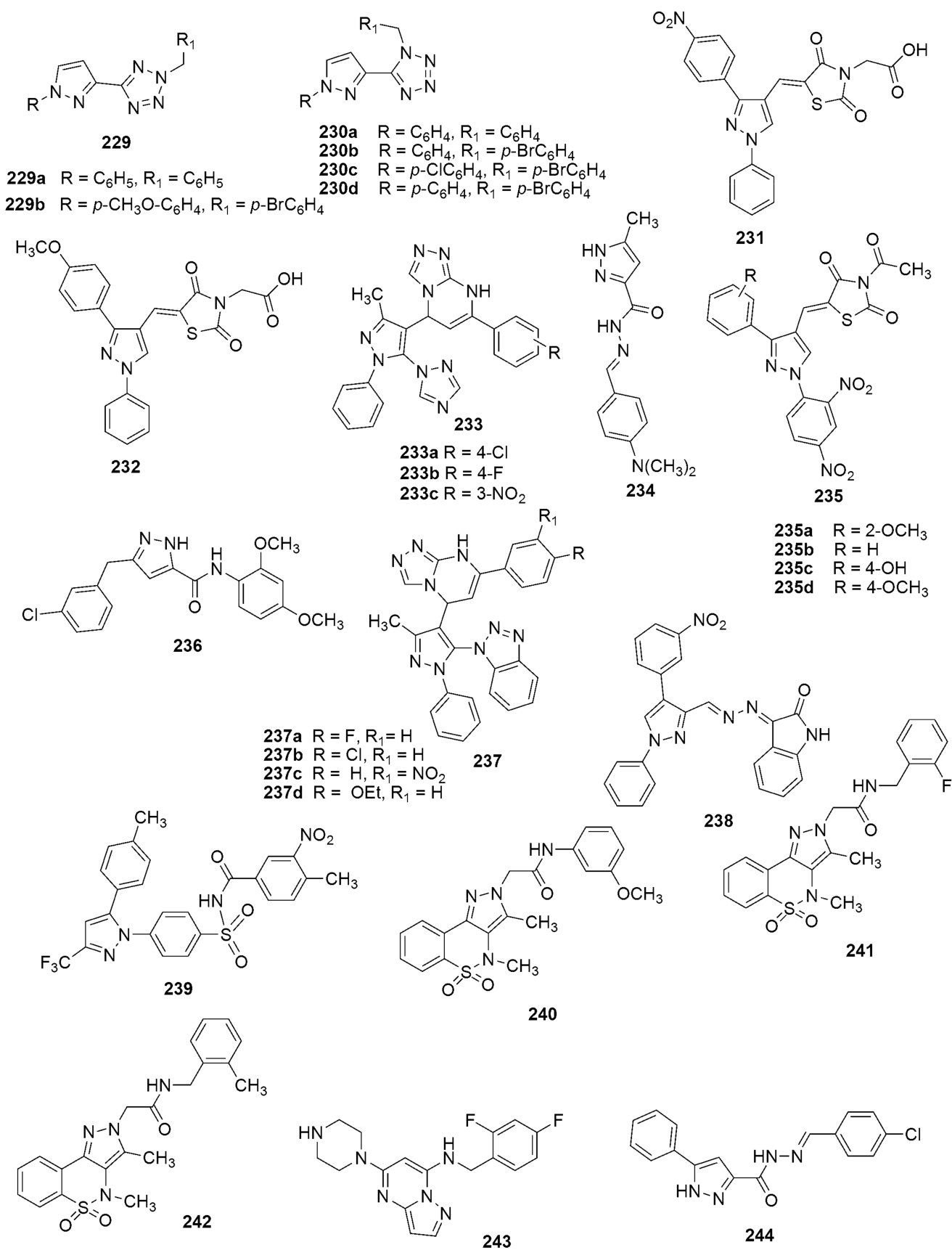


Figure 12. Structures of pyrazole hybrids with antidiabetic activity.

Kaur et al. reported a series of novel isatin–pyrazole hybrids and tested their antidiabetic activity [113]. Among the tested compounds, **238** (Figure 12) appeared to be most potent with $IC_{50} = 3.26 \pm 0.25 \mu\text{M}$, which was ~146-fold more potent than acarbose ($IC_{50} = 478.07 \pm 1.53 \mu\text{M}$). Kausar and coworkers [114] synthesized Celebrex derivatives and investigated their antidiabetic effectiveness. Many of the evaluated compounds exhibited good activity. Compound **239** emerged as the most potent inhibitor of the α -glucosidase enzyme ($IC_{50} = 92.32 \pm 1.530 \mu\text{M}$), comparable to the standard drug acarbose ($IC_{50} = 875.75 \pm 2.08 \mu\text{M}$). Compound **240** exhibited excellent antidiabetic activity ($IC_{50} = 5.8 \mu\text{M}$) compared to the reference acarbose ($IC_{50} = 58.8 \mu\text{M}$) and other evaluated compounds (**241**, $IC_{50} = 65 \mu\text{M}$ and **242**, $IC_{50} = 103 \mu\text{M}$) under the same conditions [115]. Shen described a series of novel pyrazolo [1,5-*a*]pyrimidine derivatives as promising and selective DPP-4 inhibitors [116]. Compound **243** was 2-fold superior to alogliptin ($IC_{50} = 4 \text{ nM}$) and notably selective over DPP-8 and DPP-9 (>2000-fold). The in vivo IPGTT assays in diabetics showed that **243** significantly lowers blood sugar by 48% at 10 mg/kg. The in vitro antidiabetic potential of compound **244** was evaluated against α -glucosidase and α -amylase enzymes. The results revealed that **244** with $IC_{50} = 60.45 \pm 1.23 \mu\text{M}$ showed superior α -glucosidase effectiveness relative to acarbose ($IC_{50} = 89.12 \pm 2.08 \mu\text{M}$) [117]. Nevertheless, compound **244** was inactive against α -amylase (see Figure 12).

4.6. Antileishmanial

The incorporation of a heteroaromatic ring coupled with a 1,3,4-oxadiazole moiety improved the antileishmanial activity. Compounds **245**, **246**, and **247** (Figure 13) proved the dose-dependent killing of the promastigotes with corresponding IC_{50} values of 33.3 ± 1.68 , 40.1 ± 1.0 , and $19.0 \pm 1.47 \mu\text{g/mL}$, respectively [118]. Additionally, the compounds (**245**, **246**, and **247**) displayed IC_{50} values of 44.2 ± 2.72 , 66.8 ± 2.05 , and $73.1 \pm 1.69 \mu\text{g/mL}$, respectively, on amastigote infectivity. These compounds depicted a comparable point in dose-dependent parasite killing with the standard drug, pentamidine ($IC_{50} = 2.6 \pm 0.32 \mu\text{g/mL}$). Camargo et al. synthesized a series of novel pyrazole hybrids [119]. The hybrids were investigated in vitro against the promastigote of *Leishmania amazonensis*. At the same time, the hybrids were examined against the epimastigote of *Trypanosoma cruzi* (*T. cruzi*). The *S*-methyl thiosemicarbazones **248a–248c** and 2-amino-1,3,4-thiadiazole pyrazole hybrids **249a–249c** displayed significant antileishmanial and antitrypanosomal properties. The substitution of Br, OCH₃, or NO₂ at the *para* position of the aryl ring attached at position five of pyrazole favored their activity. The substituent attached to position three of the pyrazole ring also influenced the activity of the evaluated compounds. Silva et al. synthesized and screened a series of 1,5-biaryl 3-arylaminoethyl 4-carboxyethyl pyrazoles and screened against *L. amazonensis* and *T. cruzi* [120]. The most active compounds **249**, **250**, and **251** demonstrated similar profiles against both *L. amazonensis* and *T. cruzi* parasites, describing their dual activity. Meanwhile, compound **249** induced morphological and ultrastructural alterations in the promastigote of *L. amazonensis* (see Figure 13).

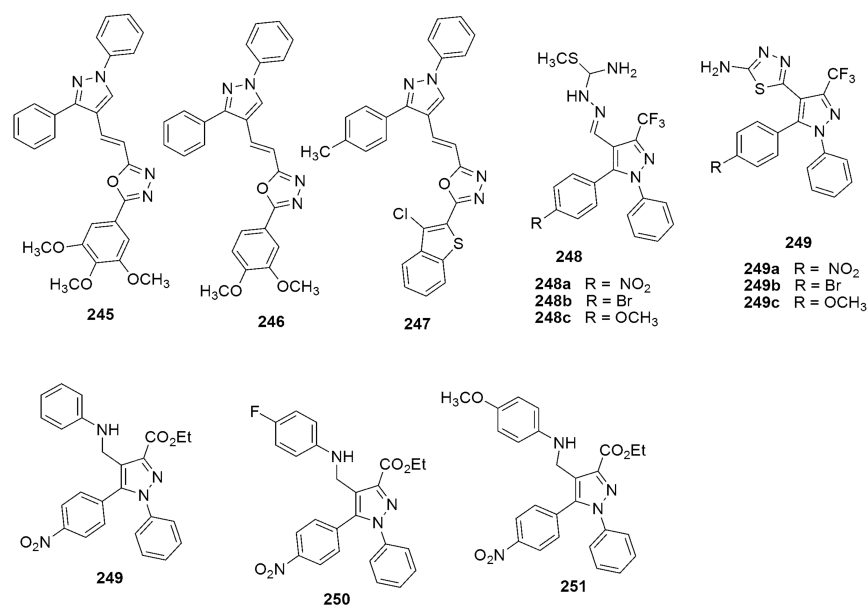


Figure 13. Structures of pyrazoles derivatives with antileishmanial activity.

4.7. Antimalarial

Compound **252** (Figure 13) has been demonstrated to be an excellent inhibitor of Falcipain-2, with an IC₅₀ value of 14 μM [118]. Akolkar et al. [121] have examined the antimalarial potency of **253**, **254**, and **255**. Compounds **253** and **254** (IC₅₀ = 0.47 μM) were equipotent regarding efficacy compared to the standard drug quinine (0.83 μM). The inhibition activity of **255** (0.21 μM) was 4-fold superior to the standard drug. Molecular hybrids of the thiophene, pyrazoline, and benzene rings enhanced the antimalarial activity. Strašek and coworkers [122] reported the synthetic route of the tetrahydropyrazolo [1,2-*a*]pyrazole-1 carboxylates. The reactions yielded mixtures of 7-oxo-2,3,5,6 tetrahydropyrazolo [1,2-*a*]pyrazole-1-carboxamides **256** and **257**. An assessment inhibition of dihydroorotate dehydrogenase of *Plasmodium falciparum* (*Pf*DHODH) was demonstrated. The strongest potency was found in compound **257** with an IC₅₀ value of 2.9 ± 0.3 μM). All the evaluated compounds developed selectivity for *Pf*DHODH more than *Hs*DHODH. Gogoi et al. [123] reported dimethoxy pyrazole 1,3,5-triazine derivatives as a novel class of potent antimalarial agents with good toxicity profiles. Within the series compound **258** was observed as a promising antimalarial agent (see Figure 14).

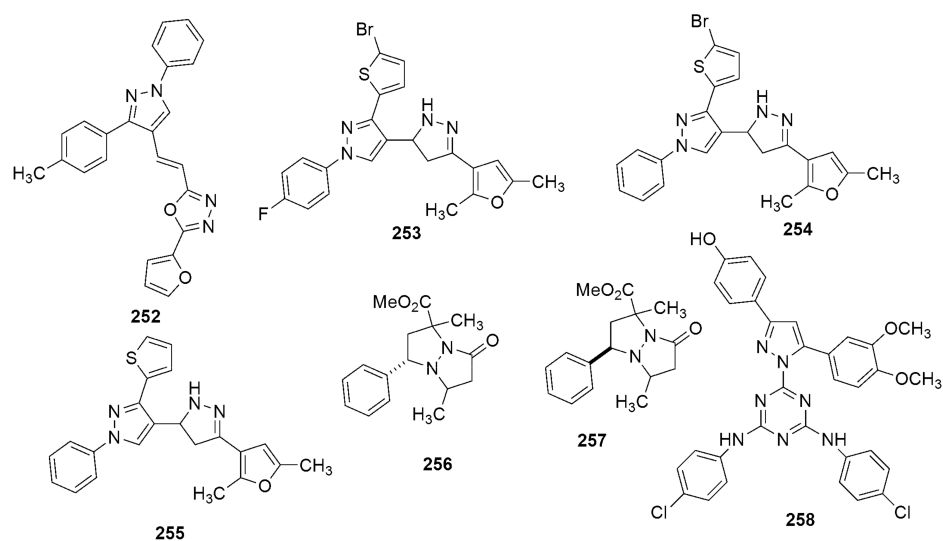


Figure 14. Structures of pyrazoles derivatives as potent antimalarial agents.

4.8. Antioxidant

Antioxidant activities of pyrazoline derivatives were screened using the 2,2-diphenyl-1-picrylhydrazyl (DPPH) radical scavenging method. All the tested compounds showed antioxidant activity [88]. Compound **197c** bearing 4-fluoro and 4-methyl substituents was the most potent antioxidant agent among all the tested compounds at all the concentrations. Compound **234** has been reported as a promising antioxidant agent [109]. Compounds **237d** and **237c** have been revealed as having effective antioxidant activity (IC_{50} values = 4.25 μ M and 5.40 μ M, respectively) [112]. The results of an evaluation of synthesized thiazolidine-2,4-dione-pyrazole conjugates as antioxidant agents showed the efficacy of all the examined compounds [107]. Compounds **259a** and **259b** and **260** (see Figure 14) showed the most potent results, with IC_{50} values of 110.88, 127.18, and 128.55 μ g/mL, respectively. The standard drug ascorbic acid showed an IC_{50} value of 81.12 μ g/mL. The synthesis of functionalized pyrano [2,3-*c*]pyrazoles and pyrazolopyrano [2,3-*d*]pyrimidines containing a bioactive chromone moiety has been achieved, along with their antioxidant activity [124]. The *in vitro* antioxidant activity was determined using DPPH radical scavenging methods. Among the tested hybrids, **261–264** displayed promising activity with all the concentrations in the evaluation with the reference drug. The hybridization of pyranopyrazole with the pyrimidine moiety with substituted NH and OH groups improved the antioxidant properties. Ali et al. [125] reported the synthesis of a novel series of pyrazoline **269a–269e**, phenylpyrazoline **270a–270e**, isoxazoline **271a–271e**, and pyrazoline carbothioamide derivatives **272a–272e** using chalcones as a precursor **268a–268e**. The hybrid compounds were vetted for *in vitro* antioxidant activity using DPPH, nitric oxide (NO), and the superoxide radical scavenging (RSA) assay, along with 15-lipoxygenase (15-LOX) inhibition activity. Pyrazoline carbothioamide derivatives **272a** and **272e** were the most potent anti-LOX compounds, 2.2- and 2.1-fold superior to quercetin, while compounds **269a**, **270e**, **271b**, **271c**, **272a**, **272c**, and **272e** exhibited substantial RSA in all the three *in vitro* assays relative to the ascorbic acid, along with 15-LOX inhibition potency. The presence of electron-donating groups (CH_3 and OCH_3) or halogens (di-Cl) on the benzene ring enhanced the inhibition activity. The potential antioxidant activity of **272a** and **272e** were comparable in all three assays. Compounds **271b**, **271c**, and **271e** (Figure 15) showed significant *in vivo* antioxidant potential compared to the standard group at a dose of 100 mg/kg B.W. Meanwhile, there was an increase in CAT activity, the GSH level, and a decrease in lipid peroxidation in the treated rat liver compared to the control treatment. The *in vitro* antioxidant effectiveness of 4-(arylchalcogenyl)-1*H*-pyrazoles bearing sulfur or 1*H*-pyrazole groups has been investigated in different assays by Oliveira et al. [126], along with their oxidative stress impacts in biological systems. Compounds **273** and **274** showed significant inhibition in the ABTS assay, revealing that the mechanisms of the antioxidant action of compounds **273** and **274** were connected to their ability to donate electrons. Additionally, compounds **273** and **275** are more potent in the NO scavenging assay, while **274** reduced the lipid peroxidation levels in the brain and the liver after 72 h of treatment remarking on the compound efficacy in oxidative stress. A new series of pyrazole-containing heterocyclic skeletons—namely, pyrimidine, triazole, triazepine, pyrrolone, and thiadiazolopyrimidine—along with acylthiourea derivatives, were synthesized from 2-cyano-3-pyrazolylpropenoyl isothiocyanate by Badawy et al. [127]. The antioxidant screening of all the synthesized compounds showed that pyrimidinethione derivatives **276** and **277** were the most potent antioxidant agents. El-Borai et al. [128] achieved a biological evaluation of the cytotoxicity, antihemolytic and antioxidant activities of some thienopyrazole compounds. The antioxidant activity of the examined compounds was achieved by utilizing the DPPH radical scavenging assay with ascorbic acid as the reference. Compound **278** exhibited excellent radical scavenging activity, with an IC_{50} value of 4.49 μ g/mL comparable to an IC_{50} of 4.76 μ g/mL. The excellent antioxidant result was obtained due to the existence of the two amino groups on the pyrimidine ring. Additionally, **279** exhibited strong antihemolytic and antioxidants, justifying that the antioxidant activity may protect red blood cells from hemolysis. The insertion of chlorine atoms, hydroxyl, and

cyanide with a pyrimidine ring in a single moiety enhanced the activity of **279**. In addition, **280** was noxious to all the tested cancerous cell lines; however, a lower cytotoxicity activity against the normal fibroblast cell line was observed. Elnagdy and colleagues [129] described a synthetic route to pyrazole analogs by using copper oxide nanoparticles (CuO-NPs) as catalyzed. The compounds were evaluated for their antioxidant activity using the DPPH radical scavenging assay. Most of the compounds tested demonstrated a greater interaction with the DPPH radical relative to the standard compound Trolox ($IC_{50} = 11.48$ mM). The compounds **281**, **282**, and **283** showed maximum antioxidant activity in the order of **282** > **281** > **283**, with IC_{50} values of 3.06, 3.53, and 5.42 mM, respectively. The ability of **281** and **282** to recover the DPPH radical assay resulted from the prolonged conjugation in compounds, while that of compound **283** was due to a phenolic hydroxyl group at the *ortho*-position and a fluorine group. The condensation reaction between 1,3-thiazole or aminopyridine derivatives and 1*H*-pyrazole,3,5-dimethyl-1*H*-pyrazole or 1,2,4-triazole was described by Kaddouri and colleagues [130]. The reaction produced novel heterocyclic compounds containing pyrazole, thiazole, and pyridine. Additionally, the DPPH scavenging assay was utilized to investigate their antioxidant activity. Ligand **284** showed the best antioxidant activity, with an IC_{50} value of 4.67 $\mu\text{g/mL}$, while the IC_{50} value for the reference compound was 2 $\mu\text{g/mL}$ (ascorbic acid). The applicable route for the direct synthesis of (*E*)-ethyl 2-benzylidene-3-oxobutanoate through the 3 + 2 annulation method, including the investigated in vitro antioxidant vulnerabilities through the DPPH and hydroxyl radical scavenging methods of this compound, have been reported [131]. The assays showed that compound **285** has a strong antioxidant power (see Figure 16).

The multicomponent reaction of some heterocyclic compounds with activated acetylenic, alkyl bromides, triphenylphosphine, and hydrazine in water under ultrasonic irradiation yielded pyrazole derivatives in better yields [132]. Additionally, the antioxidant activities of the compounds were examined using DPPH radical scavenging and the ferric-reducing power assay. Compound **286** (Figure 16) exhibited exceptional DPPH radical scavenging activity and greater reducing power compared to the standard reference butylated hydroxytoluene (BHT) and 2-tertbutylhydroquinone (TBHQ). Compounds **287** and **288** have been reported as more potent antioxidant inhibitors than ascorbic acid and butylated hydroxyanisole (BHA) [133]. The corresponding IC_{50} values for **287** and **288** from the DPPH radical assay were 0.245 ± 0.01 and 0.284 ± 0.02 μM , respectively. These compounds have more potent RSA than ascorbic acid ($IC_{50} = 0.483 \pm 0.01$ μM). In the hydroxyl radical scavenging assay, compounds **287** and **288** showed IC_{50} values of 0.905 ± 0.01 μM and 0.892 ± 0.01 μM , respectively. They displayed greater RSA than BHA ($IC_{50} = 1.739 \pm 0.01$ μM).

Patil et al. [134] prepared sulfonic acid functionalized 1,4-diazabicyclo [2.2.2]octane assisted on Merrifield resin, [MerDABCO- SO_3H]Cl as a catalyst to synthesized pyrazolopyranopyrimidines in one-pot four-component reactions in an excellent yield. The antioxidant effect of the synthesized compounds was determined using the 1,1-diphenyl-2- DPPH radicals scavenging assay, and ascorbic acid was used as a standard control. Among the evaluated compounds, **289–292** showed excellent antioxidant activity compared to the standard ascorbic acid due to the incorporation of an electron-withdrawing substituent (nitro group) on the phenyl ring, enhancing the resonance impact stabilizing the consistently formed radical. Compounds **293** and **294** have been reported as promising antioxidant agents [135] (see Figure 16).

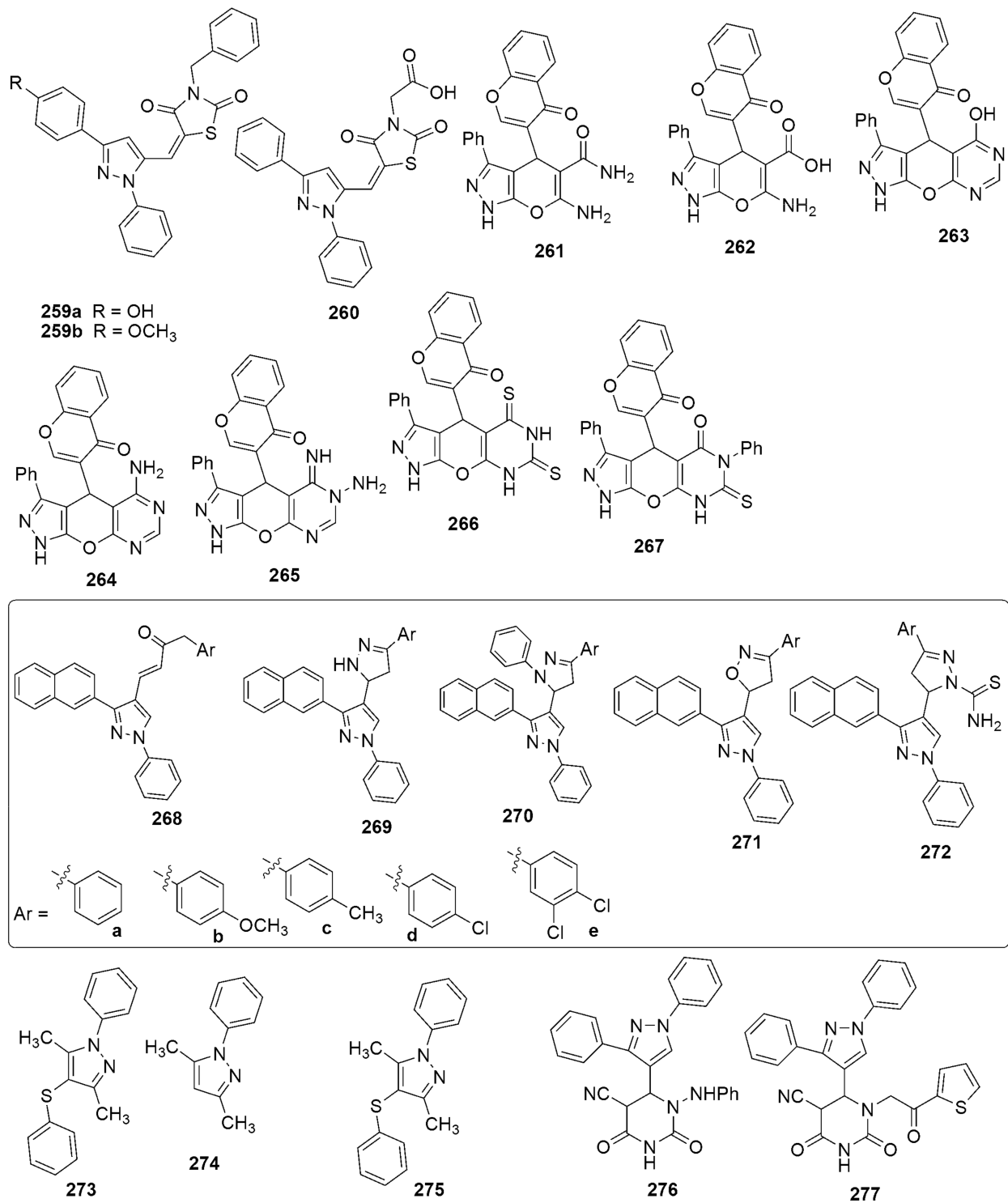


Figure 15. Structures of promising pyrazole derivatives with antioxidant activity.

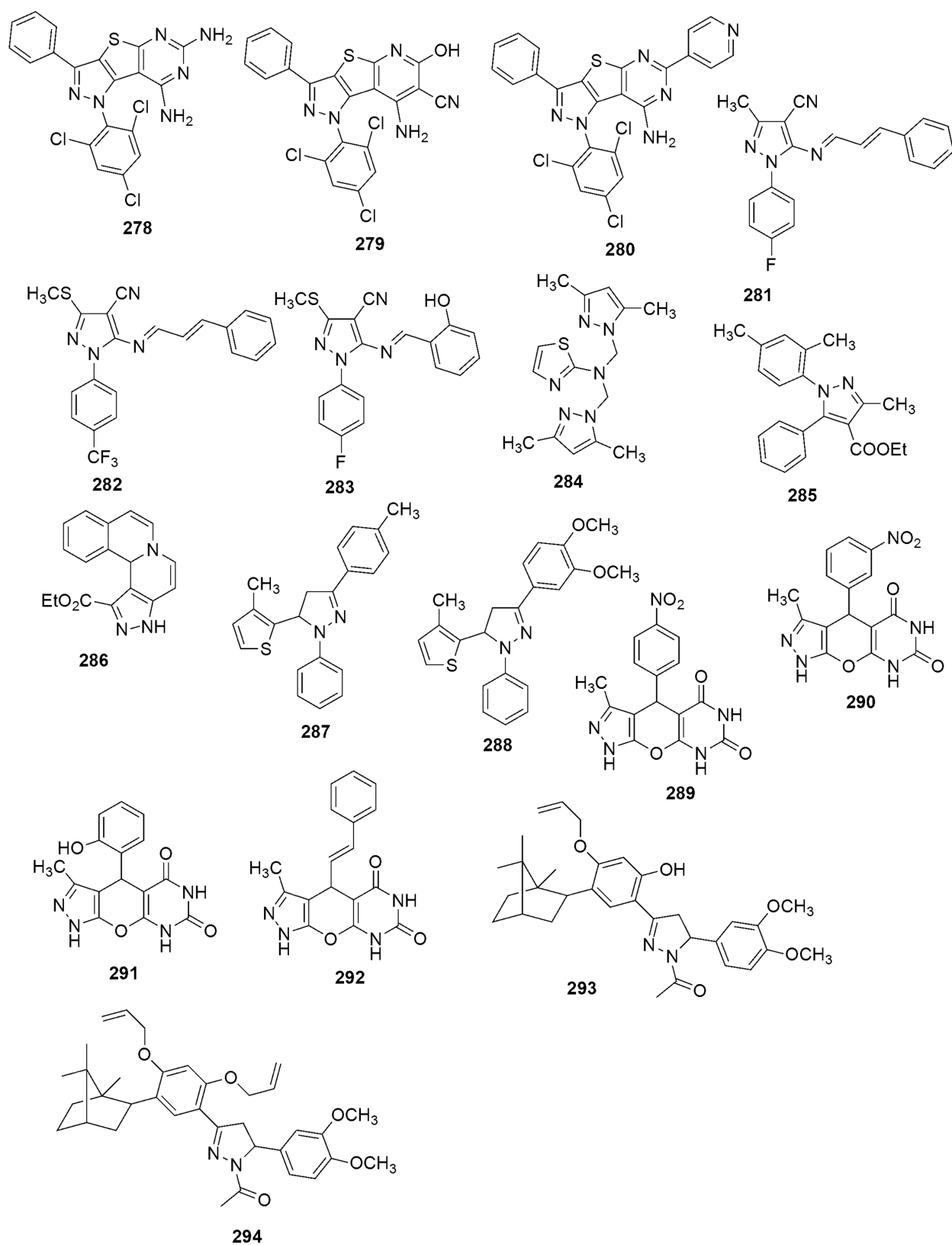


Figure 16. Structures of pyrazole hybrids with antioxidant activity.

4.9. Antituberculosis

Jagdale et al. [136] described the pathway to synthesize thiazolyl-pyrazolyl-1,2,3-triazole derivative **295** and bis-pyrazolyl-1,2,3-triazole **296** derivative, along with their

antimycobacterial activity against *M. tuberculosis* (*Mtb*) with H37Ra dormant and active. The antimycobacterial activity revealed that most of the compounds showed moderate to good activity against both strains of *M. tuberculosis*. Compounds **295a–295c** and **296a** and **296b** exhibited good activity against the *Mtb* H37Ra active strain; also, compounds **295d** and **295e** and **296c–296e** displayed good activity against the *Mtb* H37Ra dormant strain. Using Pd/Cu catalyst coupling-cyclization strategy, 3-indolylmethyl substituted (pyrazolo/benzo) triazinone derivatives have been expediently prepared in a one-pot reaction [137]. The synthesized compounds were tested for chorismate mutase (CM) inhibitory properties in vitro using an assay that measured the enzyme's catalytic activity (MC) in converting chorismate (substrate) to prehenate. The best active compounds, **297** and **298**, showed 78% inhibition at 30 μ M. Meanwhile the concentration-dependent evaluation resulted in IC_{50} values of $0.40 \pm 0.05 \mu$ M and $0.85 \pm 0.10 \mu$ M for compounds **297** and **298**, respectively. Compound **299** has also been shown to maintain good potency against clinical samples from the four main lines and strains containing isoniazid or rifampin resistance mutations [138]. The mutated strains in MmpL3 were resistant to **299** and under replication conditions, and it exhibited bactericidal activity against *Mtb*. However, compound **299** was not effective in an acute model of tubercular infection. This is likely the result of in vivo exposure remaining above the minimum inhibitory level for a restricted period (see Figure 17).

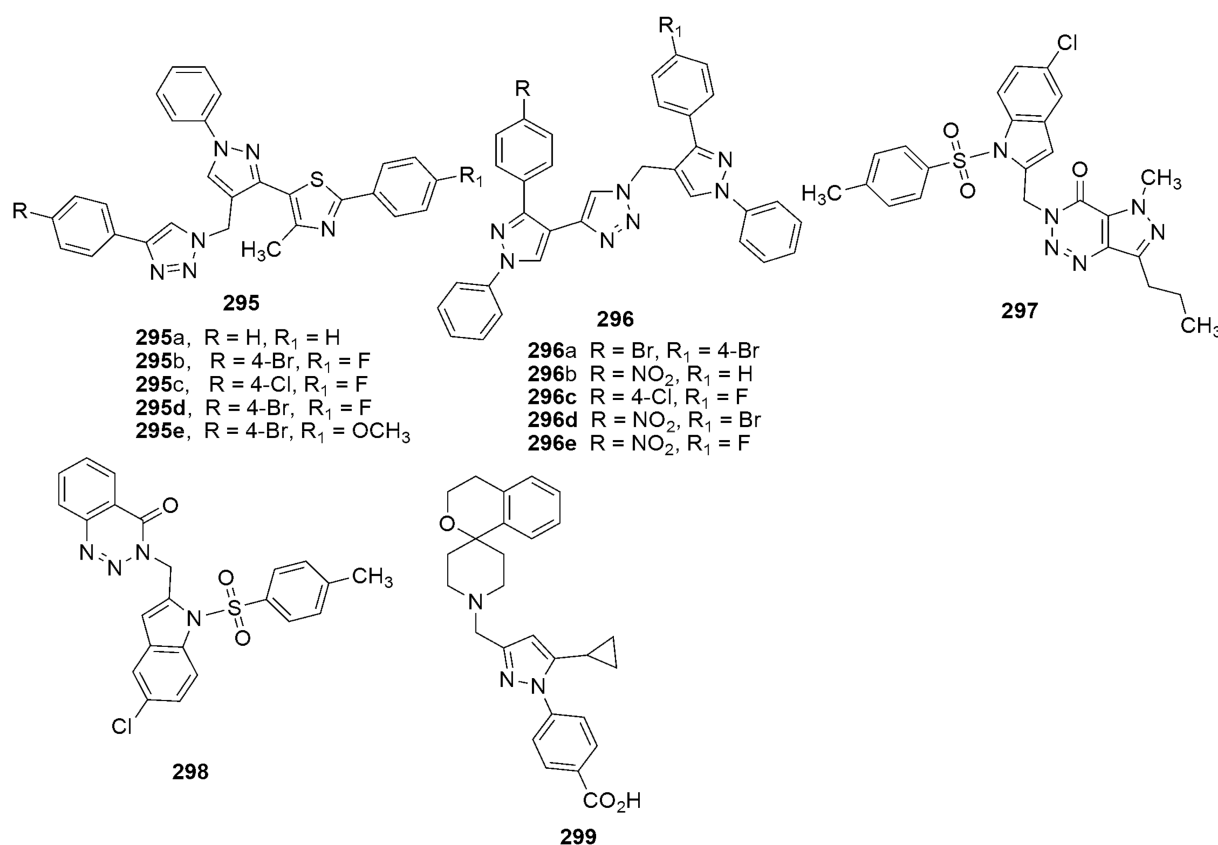


Figure 17. Structures of pyrazole hybrids with antitubercular activity.

Hu and coworkers [139] reported novel series of pyrazolo [1,5-a]pyridine-3-carboxamide (PPA) conjugates bearing diaryl side chains and their antitubercular activity. Most of the evaluated compounds were highly potent in vitro against *Mtb* strains, including H37Rv (MIC = < 0.002–0.381 μ g/mL), rINH (MIC = < 0.002–0.465 μ g/mL), and rRMP (MIC = < 0.002–0.004 μ g/mL). Notably, compound **300** demonstrated favorable in vitro activity against *Mtb* H37Rv, rRMP, and rINH, with corresponding MIC values $\leq 0.002 \mu$ g/mL and a lack of toxicity against Vero cells. Moreover, in vivo studies showed that **300** sub-

stantially lessened the mycobacterial load in a mouse model infected with H37Ra. Other reported antituberculosis pyrazole derivatives and the corresponding references are shown in Table 1.

Table 1. Reported antituberculosis pyrazole derivatives, along with the corresponding references.

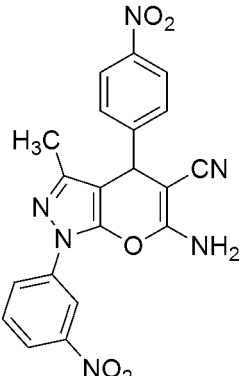
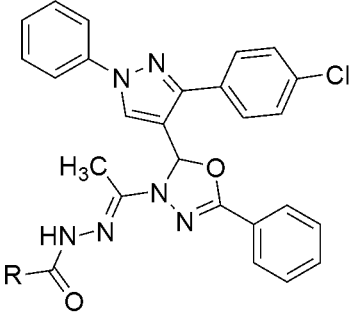
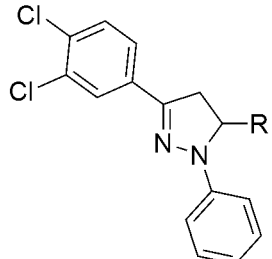
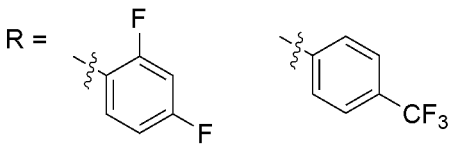
| | | | |
|---|------|--|------|
|  <p style="text-align: center;">301</p> | | [140] | |
| MIC ($\mu\text{g/mL}$) = 25 against H37R _V strain | | | |
|  <p style="text-align: center;">302</p> | | [141] | |
| IC ₅₀ ($\mu\text{g/mL}$) | | | |
| H37Ra | | <i>M. bovis</i> BCG | |
| 302a R = 4-NO ₂ -C ₆ H ₄ | 0.52 | 302f R = 3-CH ₃ -C ₆ H ₄ | 0.92 |
| 302b R = 4-OCH ₃ -C ₆ H ₄ | 0.50 | 302g R = 4-CH ₃ -C ₆ H ₄ | 0.97 |
| 302c R = 4-Cl-C ₆ H ₄ | 0.79 | 302e R = CH ₂ -O-C ₆ H ₄ -2-Cl | 0.62 |
| 302d R = CH ₂ -O-C ₆ H ₄ -2-NO ₂ | 1.48 | | |
| 302e R = CH ₂ -O-C ₆ H ₄ -2-Cl | 0.53 | | |
|  | | [142] | |
|  <p style="text-align: center;">303a 303b</p> | | | |
| MIC (μM) = 3.96 and 3.67 μM against H37R _V | | | |

Table 1. Cont.

| | | | | | | | | | |
|---|--|-----|---|------|--|------|--|------|--|
| | [143] | | | | | | | | |
| <p style="text-align: center;">304 MIC(μM) = 6.25, against H37R_v</p> | | | | | | | | | |
| | [144] | | | | | | | | |
| <p style="text-align: center;">305 MIC (μg/mL) = 25 against H37R_v</p> | | | | | | | | | |
| | [145] | | | | | | | | |
| <p style="text-align: center;">H37R_v MIC(μg/mL)</p> <table border="0" style="width: 100%;"> <tbody> <tr> <td>306a R₁ = 4-F-C₆H₅, R₂ = 3,4-di-F-C₆H₄</td> <td style="text-align: right;">0.8</td> </tr> <tr> <td>306b R₁ = 4-CH₃-C₆H₅, R₂ = 4-Cl-C₆H₅</td> <td style="text-align: right;">3.12</td> </tr> <tr> <td>306c R₁ = 2-OCH₃-C₆H₅, R₂ = 3-CH₃-C₆H₅</td> <td style="text-align: right;">3.12</td> </tr> <tr> <td>306d R₁ = H, R₂ = 3,4-di-Cl-C₆H₄</td> <td style="text-align: right;">6.25</td> </tr> </tbody> </table> | 306a R ₁ = 4-F-C ₆ H ₅ , R ₂ = 3,4-di-F-C ₆ H ₄ | 0.8 | 306b R ₁ = 4-CH ₃ -C ₆ H ₅ , R ₂ = 4-Cl-C ₆ H ₅ | 3.12 | 306c R ₁ = 2-OCH ₃ -C ₆ H ₅ , R ₂ = 3-CH ₃ -C ₆ H ₅ | 3.12 | 306d R ₁ = H, R ₂ = 3,4-di-Cl-C ₆ H ₄ | 6.25 | |
| 306a R ₁ = 4-F-C ₆ H ₅ , R ₂ = 3,4-di-F-C ₆ H ₄ | 0.8 | | | | | | | | |
| 306b R ₁ = 4-CH ₃ -C ₆ H ₅ , R ₂ = 4-Cl-C ₆ H ₅ | 3.12 | | | | | | | | |
| 306c R ₁ = 2-OCH ₃ -C ₆ H ₅ , R ₂ = 3-CH ₃ -C ₆ H ₅ | 3.12 | | | | | | | | |
| 306d R ₁ = H, R ₂ = 3,4-di-Cl-C ₆ H ₄ | 6.25 | | | | | | | | |
| | [146] | | | | | | | | |
| <p style="text-align: center;">MIC(μg/mL) H37R_v</p> | | | | | | | | | |
| 307a R ₁ = H, R ₂ = Cl | 0.78 | | | | | | | | |
| 307b R ₁ = 4-Br, R ₂ = H | 1.56 | | | | | | | | |
| 307c R ₁ = 4-Cl, R ₂ = Cl | 1.56 | | | | | | | | |
| 307d R ₁ = 4-Br, R ₂ = Cl | 1.56 | | | | | | | | |
| 307e R ₁ = 4-Cl, R ₂ = Cl | 1.56 | | | | | | | | |
| 307f R ₁ = 4-Cl, R ₂ = Br | 1.56 | | | | | | | | |
| 307g R ₁ = Br, R ₂ = Br | 1.56 | | | | | | | | |

Table 1. Cont.

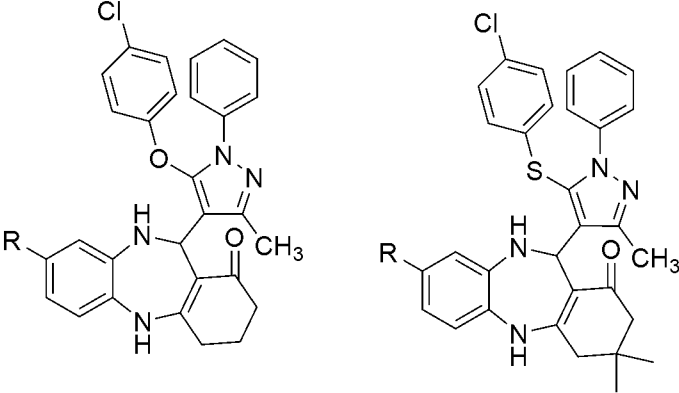
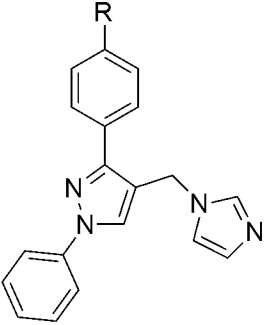
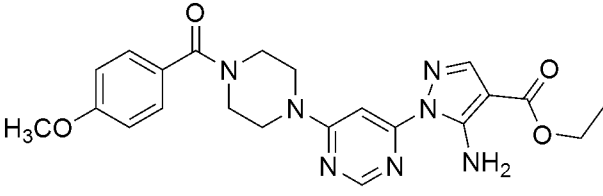
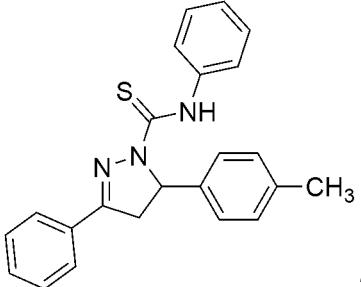
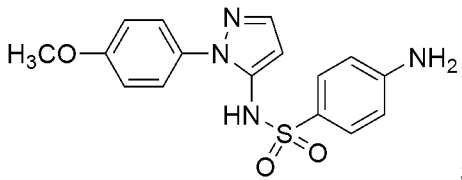
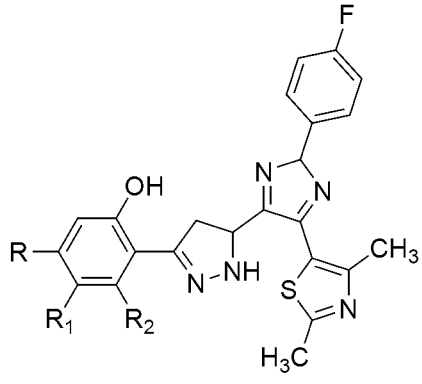
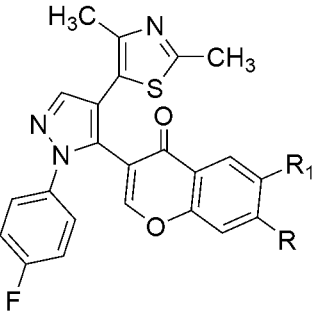
| | | |
|---|-------|-------|
|  | | [147] |
| 308 309 Growth Inhibition (%GI) H37R _v | | |
| 308a R = H | 86 | |
| 308b R = C ₆ H ₅ | 85 | |
| 309a R = H | 90 | |
| 309b R = C ₆ H ₅ | 88 | |
|  | | [148] |
| 310 MIC(μg/mL) H37R _v | | |
| 310a R = isobutyl | 1.562 | |
| 310b R = <i>tert</i> -butyl | 1.562 | |
|  | | [149] |
| 311 MIC(μg/mL) = 1.6, against H37R _v | | |
|  | | [150] |
| 312 MIC(μM) = 17, and MBC(μM) = 34 against H37Ra | | |

Table 1. Cont.

| | | | |
|--|-------|---------------------|-------|
|  | | | [151] |
| <p style="text-align: center;">313</p> <p style="text-align: center;">MIC($\mu\text{g}/\text{mL}$) = 5.96, H37R_v MIC($\mu\text{g}/\text{mL}$) = 10.62, DR-TB</p> | | | |
|  | | | [152] |
| <p style="text-align: center;">314</p> <p style="text-align: center;">MIC($\mu\text{g}/\text{mL}$)</p> | | | |
|  | | | |
| <p style="text-align: center;">315</p> | | | |
| | H37Ra | <i>M. bovis</i> BCG | |
| 314a R = H, R ₁ = Br, R ₂ = H | 2.96 | 0.20 | |
| 314b R = H, R ₁ = Cl, R ₂ = H | 1.16 | 0.72 | |
| 314c R = CH ₃ , R ₁ = H, R ₂ = H | 4.65 | 2.3 | |
| 314d R = CH ₃ , R ₁ = Cl, R ₂ = CH ₃ | 2.5 | 2.26 | |
| 315a R = H, R ₁ = Cl | 2.54 | 0.51 | |
| 315b R = CH ₃ , R ₁ = Cl | 1.72 | 1.33 | |

4.10. Agrochemical

Series of novel pyrazole–isoindoline-1,3-dione hybrids as favorable 4-hydroxyphenylpyruvate dioxygenase (HPPD) inhibitors were designed by combining 2-benzoylthien-1-ol and isoindoline-1,3-dione into a single moiety [153]. Among the evaluated compounds against *Arabidopsis thaliana* HPPD in vitro, using mesotrione and pyrasulfotole as the positive control, the IC₅₀ of **316** (Figure 18) was extended to 90 nM. In addition, **316** was identified as the most promising inhibitor, with a K_i value of 3.92 nM, which was ~10 times superior to pyrasulfotole (K_i = 44 nM) and 300 times marginally superior to mesotrione (K_i = 4.56 nM). Jiang et al. [154] designed and synthesized novel heptacyclic pyrazolamide conjugates using the scaffold hopping approach. The insecticidal activities of all synthesized compounds were examined against *P. xylostella* in vivo at 500 mg/L. Meanwhile, the marketed insecticide—namely, tebufenozide—was used as the reference drug. Compounds **317** and **318** flaunted excellent insecticidal activities (>90%) against *P. xylostella*. Additionally, compound **317** displayed 100% insecticidal activity at the dose of 200 mg/L. The lower dose and LC₅₀ value of **317** (64.13 mg/L) was akin to tebufenozide (LC₅₀ = 33.83 mg/L). Zhao et al. [155] reported a novel series of fluoro-substituted compounds bearing altered pyrazole and their anti-larvicidal effects. The larvicidal activity unveiled fluoro-substituted compounds to have good to excellent activities against *M. separata* and *P. xylostella*. The corresponding LC₅₀ values for **320a** and **320b** against *P. xylostella* were 2.9×10^{-6} mg/L and 3.1×10^{-6} mg/L, respectively, superior to the LC₅₀ of chlorantraniliprole (4.6×10^{-5} mg/L). In addition, fluoro-substituted compounds **320a–320c** bearing ether groups at position three of the pyrazole showed better inhibitory effects than compounds with halogen, amide, or ester groups substituents. The

insertion of fluorine atoms on the ethoxy group enhanced the larvicidal activity. Compound **320a** exhibited the 50% larvicidal mortality against *M. separata* to 0.1 mg/L. Moreover, **320a** displayed 90% larvicidal activity against *P. xylostella* at 10^{-5} mg/L, higher than that of chlorantraniliprole. Judge and colleagues [156] revealed substituted 3-hydroxyproazole derivative **321** as a promising herbicidal agent. Pyridylpyrazole-4-carboxamides bearing 1,3,4-oxadiazole rings were designed and synthesized by dehydration of aromatic hydrazine derivatives and formanilides [157]. The synthesized compounds were further evaluated for their insecticidal activities (*Plutella xylostella*). Among the examined compounds, **322** displayed promising activity as follows, 67%, 50%, 34%, 20%, and 17% activity at the concentrations of 100, 50, 10, 5, and 1 $\mu\text{g/mL}$, respectively (see Figure 18).

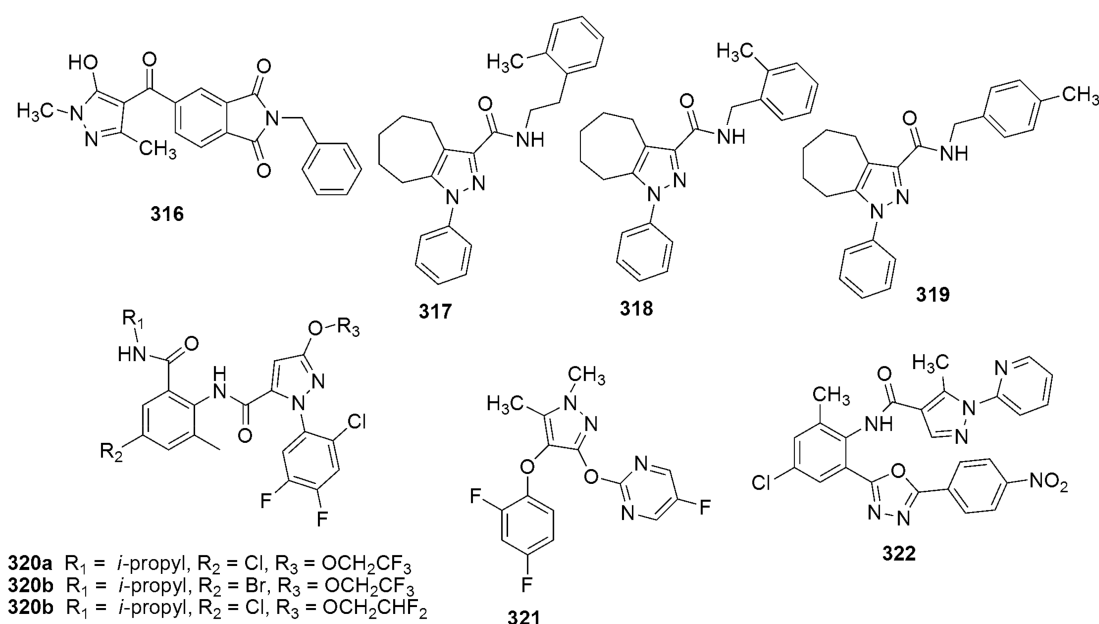


Figure 18. Structures of pyrazole a derivative acting as promising agrochemical agents.

5. Conclusions

Pyrazoles are five-membered heterocyclic compounds containing nitrogen. They are an important class of compounds for drug development; they constitute an essential class of hit compounds to develop new pharmacological agents to treat various infections of clinical primacy. With such a diverse range of biological activities, they have attracted much attention from researchers focusing on synthesizing different pyrazole analogs to develop novel and more effective drugs. This literature review documented various synthetic pathways to pyrazole derivatives and the biological potential of some pyrazole derivatives in recent years. Their biological activity properties, such as antibacterial, analgesic, anti-inflammatory, anticancer, antibacterial, antidiabetic, antioxidant, and agrochemical, were detailed in this review. The information presented in this review will assist prospective researchers in further investigating pyrazole derivatives and update scientists with promising biological activities of recently developed derivatives. Additionally, this will allow them to identify other derivatizations that can be explored. However, where the pyrazole unit itself plays a significant role in the compound's mode of action, including cases where the pyrazole is more of a structural element, still needs to be explored. Additionally, the molecular hybridization of pyrazole with other bioactive compounds will be explored in our future work.

Author Contributions: Conceptualization, O.E. and J.A.T.; Data curation, O.E.; Project administration, J.A.T.; Resources, J.A.T. and M.S.; Supervision, J.A.T. and M.S.; Visualization, O.E.; Roles/Writing—original draft; O.E. Writing—review and editing, O.E. and J.A.T. All authors have read and agreed to the published version of the manuscript.

Funding: This research received no external funding.

Institutional Review Board Statement: Not applicable.

Informed Consent Statement: Not applicable.

Data Availability Statement: Not applicable.

Acknowledgments: J.A.T. acknowledges research funding support from NSERC (Canada).

Conflicts of Interest: The authors declare no conflict of interest.

References

1. Ansari, A.; Ali, A.; Asif, M. Biologically active pyrazole derivatives. *New J. Chem.* **2017**, *41*, 16–41. [[CrossRef](#)]
2. Alam, R.; Wahi, D.; Singh, R.; Sinha, D.; Tandon, V.; Grover, A.; Rahisuddin. Design, synthesis, cytotoxicity, HuTopoII α inhibitory activity and molecular docking studies of pyrazole derivatives as potential anticancer agents. *Bioorg. Chem.* **2016**, *69*, 77–90. [[CrossRef](#)] [[PubMed](#)]
3. Gregory, W.A.; Brittelli, D.R.; Wang, C.; Wuonola, M.A.; McRipley, R.J.; Eustice, D.C.; Eberly, V.S.; Slee, A.M.; Forbes, M.; Bartholomew, P. Antibacterials. Synthesis and structure-activity studies of 3-aryl-2-oxooxazolidines. 1. The B group. *J. Med. Chem.* **1989**, *32*, 1673–1681. [[CrossRef](#)] [[PubMed](#)]
4. Ferreira, S.B.; Sodero, A.C.; Cardoso, M.F.; Lima, E.S.; Kaiser, C.R.; Silva, F.P., Jr.; Ferreira, V.F. Synthesis, biological activity, and molecular modeling studies of 1-h-1, 2, 3-triazole derivatives of carbohydrates as α -glucosidases inhibitors. *J. Med. Chem.* **2010**, *53*, 2364–2375. [[CrossRef](#)] [[PubMed](#)]
5. Ramtohul, Y.K.; Black, C.; Chan, C.-C.; Crane, S.; Guay, J.; Guiral, S.; Huang, Z.; Oballa, R.; Xu, L.-J.; Zhang, L. SAR and optimization of thiazole analogs as potent stearyl-CoA desaturase inhibitors. *Bioorg. Med. Chem. Lett.* **2010**, *20*, 1593–1597. [[CrossRef](#)] [[PubMed](#)]
6. Guo, Y.H.; Wang, G.D.; Wei, L.; Wan, J.P. Domino C-H Sulfonylation and Pyrazole Annulation for Fully Substituted Pyrazole Synthesis in Water Using Hydrophilic Enaminones. *J. Org. Chem.* **2019**, *84*, 2984–2990. [[CrossRef](#)] [[PubMed](#)]
7. Wan, C.; Pang, J.Y.; Jiang, W.; Zhang, X.W.; Hu, X.G. Copper-Catalyzed Reductive Ring-Cleavage of Isoxazoles: Synthesis of Fluoroalkylated Enaminones and Application for the Preparation of Celecoxib, Deracoxib, and Mavacoxib. *J. Org. Chem.* **2021**, *86*, 4557–4566. [[CrossRef](#)]
8. Zhu, C.; Zeng, H.; Liu, C.; Cai, Y.; Fang, X.; Jiang, H. Regioselective Synthesis of 3-Trifluoromethylpyrazole by Coupling of Aldehydes, Sulfonyl Hydrazides, and 2-Bromo-3,3,3-trifluoropropene. *Org. Lett.* **2020**, *22*, 809–813. [[CrossRef](#)]
9. Penning, T.D.; Talley, J.J.; Bertenshaw, S.R.; Carter, J.S.; Collins, P.W.; Docter, S.; Graneto, M.J.; Lee, L.F.; Malecha, J.W.; Miyashiro, J.M.; et al. Synthesis and biological evaluation of the 1,5-diarylpyrazole class of cyclooxygenase-2 inhibitors: Identification of 4-[5-(4-methylphenyl)-3-(trifluoromethyl)-1H-pyrazol-1-yl]benzene nesulfonamide (SC-58635, celecoxib). *J. Med. Chem.* **1997**, *40*, 1347–1365. [[CrossRef](#)]
10. Muzalevskiy, V.M.; Rulev, A.Y.; Romanov, A.R.; Kondrashov, E.V.; Ushakov, I.A.; Chertkov, V.A.; Nenajdenko, V.G. Selective, Metal-Free Approach to 3- or 5-CF(3)-Pyrazoles: Solvent Switchable Reaction of CF(3)-Ynones with Hydrazines. *J. Org. Chem.* **2017**, *82*, 7200–7214. [[CrossRef](#)]
11. Xu, Y.H.; Chen, Q.L.; Tian, Y.S.; Wu, W.; You, Y.; Weng, Z.Q. Silver-catalyzed synthesis of 5-aryl-3-trifluoromethyl pyrazoles. *Tetrahedron Lett.* **2020**, *61*, 151455. [[CrossRef](#)]
12. Poletto, J.; Ribeiro, G.M.; Da Silva, M.J.V.; Jacomini, A.P.; Basso, E.A.; Back, D.F.; Moura, S.; Rosa, F.A. One-Pot Highly Regioselective Synthesis of α -Ketoamide N-Arylpyrazoles from Secondary β -Enamino Diketones. *Org. Lett.* **2019**, *21*, 6325–6328. [[CrossRef](#)] [[PubMed](#)]
13. Golovanov, A.A.; Odin, I.S.; Gusev, D.M.; Vologzhanina, A.V.; Sosnin, I.M.; Grabovskiy, S.A. Reactivity of Cross-Conjugated Enynones in Cyclocondensations with Hydrazines: Synthesis of Pyrazoles and Pyrazolines. *J. Org. Chem.* **2021**, *86*, 7229–7241. [[CrossRef](#)] [[PubMed](#)]
14. Fang, Z.; Yin, H.; Lin, L.; Wen, S.; Xie, L.; Huang, Y.; Weng, Z. Collaborative Activation of Trifluoroacetyl Diazoester by a Lewis Acid and Base for the Synthesis of Polysubstituted 4-Trifluoromethylpyrazoles. *J. Org. Chem.* **2020**, *85*, 8714–8722. [[CrossRef](#)] [[PubMed](#)]
15. Chen, H.H.; Wen, S.L.; Cui, Y.B.; Lin, L.; Zhang, H.B.; Fang, Z.; You, Y.; Weng, Z.Q. A method for synthesis of polysubstituted 4-difluoromethyl and perfluoroalkyl pyrazoles. *Tetrahedron* **2021**, *85*, 132062. [[CrossRef](#)]
16. Kardile, R.D.; Liu, R.S. Gold(I)-Catalyzed Reactions between 2-(1-Alkynyl)-2-alken-1-ones and Vinyldiazo Ketones for Divergent Synthesis of Nonsymmetric Heteroaryl-Substituted Triarylmethanes: N- versus C-Attack Paths. *Org. Lett.* **2020**, *22*, 8229–8233. [[CrossRef](#)]
17. Zhu, J.N.; Wang, W.K.; Jin, Z.H.; Wang, Q.K.; Zhao, S.Y. Pyrrolo 3,4-c pyrazole Synthesis via Copper(I) Chloride-Catalyzed Oxidative Coupling of Hydrazones to Maleimides. *Org. Lett.* **2019**, *21*, 5046–5050. [[CrossRef](#)]
18. Zhu, J.N.; Wang, W.K.; Zheng, J.; Lin, H.P.; Deng, Y.X.; Zhao, S.Y. Iodine-Catalyzed Regioselective Oxidative Cyclization of Aldehyde Hydrazones with Electron-Deficient Olefins for the Synthesis of Mefenpyr-Diethyl. *J. Org. Chem.* **2019**, *84*, 11032–11041. [[CrossRef](#)]

19. Fan, Z.W.; Feng, J.H.; Hou, Y.C.; Rao, M.; Cheng, J.J. Copper-Catalyzed Aerobic Cyclization of α,γ -Unsaturated Hydrazones with Concomitant C=C Bond Cleavage. *Org. Lett.* **2020**, *22*, 7981–7985. [[CrossRef](#)]
20. Veerakanellore, G.B.; Smith, C.M.; Vasiliu, M.; Oliver, A.G.; Dixon, D.A.; Carrick, J.D. Synthesis of 1H-Pyrazol-5-yl-pyridin-2-yl-1,2,4-triazinyl Soft-Lewis Basic Complexants via Metal and Oxidant Free 3+2 Dipolar Cycloaddition of Terminal Ethynyl Pyridines with Tosylhydrazides. *J. Org. Chem.* **2019**, *84*, 14558–14570. [[CrossRef](#)]
21. Zheng, P.F.; Zeng, R.; Jiang, K.; Li, H.W.; Ye, Y.; Mu, C.; Shuai, L.; Quyang, Q.; Chen, Y.C. (3+1) Annulation/Rearrangement Cascade of C,N-Cyclic Azomethine Imines and 3-Chlorooxindoles: Construction of Hexahydroindeno 2,1-c pyrazole Spirooxindole Frameworks. *Org. Lett.* **2019**, *21*, 10052–10056. [[CrossRef](#)] [[PubMed](#)]
22. Dimirjian, C.A.; Reis, M.C.; Balmond, E.I.; Turman, N.C.; Rodriguez, E.P.; Di Maso, M.J.; Fettingner, J.C.; Tantillo, D.J.; Shaw, J.T. Synthesis of Spirobicyclic Pyrazoles by Intramolecular Dipolar Cycloadditions/1s, 5s Sigmatropic Rearrangements. *Org. Lett.* **2019**, *21*, 7209–7212. [[CrossRef](#)] [[PubMed](#)]
23. Carlson, A.S.; Petre, A.M.; Topczewski, J.J. A cascade reaction of cinnamyl azides with vinyl sulfones directly generates dihydropyrrolo-pyrazole heterocycles. *Tetrahedron Lett.* **2021**, *67*, 152860. [[CrossRef](#)] [[PubMed](#)]
24. Bania, N.; Mondal, B.; Ghosh, S.; Pan, S.C. DMAP Catalyzed Domino Rauhut-Currier Cyclization Reaction between Alkylidene Pyrazolones and Nitro-olefins: Access to Tetra hydro-pyrano 2,3-c pyrazoles. *J. Org. Chem.* **2021**, *86*, 4304–4312. [[CrossRef](#)] [[PubMed](#)]
25. Meng, Y.G.; Zhang, T.; Gong, X.C.; Zhang, M.; Zhu, C.Y. Visible-light promoted one-pot synthesis of pyrazoles from alkynes and hydrazines. *Tetrahedron Lett.* **2019**, *60*, 171–174. [[CrossRef](#)]
26. Li, H.X.; Shi, W.Y.; Wang, C.; Liu, H.; Wang, W.; Wu, Y.J.; Guo, H.C. Phosphine-Catalyzed Cascade Annulation of MBH Carbonates and Diazenes: Synthesis of Hexahydrocyclopenta c pyrazole Derivatives. *Org. Lett.* **2021**, *23*, 5571–5575. [[CrossRef](#)]
27. Ahmadzadeh, M.; Sadeghi, M.; Safari, J. Copper(II) Anchored on Amine-Functionalized MMT: A Highly Efficient Catalytic System for the One-Pot Synthesis of Bispyrano 2,3-c pyrazole Derivatives. *J. Chem.* **2021**, *2021*, 1784142. [[CrossRef](#)]
28. Alizadeh-Kouzehrash, M.; Rahmati, A. Synthesis of a structure containing three N-fused heterocycles with very high bond-forming through a one-pot reaction. *Tetrahedron* **2020**, *76*, 130923. [[CrossRef](#)]
29. Dvorak, C.A.; Liang, J.; Mani, N.S.; Carruthers, N.I. Regioselective assembly of fused pyrazole-azepine heterocycles: Synthesis of the 5-HT7 antagonist 1-benzy-1-3-(4-chlorophenyl)-1,4,5,6,7,8-hexahydropyrazolo 3,4-d azepine. *Tetrahedron Lett.* **2021**, *67*, 152843. [[CrossRef](#)]
30. Everson, N.; Yniguez, K.; Loop, L.; Lazaro, H.; Belanger, B.; Koch, G.; Bach, J.; Manjunath, A.; Schioldager, R.; Law, J.; et al. Microwave synthesis of 1-aryl-1H-pyrazole-5-amines. *Tetrahedron Lett.* **2019**, *60*, 72–74. [[CrossRef](#)]
31. Bhale, P.S.; Bandgar, B.P.; Dongare, S.B.; Shringare, S.N.; Sirsat, D.M.; Chavan, H.V. Ketene dithioacetal mediated synthesis of 1,3,4,5-tetrasubstituted pyrazole derivatives and their biological evaluation. *Phosphorus Sulfur Relat. Elem.* **2019**, *194*, 843–849. [[CrossRef](#)]
32. Abd El-Karim, S.S.; Mohamed, H.S.; Abdelhameed, M.F.; Amr, A.E.; Almehezia, A.A.; Nossier, E.S. Design, synthesis and molecular docking of new pyrazole-thiazolidinones as potent anti-inflammatory and analgesic agents with TNF- α inhibitory activity. *Bioorg. Chem.* **2021**, *111*, 104827. [[CrossRef](#)] [[PubMed](#)]
33. Akhtar, W.; Marella, A.; Alam, M.M.; Khan, M.F.; Akhtar, M.; Anwer, T.; Khan, F.; Naematullah, M.; Azam, F.; Rizvi, M.A.; et al. Design and synthesis of pyrazole-pyrazoline hybrids as cancer-associated selective COX-2 inhibitors. *Archiv. Pharm.* **2021**, *354*, 2000116. [[CrossRef](#)] [[PubMed](#)]
34. Abdellatif, K.R.A.; Abdelall, E.K.A.; Elshemy, H.A.H.; El-Nahass, E.; Abdel-Fattah, M.M.; Abdelgawad, Y.Y.M. New indomethacin analogs as selective COX-2 inhibitors: Synthesis, COX-1/2 inhibitory activity, anti-inflammatory, ulcerogenicity, histopathological, and docking studies. *Arch. Pharm.* **2021**, *354*, 2000328. [[CrossRef](#)] [[PubMed](#)]
35. Shi, J.B.; Chen, L.Z.; Wang, B.S.; Huang, X.; Jiao, M.M.; Liu, M.M.; Tang, W.J.; Liu, X.H. Novel Pyrazolo 4,3-d pyrimidine as Potent and Orally Active Inducible Nitric Oxide Synthase (iNOS) Dimerization Inhibitor with Efficacy in Rheumatoid Arthritis Mouse Model. *J. Med. Chem.* **2019**, *62*, 4013–4031. [[CrossRef](#)]
36. Sivaramakarthiskeyan, R.; Shunmugam, I.; Vadivel, S.; Lim, W.M.; Mai, C.W.; Ramalingan, C. Molecular Hybrids Integrated with Benzimidazole and Pyrazole Structural Motifs: Design, Synthesis, Biological Evaluation, and Molecular Docking Studies. *ACS Omega* **2020**, *5*, 10089–10098. [[CrossRef](#)]
37. Nayak, S.G.; Poojary, B.; Kamat, V. Novel pyrazole-clubbed thiophene derivatives via Gewald synthesis as antibacterial and anti-inflammatory agents. *Arch. Pharm.* **2020**, *353*, 2000103. [[CrossRef](#)]
38. Dimmito, M.P.; Stefanucci, A.; Pieretti, S.; Minosi, P.; Dvoracsco, S.; Tomboly, C.; Zengin, G.; Mollica, A. Discovery of Orexant and Anorexant Agents with Indazole Scaffold Endowed with Peripheral Antiedema Activity. *Biomolecules* **2019**, *9*, 492. [[CrossRef](#)]
39. Harras, M.F.; Sabour, R.; Alkamali, O.M. Discovery of new non-acidic lonazolac analogues with COX-2 selectivity as potent anti-inflammatory agents. *MedChemComm* **2019**, *10*, 1775–1788. [[CrossRef](#)]
40. Sivaramakarthiskeyan, R.; Iniyaval, S.; Lim, W.M.; Hii, L.W.; Mai, C.W.; Ramalingan, C. Pyrazolyphenanthroimidazole heterocycles: Synthesis, biological and molecular docking studies. *New J. Chem.* **2020**, *44*, 19612–19622. [[CrossRef](#)]
41. Abdellatif, K.R.A.; El-Saadi, M.T.; Elzayat, S.G.; Amin, N.H. New substituted pyrazole derivatives targeting COXs as potential safe anti-inflammatory agents. *Future Med. Chem.* **2019**, *11*, 1871–1887. [[CrossRef](#)] [[PubMed](#)]

42. Abdellatif, K.R.A.; Fadaly, W.A.A.; Kamel, G.M.; Elshaier, Y.; El-Magd, M.A. Design, synthesis, modeling studies and biological evaluation of thiazolidine derivatives containing pyrazole core as potential anti-diabetic PPAR-gamma agonists and anti-inflammatory COX-2 selective inhibitors. *Bioorg. Chem.* **2019**, *82*, 86–99. [[CrossRef](#)] [[PubMed](#)]
43. Abdelall, E.K.A.; Lamie, P.F.; Ahmed, A.K.M.; El-Nahass, E.S. COX-1/COX-2 inhibition assays and histopathological study of the new designed anti-inflammatory agent with a pyrazolopyrimidine core. *Bioorg. Chem.* **2019**, *86*, 235–253. [[CrossRef](#)] [[PubMed](#)]
44. Thangarasu, P.; Manikandan, A.; Thamaraiselvi, S. Discovery, synthesis and molecular corroborations of medicinally important novel pyrazoles; drug efficacy determinations through in silico, in vitro and cytotoxicity validations. *Bioorg. Chem.* **2019**, *86*, 410–419. [[CrossRef](#)] [[PubMed](#)]
45. Murahari, M.; Mahajan, V.; Neeladri, S.; Kumar, M.S.; Mayur, Y.C. Ligand based design and synthesis of pyrazole based derivatives as selective COX-2 inhibitors. *Bioorg. Chem.* **2019**, *86*, 583–597. [[CrossRef](#)]
46. El-Shoukrofy, M.S.; Abd El Razik, H.A.; Aboulwafa, O.M.; Bayad, A.E.; El-Ashrawy, I.M. Pyrazoles containing thiophene, thienopyrimidine and thienotriazolopyrimidine as COX-2 selective inhibitors: Design, synthesis, in vivo anti-inflammatory activity, docking and in silico chemo-informatic studies. *Bioorg. Chem.* **2019**, *85*, 541–557. [[CrossRef](#)]
47. Khan, M.F.; Anwer, T.; Bakht, A.; Verma, G.; Akhtar, W.; Alam, M.M.; Rizvi, M.A.; Akhter, M.; Shaquiquzzaman, M. Unveiling novel diphenyl-1H-pyrazole based acrylates tethered to 1,2,3-triazole as promising apoptosis inducing cytotoxic and anti-inflammatory agents. *Bioorg. Chem.* **2019**, *87*, 667–678. [[CrossRef](#)]
48. Taher, A.T.; Sarg, M.T.M.; Ali, N.R.E.; Elnagdi, N.H. Design, synthesis, modeling studies and biological screening of novel pyrazole derivatives as potential analgesic and anti-inflammatory agents. *Bioorg. Chem.* **2019**, *89*, 103023. [[CrossRef](#)]
49. Mustafa, G.; Angeli, A.; Zia-ur-Rehman, M.; Akbar, N.; Ishtiaq, S.; Supuran, C.T. An efficient method for the synthesis of novel derivatives 4-[5-(4-(4-amino-5-mercapto-4H-1,2,4-triazol-3-yl)-phenyl)-3-(trifluoroethyl)-pyrazol-1-yl]-benzenesulfonamide and their anti-inflammatory potential. *Bioorg. Chem.* **2019**, *91*, 103110. [[CrossRef](#)]
50. Zabiulla; Gulnaz, A.R.; Mohammed, Y.H.E.; Khanum, S.A. Design, synthesis and molecular docking of benzophenone conjugated with oxadiazole sulphur bridge pyrazole pharmacophores as anti-inflammatory and analgesic agents. *Bioorg. Chem.* **2019**, *92*, 103220. [[CrossRef](#)]
51. Abdellatif, K.R.A.; Fadaly, W.A.A.; Mostafa, Y.A.; Zaher, D.M.; Omar, H.A. Thiohydantoin derivatives incorporating a pyrazole core: Design, synthesis and biological evaluation as dual inhibitors of topoisomerase-I and cyclooxygenase-2 with anti-cancer and anti-inflammatory activities. *Bioorg. Chem.* **2019**, *91*, 103132. [[CrossRef](#)] [[PubMed](#)]
52. Abdellatif, K.R.A.; Abdelall, E.K.A.; Lamie, P.F.; Labib, M.B.; El-Nahaas, E.; Abdelhakeem, M.M. New pyrazole derivatives possessing amino/methanesulphonyl pharmacophore with good gastric safety profile: Design, synthesis, cyclooxygenase inhibition, anti-inflammatory activity and histopathological studies. *Bioorg. Chem.* **2020**, *95*, 103540. [[CrossRef](#)] [[PubMed](#)]
53. Fadaly, W.A.A.; Elshaier, Y.; Hassanein, E.H.M.; Abdellatif, K.R.A. New 1,2,4-triazole/pyrazole hybrids linked to oxime moiety as nitric oxide donor celecoxib analogs: Synthesis, cyclooxygenase inhibition anti-inflammatory, ulcerogenicity, anti-proliferative activities, apoptosis, molecular modeling and nitric oxide release studies. *Bioorg. Chem.* **2020**, *98*, 103752. [[CrossRef](#)] [[PubMed](#)]
54. Gedawy, E.M.; Kassab, A.E.; El Kerdawy, A.M. Design, synthesis and biological evaluation of novel pyrazole sulfonamide derivatives as dual COX-2/5-LOX inhibitors. *Eur. J. Med. Chem.* **2020**, *189*, 112066. [[CrossRef](#)] [[PubMed](#)]
55. Yao, H.Y.; Guo, Q.P.; Wang, M.R.; Wang, R.; Xu, Z.Q. Discovery of pyrazole N-aryl sulfonate: A novel and highly potent cyclooxygenase-2 (COX-2) selective inhibitors. *Bioorg. Med. Chem.* **2021**, *46*, 116344. [[CrossRef](#)]
56. Hendawy, O.M.; Gomaa, H.A.M.; Alzarea, S.I.; Alshammari, M.S.; Mohamed, F.A.M.; Mostafa, Y.A.; Abdelazeem, A.H.; Abdelrahman, M.H.; Trembleau, L.; Youssif, B.G.M. Novel 1,5-diaryl pyrazole-3-carboxamides as selective COX-2/sEH inhibitors with analgesic, anti-inflammatory, and lower cardiotoxicity effects. *Bioorg. Chem.* **2021**, *116*, 105302. [[CrossRef](#)]
57. Amer, M.M.K.; Abdellatif, M.H.; Mouneir, S.M.; Zordok, W.A.; Shehab, W.S. Synthesis, DFT calculation, pharmacological evaluation, and catalytic application in the synthesis of diverse pyrano 2,3-c pyrazole derivatives. *Bioorg. Chem.* **2021**, *114*, 105136. [[CrossRef](#)]
58. Dawood, D.H.; Nossier, E.S.; Ali, M.M.; Mahmoud, A.E. Synthesis and molecular docking study of new pyrazole derivatives as potent anti-breast cancer agents targeting VEGFR-2 kinase. *Bioorg. Chem.* **2020**, *101*, 103916. [[CrossRef](#)]
59. Philoppes, J.N.; Khedr, M.A.; Hassan, M.H.A.; Kamel, G.; Lamie, P.F. New pyrazolopyrimidine derivatives with anticancer activity: Design, synthesis, PIM-1 inhibition, molecular docking study and molecular dynamics. *Bioorg. Chem.* **2020**, *100*, 103944. [[CrossRef](#)]
60. Song, Y.L.; Feng, S.R.; Feng, J.J.; Dong, J.J.; Yang, K.; Liu, Z.M.; Qiao, X.Q. Synthesis and biological evaluation of novel pyrazoline derivatives containing indole skeleton as anti-cancer agents targeting topoisomerase II. *Eur. J. Med. Chem.* **2020**, *200*, 112459. [[CrossRef](#)]
61. Sener, N.; Ozkinali, S.; Altunoglu, Y.C.; Yerlikaya, S.; Gokce, H.; Zurnaci, M.; Gur, M.; Baloglu, M.C.; Sener, I. Antiproliferative properties and structural analysis of newly synthesized Schiff bases bearing pyrazole derivatives and molecular docking studies. *J. Mol. Struct.* **2021**, *1241*, 130520. [[CrossRef](#)]
62. Cai, W.X.; Wu, J.W.; Sun, Y.Z.; Liu, A.L.; Wang, R.L.; Ma, Y.; Wang, S.Q.; Dong, W.L. Synthesis, evaluation, molecular dynamics simulation and targets identification of novel pyrazole-containing imide derivatives. *J. Biomol. Struct. Dyn.* **2021**, *39*, 2176–2188. [[CrossRef](#)]

63. Zimnitskiy, N.S.; Barkov, A.Y.; Ulitko, M.V.; Kutyashev, I.B.; Korotaev, V.Y.; Sosnovskikh, V.Y. An expedient synthesis of novel spiro indenoquinoxaline-pyrrolizidine-pyrazole conjugates with anticancer activity from 1,5-diarylpent-4-ene-1,3-diones through the 1,3-dipolar cycloaddition/cyclocondensation sequence. *New J. Chem.* **2020**, *44*, 16185–16199. [[CrossRef](#)]
64. El Azab, I.H.; El-Sheshtawy, H.S.; Bakr, R.B.; Elkanzi, N.A.A. New 1,2,3-Triazole-Containing Hybrids as Antitumor Candidates: Design, Click Reaction Synthesis, DFT Calculations, and Molecular Docking Study. *Molecules* **2021**, *26*, 708. [[CrossRef](#)] [[PubMed](#)]
65. Ragab, F.A.; Nissan, Y.M.; Seif, E.M.; Maher, A.; Arafa, R.K. Synthesis and in vitro investigation of novel cytotoxic pyrimidine and pyrazolopyrimidine derivatives showing apoptotic effect. *Bioorg. Chem.* **2020**, *96*, 103621. [[CrossRef](#)]
66. Mohamady, S.; Ismail, M.I.; Mogheith, S.M.; Attia, Y.M.; Taylor, S.D. Discovery of 5-aryl-3-thiophen-2-yl-1H-pyrazoles as a new class of Hsp90 inhibitors in hepatocellular carcinoma. *Bioorg. Chem.* **2020**, *94*, 103433. [[CrossRef](#)]
67. El Azab, I.H.; Bakr, R.B.; Elkanzi, N.A.A. Facile One-Pot Multicomponent Synthesis of Pyrazolo-Thiazole Substituted Pyridines with Potential Anti-Proliferative Activity: Synthesis, In Vitro and In Silico Studies. *Molecules* **2021**, *26*, 3103. [[CrossRef](#)]
68. Wang, G.C.; Liu, W.J.; Peng, Z.Y.; Huang, Y.; Gong, Z.P.; Li, Y.J. Design, synthesis, molecular modeling, and biological evaluation of pyrazole-naphthalene derivatives as potential anticancer agents on MCF-7 breast cancer cells by inhibiting tubulin polymerization. *Bioorg. Chem.* **2020**, *103*, 104141. [[CrossRef](#)]
69. Mohamed, M.F.; Saddiq, A.A.; Abdelhamid, I.A. Attacking the mitochondria of colorectal carcinoma by novel 2-cyanoacrylamides linked to ethyl 1,3-diphenylpyrazole-4-carboxylates moiety as a new trend for chemotherapy. *Bioorg. Chem.* **2020**, *103*, 104195. [[CrossRef](#)]
70. Burgart, Y.V.; Agafonova, N.A.; Shchegolkov, E.V.; Krasnykh, O.P.; Kushch, S.O.; Evstigneeva, N.P.; Gerasimova, N.A.; Maslova, V.V.; Triandafilova, G.A.; Solodnikov, S.Y.; et al. Multiple biological active 4-aminopyrazoles containing trifluoromethyl and their 4-nitroso-precursors: Synthesis and evaluation. *Eur. J. Med. Chem.* **2020**, *208*, 112768. [[CrossRef](#)]
71. Anwer, K.E.; Sayed, G.H. Conventional and microwave reactions of 1,3-diaryl-5,4-enaminonitrile-pyrazole derivative with expected antimicrobial and anticancer activities. *J. Heterocycl. Chem.* **2020**, *57*, 2339–2353. [[CrossRef](#)]
72. Hassan, A.Y.; Saleh, N.M.; Kadh, M.S.; Abou-Amra, E.S. New fused pyrazolopyrimidine derivatives; heterocyclic styling, synthesis, molecular docking and anticancer evaluation. *J. Heterocycl. Chem.* **2020**, *57*, 2704–2721. [[CrossRef](#)]
73. Kolluri, P.K.; Gurrupu, N.; Subhashini, N.; Putta, S.; Singh, S.S.; Vani, T.; Manga, V. Design, synthesis of novel (Z)-2-(3-(4-((3-benzyl-2,4-dioxothiazolidin-5-ylidene) methyl)-1-phenyl-1H-pyrazol-3-yl) phenoxy)-N-arylacetamide derivatives: Evaluation of cytotoxic activity and molecular docking studies. *J. Mol. Struct.* **2020**, *1202*, 127300. [[CrossRef](#)]
74. Mamidala, S.; Aravilli, R.K.; Ramesh, G.; Khajavali, S.; Chedupaka, R.; Manga, V.; Vedula, R.R. A facile one-pot, three-component synthesis of a new series of thiazolyl pyrazole carbaldehydes: In vitro anticancer evaluation, in silico ADME/T, and molecular docking studies. *J. Mol. Struct.* **2021**, *1236*, 130356. [[CrossRef](#)]
75. Raghu, M.S.; Kumar, C.B.P.; Prashanth, M.K.; Kumar, K.Y.; Prathibha, B.S.; Kanthimathi, G.; Alissa, S.A.; Alghulikah, H.A.; Osman, S.M. Novel 1,3,5-triazine-based pyrazole derivatives as potential antitumor agents and EGFR kinase inhibitors: Synthesis, cytotoxicity, DNA binding, molecular docking and DFT studies. *New J. Chem.* **2021**, *45*, 13909–13924. [[CrossRef](#)]
76. Mohammed, E.Z.; Mahmoud, W.R.; George, R.F.; Hassan, G.S.; Omar, F.A.; Georgey, H.H. Synthesis, in vitro anticancer activity and in silico studies of certain pyrazole-based derivatives as potential inhibitors of cyclin dependent kinases (CDKs). *Bioorg. Chem.* **2021**, *116*, 105347. [[CrossRef](#)]
77. Suryanarayana, K.; Robert, A.R.; Kerru, N.; Pooventhiran, T.; Thomas, R.; Maddila, S.; Jonnalagadda, S.B. Design, synthesis, anticancer activity and molecular docking analysis of novel dinitrophenylpyrazole bearing 1,2,3-triazoles. *J. Mol. Struct.* **2021**, *1243*, 130865. [[CrossRef](#)]
78. Wang, Y.Y.; Shi, W.; Wu, C.L.; Wan, L.; Zhao, Y.X.; Zhang, C.L.; Gu, W.; Wang, S.F. Pyrazole ring-containing isolongifolanone derivatives as potential CDK2 inhibitors: Evaluation of anticancer activity and investigation of action mechanism. *Biomed. Pharmacother.* **2021**, *139*, 111663. [[CrossRef](#)]
79. Signorello, M.G.; Rapetti, F.; Meta, E.; Sidibè, A.; Bruno, O.; Brullo, C. New Series of Pyrazoles and Imidazo-Pyrazoles Targeting Different Cancer and Inflammation Pathways. *Molecules* **2021**, *26*, 5735. [[CrossRef](#)]
80. Alfei, S.; Brullo, C.; Caviglia, D.; Piatti, G.; Zorzoli, A.; Marimpietri, D.; Zuccari, G.; Schito, A.M. Pyrazole-Based Water-Soluble Dendrimer Nanoparticles as a Potential New Agent against Staphylococci. *Biomedicines* **2021**, *10*, 17. [[CrossRef](#)]
81. Morretta, E.; Sidibè, A.; Spallarossa, A.; Petrella, A.; Meta, E.; Bruno, O.; Monti, M.C.; Brullo, C. Synthesis, functional proteomics and biological evaluation of new 5-pyrazolyl ureas as potential anti-angiogenic compounds. *Eur. J. Med. Chem.* **2021**, *226*, 113872. [[CrossRef](#)] [[PubMed](#)]
82. Ebenezer, O.; Awolade, P.; Koorbanally, N.; Singh, P. New library of pyrazole-imidazo 1,2-alpha pyridine molecular conjugates: Synthesis, antibacterial activity and molecular docking studies. *Chem. Biol. Drug Des.* **2020**, *95*, 162–173. [[CrossRef](#)] [[PubMed](#)]
83. El-Shershaby, M.H.; El-Gamal, K.M.; Bayoumi, A.H.; El-Adl, K.; Alswah, M.; Ahmed, H.E.A.; Al-Karmalamy, A.A.; Abulkhair, H.S. The antimicrobial potential and pharmacokinetic profiles of novel quinoline-based scaffolds: Synthesis and in silico mechanistic studies as dual DNA gyrase and DHFR inhibitors. *New J. Chem.* **2021**, *45*, 13986–14004. [[CrossRef](#)]
84. Hansa, R.K.C.; Khan, M.M.K.; Frangie, M.M.; Gilmore, D.F.; Shelton, R.S.; Savenka, A.V.; Basnakian, A.G.; Shuttleworth, S.L.; Smeltzer, M.S.; Alam, M.A. 4-(4-(Anilinomethyl)-3-(4-(trifluoromethyl)phenyl)-1H-pyrazol-1-yl)benzoic acid derivatives as potent anti-gram-positive bacterial agents. *Eur. J. Med. Chem.* **2021**, *219*, 113402. [[CrossRef](#)]
85. Liu, H.; Chu, Z.W.; Xia, D.G.; Cao, H.Q.; Lv, X.H. Discovery of novel multi-substituted benzo-indole pyrazole schiff base derivatives with antibacterial activity targeting DNA gyrase. *Bioorg. Chem.* **2020**, *99*, 103807. [[CrossRef](#)]

86. Patel, B.; Zunk, M.; Grant, G.; Rudrawar, S. Design, synthesis and bioactivity evaluation of novel pyrazole linked phenylthiazole derivatives in context of antibacterial activity. *Bioorg. Med. Chem. Lett.* **2021**, *39*, 127853. [[CrossRef](#)]
87. Ebenezer, O.; Singh-Pillay, A.; Koorbanally, N.A.; Singh, P. Antibacterial evaluation and molecular docking studies of pyrazole-thiosemicarbazones and their pyrazole-thiazolidinone conjugates. *Mol. Divers.* **2021**, *25*, 191–204. [[CrossRef](#)]
88. Bhirud, J.D.; Patil, R.D.; Narkhede, H.P. Sulfamic acid catalyzed synthesis of new 3,5- (sub)phenyl -1H-pyrazole bearing N-1-isonicotinoyl: And their pharmacological activity evaluation. *Bioorg. Med. Chem. Lett.* **2020**, *30*, 127558. [[CrossRef](#)]
89. Ibrahim, S.A.; Fayed, E.A.; Rizk, H.F.; Desouky, S.E.; Ragab, A. Hydrazonoyl bromide precursors as DHFR inhibitors for the synthesis of bis-thiazolyl pyrazole derivatives; antimicrobial activities, antibiofilm, and drug combination studies against MRSA. *Bioorg. Chem.* **2021**, *116*, 105339. [[CrossRef](#)]
90. Desai, N.C.; Vaja, D.V.; Monapara, J.D.; Manga, V.; Vani, T. Synthesis, biological evaluation, and molecular docking studies of novel pyrazole, pyrazoline-clubbed pyridine as potential antimicrobial agents. *J. Heterocycl. Chem.* **2021**, *58*, 737–750. [[CrossRef](#)]
91. Saber, A.F.; Zaki, R.M.; El-Dean, A.M.K.; Radwan, S.M. Synthesis, reactions, and spectral characterization of some new biologically active compounds derived from thieno 2,3-c pyrazole-5-carboxamide. *J. Heterocycl. Chem.* **2020**, *57*, 238–247. [[CrossRef](#)]
92. Othman, I.M.M.; Gad-Elkareem, M.A.M.; Amr, A.E.; Al-Omar, M.A.; Nossier, E.S.; Elsayed, E.A. Novel heterocyclic hybrids of pyrazole targeting dihydrofolate reductase: Design, biological evaluation and insilicostudies. *J. Enzyme Inhib. Med. Chem.* **2020**, *35*, 1491–1502. [[CrossRef](#)] [[PubMed](#)]
93. Yu, B.; Zhou, S.; Cao, L.; Hao, Z.; Yang, D.; Guo, X.; Zhang, N.; Bakulev, V.A.; Fan, Z. Design, Synthesis, and Evaluation of the Antifungal Activity of Novel Pyrazole–Thiazole Carboxamides as Succinate Dehydrogenase Inhibitors. *J. Agric. Food Chem.* **2020**, *68*, 7093–7102. [[CrossRef](#)] [[PubMed](#)]
94. Wang, X.B.; Wang, A.; Qu, L.L.; Chen, M.; Lu, A.M.; Li, G.H.; Yang, C.L.; Xue, W. Expedient Discovery for Novel Antifungal Leads Targeting Succinate Dehydrogenase: Pyrazole-4-formylhydrazide Derivatives Bearing a Diphenyl Ether Fragment. *J. Agric. Food Chem.* **2020**, *68*, 14426–14437. [[CrossRef](#)]
95. Zhao, Y.T.; Yang, N.; Deng, Y.M.; Tao, K.; Jin, H.; Hou, T.P. Mechanism of Action of Novel Pyrazole Carboxamide Containing a Diarylamine Scaffold against *Rhizoctonia solani*. *J. Agric. Food Chem.* **2020**, *68*, 11068–11076. [[CrossRef](#)]
96. Tan, F.S.; Su, S.N.; Liu, Z.Z. Green synthesis and antifungal activities of novel 3-(trifluoromethyl)-4,5-dihydro-1H-furo 2,3-c pyrazole derivatives. *J. Heterocycl. Chem.* **2020**, *57*, 2904–2910. [[CrossRef](#)]
97. Kaddouri, Y.; Abridgach, F.; Ouahhoud, S.; Benabbes, R.; El Kodadi, M.; Alsalmé, A.; Al-Zaqri, N.; Warad, I.; Touzani, R. Synthesis, characterization, reaction mechanism prediction and biological study of mono, bis and tetrakis pyrazole derivatives against *Fusarium oxysporum* f. sp. *Albedinis* with conceptual DFT and ligand-protein docking studies. *Bioorg. Chem.* **2021**, *110*, 104696. [[CrossRef](#)]
98. Masaret, G.S. A New Approach for the Synthesis and Biological Activities of Novel Thiazolyl-Pyrazole Derivatives. *ChemistrySelect* **2021**, *6*, 974–982. [[CrossRef](#)]
99. Phougat, H.; Devi, V.; Rai, S.; Reddy, T.S.; Singh, K. Urea derivatives of piperazine doped with pyrazole-4-carboxylic acids: Synthesis and antimicrobial evaluation. *J. Heterocycl. Chem.* **2021**, *58*, 1992–1999. [[CrossRef](#)]
100. Dong, C.T.; Gao, W.; Li, X.T.; Sun, S.S.; Huo, J.Q.; Wang, Y.E.; Ren, D.; Zhang, J.L.; Chen, L. Synthesis of pyrazole-4-carboxamides as potential fungicide candidates. *Mol. Divers.* **2021**, *25*, 2379–2388. [[CrossRef](#)]
101. Makhanya, T.R.; Gengan, R.M.; Kasumbwe, K. Synthesis of Fused Indolo-Pyrazoles and Their Antimicrobial and Insecticidal Activities against *Anopheles arabiensis* Mosquito. *ChemistrySelect* **2020**, *5*, 2756–2762. [[CrossRef](#)]
102. Bayazeed, A.; Alshehrei, F.; Muhammad, Z.A.; Alfahmi, G.; El-Metwally, N.; Farghaly, T.A. Synthesis of Coumarin-Analogues: Analytical, Spectral, Conformational, MOE-Docking and Antimicrobial Studies. *ChemistrySelect* **2020**, *5*, 3874–3891. [[CrossRef](#)]
103. Wang, X.B.; Wang, M.Q.; Han, L.; Jin, F.; Jiao, J.; Chen, M.; Yang, C.L.; Xue, W. Novel Pyrazole-4-acetohydrazide Derivatives Potentially Targeting Fungal Succinate Dehydrogenase: Design, Synthesis, Three-Dimensional Quantitative Structure-Activity Relationship, and Molecular Docking. *J. Agric. Food Chem.* **2021**, *69*, 9557–9570. [[CrossRef](#)] [[PubMed](#)]
104. Wu, Z.B.; Park, H.Y.; Xie, D.W.; Yang, J.X.; Hou, S.T.; Shahzad, N.; Kim, C.K.; Yang, S. Synthesis, Biological Evaluation, and 3D-QSAR Studies of N-(Substituted pyridine-4-yl)-1-(substituted phenyl)-5-trifluoromethyl-1H-pyrazole-4-carboxamide Derivatives as Potential Succinate Dehydrogenase Inhibitors. *J. Agric. Food Chem.* **2021**, *69*, 1214–1223. [[CrossRef](#)] [[PubMed](#)]
105. Xia, D.G.; Cheng, X.; Liu, X.H.; Zhang, C.Q.; Wang, Y.X.; Liu, Q.Y.; Zeng, Q.; Huang, N.Q.; Cheng, Y.; Lv, X.H. Discovery of Novel Pyrazole Carboxylate Derivatives Containing Thiazole as Potential Fungicides. *J. Agric. Food Chem.* **2021**, *69*, 8358–8365. [[CrossRef](#)] [[PubMed](#)]
106. Kattimani, P.P.; Somagond, S.M.; Bayannavar, P.K.; Kamble, R.R.; Bijjaragi, S.C.; Hunnur, R.K.; Joshi, S.D. Novel 5-(1-aryl-1H-pyrazol-3-yl)-1H-tetrazoles as glycogen phosphorylase inhibitors: An in vivo antihyperglycemic activity study. *Drug Dev. Res.* **2020**, *81*, 70–84. [[CrossRef](#)]
107. Bansal, G.; Singh, S.; Monga, V.; Thanikachalam, P.V.; Chawla, P. Synthesis and biological evaluation of thiazolidine-2,4-dione-pyrazole conjugates as antidiabetic, anti-inflammatory and antioxidant agents. *Bioorg. Chem.* **2019**, *92*, 103271. [[CrossRef](#)]
108. Pogaku, V.; Gangarapu, K.; Basavoju, S.; Tatapudi, K.K.; Katragadda, S.B. Design, synthesis, molecular modelling, ADME prediction and antihyperglycemic evaluation of new pyrazole-triazolopyrimidine hybrids as potent alpha-glucosidase inhibitors. *Bioorg. Chem.* **2019**, *93*, 103307. [[CrossRef](#)]

109. Karrouchi, K.; Brandan, S.A.; Sert, Y.; El-marzouqi, H.; Radi, S.; Ferbinteanu, M.; Faouzi, M.E.; Garcia, Y.; Ansar, M. Synthesis, X-ray structure, vibrational spectroscopy, DFT, biological evaluation and molecular docking studies of (E)-N'-(4-(dimethylamino)benzylidene)-5-methyl-1H-pyrazole-3-carbohydrazide. *J. Mol. Struct.* **2020**, *1219*, 128541. [[CrossRef](#)]
110. Singh, P.; Mothilal, S.; Kerru, N.; Singh-Pillay, A.; Gummidi, L.; Erukainure, O.L.; Islam, M.S. Comparative -glucosidase and -amylase inhibition studies of rhodanine-pyrazole conjugates and their simple rhodanine analogues. *Med. Chem. Res.* **2019**, *28*, 143–159. [[CrossRef](#)]
111. Jo, J.; Lee, D.; Park, Y.H.; Choi, H.; Han, J.; Park, D.H.; Choi, Y.K.; Kwak, J.; Yang, M.K.; Yoo, J.W.; et al. Discovery and optimization of novel 3-benzyl-N-phenyl-1H-pyrazole-5-carboxamides as bifunctional antidiabetic agents stimulating both insulin secretion and glucose uptake. *Eur. J. Med. Chem.* **2021**, *217*, 113325. [[CrossRef](#)] [[PubMed](#)]
112. Pogaku, V.; Krishnan, R.; Basavoju, S. Synthesis and biological evaluation of new benzo d 1,2,3 triazol-1-yl-pyrazole-based dihydro- 1,2,4 triazolo 4,3-a pyrimidines as potent antidiabetic, anticancer and antioxidant agents. *Res. Chem. Intermed.* **2021**, *47*, 551–571. [[CrossRef](#)]
113. Kaur, R.; Palta, K.; Kumar, M. Hybrids of Isatin-Pyrazole as Potential α -Glucosidase Inhibitors: Synthesis, Biological Evaluations and Molecular Docking Studies. *ChemistrySelect* **2019**, *4*, 13219–13227. [[CrossRef](#)]
114. Kausar, N.; Ullah, S.; Khan, M.A.; Zafar, H.; Atia tul, W.; Choudhary, M.I.; Yousuf, S. Celebex derivatives: Synthesis, α -glucosidase inhibition, crystal structures and molecular docking studies. *Bioorg. Chem.* **2021**, *106*, 104499. [[CrossRef](#)] [[PubMed](#)]
115. Taj, S.; Ahmad, M.; Alshammari, A.; Alghamdi, A.; Ali Ashfaq, U. Exploring the therapeutic potential of benzothiazine-pyrazole hybrid molecules against alpha-glucosidase: Pharmacological and molecular modelling based approach. *Saudi J. Biol. Sci.* **2021**, *29*, 1416–1421. [[CrossRef](#)]
116. Shen, J.; Deng, X.; Sun, R.; Tavallaie, M.S.; Wang, J.; Cai, Q.; Lam, C.; Lei, S.; Fu, L.; Jiang, F. Structural optimization of pyrazolo[1,5-a]pyrimidine derivatives as potent and highly selective DPP-4 inhibitors. *Eur. J. Med. Chem.* **2020**, *208*, 112850. [[CrossRef](#)]
117. Karrouchi, K.; Fettach, S.; Anouar, E.H.; Tüzün, B.; Radi, S.; Alharthi, A.I.; Ghabbour, H.A.; Mabkhot, Y.N.; Faouzi, M.E.A.; Ansar, M.; et al. Synthesis, crystal structure, DFT, α -glucosidase and α -amylase inhibition and molecular docking studies of (E)-N'-(4-chlorobenzylidene)-5-phenyl-1H-pyrazole-3-carbohydrazide. *J. Mol. Struct.* **2021**, *1245*, 131067. [[CrossRef](#)]
118. Verma, G.; Khan, M.F.; Nainwal, L.M.; Ishaq, M.; Akhter, M.; Bakht, A.; Anwer, T.; Afrin, F.; Islamuddin, M.; Husain, I.; et al. Targeting malaria and leishmaniasis: Synthesis and pharmacological evaluation of novel pyrazole-1,3,4-oxadiazole hybrids. Part II. *Bioorg. Chem.* **2019**, *89*, 102986. [[CrossRef](#)]
119. Camargo, J.D.A.; Pianoski, K.E.; Dos Santos, M.G.; Lazarin-Bidoia, D.; Volpato, H.; Moura, S.; Nakamura, C.V.; Rosa, F.A. Antiparasitic Behavior of Trifluoromethylated Pyrazole 2-Amino-1,3,4-thiadiazole Hybrids and Their Analogues: Synthesis and Structure-Activity Relationship. *Front. Pharmacol.* **2020**, *11*, 591570. [[CrossRef](#)]
120. Da Silva, M.J.V.; Jacomini, A.P.; Goncalves, D.S.; Pianoski, K.E.; Poletto, J.; Lazarin-Bidoia, D.; Volpato, H.; Nakamura, C.V.; Rosa, F.A. Discovery of 1,3,4,5-tetrasubstituted pyrazoles as anti-trypanosomatid agents: Identification of alterations in flagellar structure of *L. amazonensis*. *Bioorg. Chem.* **2021**, *114*, 105082. [[CrossRef](#)]
121. Akolkar, H.N.; Dengale, S.G.; Deshmukh, K.K.; Karale, B.K.; Darekar, N.R.; Khedkar, V.M.; Shaikh, M.H. Design, Synthesis and Biological Evaluation of Novel Furan & Thiophene Containing Pyrazolyl Pyrazolines as Antimalarial Agents. *Polycycl. Aromat. Compd.* **2020**, *11*, 1–3. [[CrossRef](#)]
122. Strasek, N.; Lavrencic, L.; Ostrek, A.; Slapsak, D.; Groseelj, U.; Klemencic, M.; Zugelj, H.B.; Wagger, J.; Novinec, M.; Svete, J. Tetrahydro-1H,5H-pyrazolo 1,2-a pyrazole-1-carboxylates as inhibitors of Plasmodium falciparum dihydroorotate dehydrogenase. *Bioorg. Chem.* **2019**, *89*, 102982. [[CrossRef](#)] [[PubMed](#)]
123. Gogoi, P.; Shakya, A.; Ghosh, S.K.; Gogoi, N.; Gahtori, P.; Singh, N.; Bhattacharyya, D.R.; Singh, U.P.; Bhat, H.R. In silico study, synthesis, and evaluation of the antimalarial activity of hybrid dimethoxy pyrazole 1,3,5-triazine derivatives. *J. Biochem. Mol. Toxicol.* **2021**, *35*, 22682. [[CrossRef](#)] [[PubMed](#)]
124. Ali, T.E.; Bakhotmah, D.A.; Assiri, M.A. Synthesis of some new functionalized pyrano 2,3-c pyrazoles and pyrazolo 4',3':5,6 pyrano 2,3-d pyrimidines bearing a chromone ring as antioxidant agents. *Synth. Commun.* **2020**, *50*, 3314–3325. [[CrossRef](#)]
125. Ali, S.A.; Awad, S.M.; Said, A.M.; Mahgoub, S.; Taha, H.; Ahmed, N.M. Design, synthesis, molecular modelling and biological evaluation of novel 3-(2-naphthyl)-1-phenyl-1H-pyrazole derivatives as potent antioxidants and 15-Lipoxygenase inhibitors. *J. Enzyme Inhib. Med. Chem.* **2020**, *35*, 847–863. [[CrossRef](#)]
126. De Oliveira, D.H.; Sousa, F.S.S.; Birmann, P.T.; Pesarico, A.P.; Alves, D.; Jacob, R.G.; Savegnago, L. Evaluation of antioxidant activity and toxicity of sulfur- or selenium-containing 4-(arylchalcogenyl)-1H-pyrazoles. *Can. J. Physiol. Pharmacol.* **2020**, *98*, 441–448. [[CrossRef](#)]
127. El-Badawy, A.A.; Elgubbi, A.S.; El-Helw, E.A.E. Acryloyl isothiocyanate skeleton as a precursor for synthesis of some novel pyrimidine, triazole, triazepine, thiadiazolopyrimidine and acylthiourea derivatives as antioxidant agents. *J. Sulphur Chem.* **2021**, *42*, 295–307. [[CrossRef](#)]
128. El-Borai, M.A.; Rizk, H.F.; Ibrahim, S.A.; Fares, A.K.; El-Tahawy, M.M.T.; Beltagy, D.M. Assessment of anti-hemolytic, cytotoxicity, antioxidant activities and molecular docking study based on thienopyrazole scaffold as pharmacophore. *J. Mol. Struct.* **2021**, *1240*, 130602. [[CrossRef](#)]
129. Elnagdy, H.M.F.; Gogoi, N.G.; Handique, J.G.; Sarma, D. CuO-NPs/TFA: A New Catalytic System to Synthesize a Novel Series of Pyrazole Imines with High Antioxidant Properties. *Bionanoscience* **2021**, *11*, 929–938. [[CrossRef](#)]

130. Kaddouri, Y.; Abrigach, F.; Yousfi, E.; El Kodadi, M.; Touzani, R. New thiazole, pyridine and pyrazole derivatives as antioxidant candidates: Synthesis, DFT calculations and molecular docking study. *Heliyon* **2020**, *6*, E03185. [[CrossRef](#)]
131. Naveen, S.; Kumara, K.; Kumar, A.D.; Kumar, K.A.; Zarrouk, A.; Warad, I.; Lokanath, N.K. Synthesis, characterization, crystal structure, Hirshfeld surface analysis, antioxidant properties and DFT calculations of a novel pyrazole derivative: Ethyl 1-(2,4-dimethylphenyl)-3-methyl-5-phenyl-1H-pyrazole-4-carboxylate. *J. Mol. Struct.* **2021**, *1226*, 129350. [[CrossRef](#)]
132. Tabarsaei, N.; Hamedani, N.F.; Shafiee, S.; Khandan, S.; Hossaini, Z. Catalyst-free green synthesis and study of antioxidant activity of new pyrazole derivatives. *J. Heterocycl. Chem.* **2020**, *57*, 2945–2954. [[CrossRef](#)]
133. Kumara, K.; Prabhudeva, M.G.; Vagish, C.B.; Vivek, H.K.; Rai, K.M.L.; Lokanath, N.K.; Kumar, K.A. Design, synthesis, characterization, and antioxidant activity studies of novel thienyl-pyrazoles. *Heliyon* **2021**, *7*, E07592. [[CrossRef](#)] [[PubMed](#)]
134. Patila, P.; Yadava, A.; Bavkar, L.; Nippu, B.N.; Satyanarayana, N.D.; Maned, A.; Gurava, A.; Hangirgekar, S.; Sankpala, S. MerDABCO-SO₃H Cl catalyzed synthesis, antimicrobial and antioxidant evaluation and molecular docking study of pyrazolopyranopyrimidines. *J. Mol. Struct.* **2021**, *1242*, 130672. [[CrossRef](#)]
135. Popova, S.A.; Pavlova, E.V.; Shevchenko, O.G.; Chukicheva, I.Y.; Kutchin, A.V. Isobornylchalcones as Scaffold for the Synthesis of Diarylpyrazolines with Antioxidant Activity. *Molecules* **2021**, *26*, 3579. [[CrossRef](#)]
136. Jagadale, S.M.; Abhale, Y.K.; Pawar, H.R.; Shinde, A.; Bobade, V.D.; Chavan, A.P.; Sarkar, D.; Mhaske, P.C. Synthesis of New Thiazole and Pyrazole Clubbed 1,2,3-Triazol Derivatives as Potential Antimycobacterial and Antibacterial Agents. *Polycycl. Aromat. Compd.* **2020**, *28*, 1–22. [[CrossRef](#)]
137. Reddy, G.S.; Snehalatha, A.V.; Edwin, R.K.; Hossain, K.A.; Giliyaru, V.B.; Hariharapura, R.C.; Gautham Shenoy, G.; Misra, P.; Pal, M. Synthesis of 3-indolylmethyl substituted (pyrazolo/benzo)triazinone derivatives under Pd/Cu-catalysis: Identification of potent inhibitors of chorismate mutase (CM). *Bioorg. Chem.* **2019**, *91*, 103155. [[CrossRef](#)]
138. Ray, P.C.; Huggett, M.; Turner, P.A.; Taylor, M.; Cleghorn, L.A.T.; Early, J.; Kumar, A.; Bonnett, S.A.; Flint, L.; Joerss, D.; et al. Spirocyclic MmpL3 Inhibitors with Improved hERG and Cytotoxicity Profiles as Inhibitors of Mycobacterium tuberculosis Growth. *ACS Omega* **2021**, *6*, 2284–2311. [[CrossRef](#)]
139. Hu, X.; Wan, B.; Liu, Y.; Shen, J.; Franzblau, S.G.; Zhang, T.; Ding, K.; Lu, X. Identification of Pyrazolo[1,5-a]pyridine-3-carboxamide Diaryl Derivatives as Drug Resistant Antituberculosis Agents. *ACS Med. Chem. Lett.* **2019**, *10*, 295–299. [[CrossRef](#)]
140. Parikh, P.H.; Timaniya, J.B.; Patel, M.J.; Patel, K.P. Microwave-assisted synthesis of pyrano 2,3-c-pyrazole derivatives and their anti-microbial, anti-malarial, anti-tubercular, and anti-cancer activities. *J. Mol. Struct.* **2022**, *1249*, 131605. [[CrossRef](#)]
141. Desai, N.C.; Bhatt, K.; Monapara, J.; Pandit, U.; Khedkar, V.M. Conventional and Microwave-Assisted Synthesis, Antitubercular Activity, and Molecular Docking Studies of Pyrazole and Oxadiazole Hybrids. *ACS Omega* **2021**, *6*, 28270–28284. [[CrossRef](#)] [[PubMed](#)]
142. Shaik, A.B.; Bhandar, R.R.; Nissankararao, S.; Edis, Z.; Tangirala, N.R.; Shahanaaz, S.; Rahman, M.M. Design, facile synthesis and characterization of dichloro substituted chalcones and dihydropyrazole derivatives for their antifungal, antitubercular and antiproliferative activities. *Molecules* **2020**, *25*, 3188. [[CrossRef](#)] [[PubMed](#)]
143. Pola, S.; Banoth, K.K.; Sankaranarayanan, M.; Ummani, R.; Garlapati, A. Design, synthesis, in silico studies, and evaluation of novel chalcones and their pyrazoline derivatives for antibacterial and antitubercular activities. *Med. Chem. Res.* **2020**, *29*, 1819–1835. [[CrossRef](#)]
144. Patel, D.M.; Sharma, M.G.; Vala, R.M.; Lagunes, I.; Puerta, A.; Padron, J.M.; Rajani, D.P.; Patel, H.M. Hydroxyl alkyl ammonium ionic liquid assisted green and one-pot regioselective access to functionalized pyrazolodihydropyridine core and their pharmacological evaluation. *Bioorg. Chem.* **2019**, *86*, 137–150. [[CrossRef](#)] [[PubMed](#)]
145. Modi, P.; Patel, S.; Chhabria, M. Structure-based design, synthesis and biological evaluation of a newer series of pyrazolo[1,5-a]pyrimidine analogues as potential anti-tubercular agents. *Bioorg. Chem.* **2019**, *87*, 240–251. [[CrossRef](#)]
146. Pogaku, V.; Krishna, V.S.; Sriram, D.; Rangan, K.; Basavoju, S. Ultrasonication-ionic liquid synergy for the synthesis of new potent anti-tuberculosis 1,2,4-triazol-1-yl-pyrazole based spirooxindolopyrrolizidines. *Bioorg. Med. Chem. Lett.* **2019**, *29*, 1682–1687. [[CrossRef](#)]
147. Brahmabhatt, G.C.; Sutariya, T.R.; Atara, H.D.; Parmar, N.J.; Gupta, V.K.; Lagunes, I.; Padrón, J.M.; Murumkar, P.R.; Yadav, M.R. New pyrazolyl-dibenzo[b,e][1,4]diazepinones: Room temperature one-pot synthesis and biological evaluation. *Mol. Divers.* **2020**, *24*, 355–377. [[CrossRef](#)]
148. Kishk, S.M.; McLean, K.J.; Sood, S.; Smith, D.; Evans, J.W.D.; Helal, M.A.; Gomaa, M.S.; Salama, I.; Mostafa, S.M.; De Carvalho, L.P.S.; et al. Design and Synthesis of Imidazole and Triazole Pyrazoles as Mycobacterium Tuberculosis CYP121A1 Inhibitors. *ChemistryOpen* **2019**, *8*, 995–1011. [[CrossRef](#)]
149. Vavaiya, B.; Patel, S.; Pansuriya, V.; Marvaniya, V.; Patel, P. Synthesis, anti-tubercular evaluation and molecular docking studies of nitrogen-rich piperazine-pyrimidine-pyrazole hybrid motifs. *Curr. Chem. Lett.* **2022**, *11*, 95–104. [[CrossRef](#)]
150. Wong, K.T.; Osman, H.; Parumasivam, T.; Supratman, U.; Che Omar, M.T.; Azmi, M.N. Synthesis, characterization and biological evaluation of new 3,5-disubstituted-pyrazoline derivatives as potential anti-Mycobacterium tuberculosis H37Ra compounds. *Molecules* **2021**, *26*, 2081. [[CrossRef](#)]
151. Chen, H.; Wang, B.; Li, P.; Yan, H.; Li, G.; Huang, H.H.; Lu, Y. The optimization and characterization of functionalized sulfonamides derived from sulfaphenazole against Mycobacterium tuberculosis with reduced CYP 2C9 inhibition. *Bioorg. Med. Chem. Lett.* **2021**, *40*, 127924. [[CrossRef](#)] [[PubMed](#)]

152. Takate, S.J.; Shinde, A.D.; Karale, B.K.; Akolkar, H.; Nawale, L.; Sarkar, D.; Mhaske, P.C. Thiazolyl-pyrazole derivatives as potential antimycobacterial agents. *Bioorg. Med. Chem. Lett.* **2019**, *29*, 1199–1202. [[CrossRef](#)] [[PubMed](#)]
153. He, B.; Dong, J.; Lin, H.Y.; Wang, M.Y.; Li, X.K.; Zheng, B.F.; Chen, Q.; Hao, G.F.; Yang, W.C.; Yang, G.F. Pyrazole-Isoindoline-1,3-dione Hybrid: A Promising Scaffold for 4-Hydroxyphenylpyruvate Dioxygenase Inhibitors. *J. Agric. Food Chem.* **2019**, *67*, 10844–10852. [[CrossRef](#)]
154. Jiang, B.B.; Guo, B.B.; Cui, J.L.; Dong, Y.W.; Cui, L.; Zhang, L.; Yang, Q.; Yang, X.L. New lead discovery of insect growth regulators based on the scaffold hopping strategy. *Bioorg. Med. Chem. Lett.* **2020**, *30*, 127500. [[CrossRef](#)]
155. Zhao, Y.Y.; Li, H.G.; Sun, P.W.; Gao, L.; Liu, J.B.; Zhou, S.; Xiong, L.X.; Yang, N.; Li, Y.X.; Li, Z.M. Synthesis, biological activities, and SAR studies of novel 1-(2-chloro-4,5-difluorophenyl)-1H-pyrazole derivatives. *Bioorg. Med. Chem. Lett.* **2020**, *30*, 127535. [[CrossRef](#)] [[PubMed](#)]
156. Judge, N.R.; Chacktas, G.; Ma, L.; Schink, A.; Buckpesch, R.; Schmutzler, D.; Machettira, A.B.; Dietrich, H.; Asmus, E.; Bierer, D.; et al. Flexible Synthesis and Herbicidal Activity of Fully Substituted 3-Hydroxypyrazoles. *Eur. J. Org. Chem.* **2021**, *2021*, 5677–5684. [[CrossRef](#)]
157. Khallaf, A.; Wang, P.; Zhuo, S.P.; Zhu, H.J.; Liu, H. Synthesis, insecticidal activities, and structure-activity relationships of 1,3,4-oxadiazole-ring-containing pyridylpyrazole-4-carboxamides as novel insecticides of the anthranilic diamide family. *J. Heterocycl. Chem.* **2021**, *58*, 2189–2202. [[CrossRef](#)]